42

CIRCULATION THROUGH THE MOUTH OF LANGEBAAN LAGOON AND IMPLICATIONS

Marjolaine KRUG

Thesis submitted to the University of Cape Town in fulfilment of the requirements of the degree of Master of Science, June 1999.

Abstract

In March 1997 a two-weeks field survey was conducted in Langebaan Lagoon and Saldanha Bay. The aim of this survey was to farther our understanding of the processes driving the mixing and the exchange at the Langebaan Lagoon-Saldanha Bay interface. The parameters measured included currents, water-levels, temperature, salinity, density and wind. The nature of the flow at the Langebaan Lagoon inlets was ascertained by combining statistical analysis of the measurements to a theoretical understanding of the system hydrodynamics. The flow in the vicinity of the straight was predominantly driven by the tide. It was found that during high tidal range periods, there existed an asymmetry between the ebb and the flood flows at both of the lagoon's inlets. When tidal forcing was strong, water particles released at the lagoon inlets during the ebb were subject to long drifts. The outflow from the east inlet appeared to take the form of a turbulent jet. At the west inlet strong frictional interactions between the flow and land boundaries occurred, causing the flow to rapidly expand and lose momentum and therefore impeding the formation of a jet. It was established that, generally, buoyancy forcing on the Langebaan Lagoon outflow would be small and that water issuing from the lagoon during the ebb would remained attached to the sea-bed as it propagated into Saldanha Bay. However, when Saldanha Bay was strongly stratified, the east inlet ebb jet would lift off from the bottom as it reached the 8m depth contour. The large drifts resulting from the sink-like nature of the inflow and the jet-like nature of the outflow induced a very rapid and strong exchange between Langebaan Lagoon and Saldanha Bay. The propagation of the lagoon effluent also contributed extensively to vertically stir the water-column in Big Bay. As the tidal range weakened, the regions of influence of the ebb and the flood overlapped to a greater extent and the exchange between the lagoon and the bay decreased significantly. The asymmetry between the ebb and the flood flows at the Langebaan Lagoon inlets generated a Lagrangian residual circulation, with the east inlet constituting the entrance for Saldanha Bay water, while the west inlet would be the exit route for Langebaan Lagoon water. Southerly winds, contributed to the overall residual circulation by driving water out of the Lagoon.

Acknowledgement

- I would first like to thank my supervisor, Dr John Largier, for his guidance and encouragement. Most sincere thanks to Geoff Brundrit and Howard Waldron for the comments received on drafts of the thesis. I am very grateful to Bruce Spolander who gave me a big push at the start of this thesis, kept calm when I was not and enabled me to make the fieldwork a success. A big thank you to Penny Price, whose efficiency and enthousiasm always uplift me. I would like to acknowledge all the people who helped in the acquisition of the data, again Bruce Spolander, Howard Waldron and his family, Penny Price, Craig Attwood, Paul Hanekom and Sidney Bilski. It was a real pleasure working with you. Thank you very much to Shirley Butcher, from the ENGEO department, for being so patient and helping me solve numerous problems when using ARCVIEW.

- I am obliged to the Council for Scientific and Industrial Research (CSIR) for the ADCP data they allowed me to use in my thesis. From the CSIR, I would especially like to thank Roy Van Ballegooyen whose love of oceanography and enthusiasm are inspiring. I am also very grateful to Alan Boyd from the Sea Fisheries Research Institute (SFRI) who provided the GPS and the drifters used during the field survey. I would like to acknowledge the financial support from the Foundation for Research Development (FRD). Aslo, thank you to the National Parks Board for their collaboration during the field survey.

- Finally, I want to thank Stewart for all the nice lunch breaks.

Content

Figures

Tables

1. Introduction

Approximately 100 km from Cape Town, on the west coast of southern Africa, Langebaan Lagoon and Saldanha Bay constitute a coastal environment of great ecological importance. While Saldanha Bay is increasingly subjected to industrial or aquaculture-related developments, the Langebaan Lagoon has remained sheltered from the effects of economical growth since it was declared a National Park in 1985 (Robinson, 1989). The circulation through the two narrow inlets which connect the lagoon to the southern part of the bay, is characterised by strong tidal currents. Wind is the primary forcing of currents in Saldanha Bay, but at the lagoon entrance, winds serve only to accelerate or retard the tidal flow (Shannon and Stander, 1977). It is expected that the fast currents through the lagoon narrow entrance will contribute to large scale circulation both in the lagoon basin and in the bay. Active exchange should then occur between the two embayments and the influence of the lagoon water on the bay may be significant.

Mixing and exchange between Langebaan Lagoon and Saldanha Bay provide for the transport of water-borne materials, such as pollutants, nutrients and sediments. For example, industrial pollutants from Saldanha Bay, might slowly contaminate the lagoon. The regular visit of oil tankers into Saldanha Bay represents a significant threat to the system, as an oil spill could be fatal to the ecology of Langebaan Lagoon. It is also possible that the lagoon effluent affects the water quality within Saldanha Bay. The lagoon is a shallow and evaporative environment compared to the bay and therefore, higher temperatures and salinities are found in the lagoon. Langebaan Lagoon provides a source of heat and salt for Saldanha Bay. The lagoon effluent may thus affect local stratification and, in turn, play a role in eutrophication. Finally, the erosion of beaches located in the vicinity of the Langebaan village in the last few years, has drawn significant concern amongst the local community. A good understanding of the circulation at the interface between the lagoon and the bay is therefore essential for the successful management and monitoring of the ecology of the Saldanha-Langebaan system.

This thesis aims to address the lagoon-bay exchange and assess the role of Langebaan Lagoon effluent in Saldanha Bay. It is also hoped that through this work, our general understanding of the Langebaan-Saldanha system will be improved.

In March 1997, a two-week field survey was undertaken. Most of the data were collected in the vicinity of the lagoon inlets: the key region in terms of hydrodynamic flow and exchange. Measurements included currents, water-levels, temperature, salinity, atmospheric pressure and winds. Previous theories (Ozsoy, 1977; Joshi, 1982) on tidal inlet hydrodynamics and coastal lagoons were used. It was expected that the geometry of the lagoon entrance would lead to strong asymmetry between the ebb and the flood flows in Saldanha Bay, with the lagoon outflow having the structure of a turbulent jet and the inflow taking the form of a potential sink. The analysis conducted by Ozsoy (1977) on bottom frictional jets is applied here, with the aim of modelling the properties of the flow as lagoon water propagates into Saldanha Bay. The way by which water-level fluctuations travel into the lagoon is also assessed. Conclusions drawn through analysis of the data and use of theory serve to define the nature of the exchange between the lagoon and the bay and the effect of the Langebaan Lagoon effluent on Saldanha Bay.

This thesis starts with a description of the Saldanha Bay-Langebaan Lagoon system (Chapter 2). Chapter 3 reviews theories on the hydrodynamics at tidal inlets. The method for the data collection and analysis is described in Chapter 4, preceding the factual description of the data obtained (Chapter 5). Chapter 6, assesses the way by which water-level fluctuations propagate through the lagoon and how that reflects on the hydrodynamics at the entrance of the lagoon. Following the characterisation of the nature of the flow at the inlets (Chapter 7), the exchange at the Langebaan Lagoon-Saldanha Bay interface is described (Chapter 8). The role of the lagoon effluent and the results found in this thesis are discussed in Chapter 9. Chapter 10 reiterates the main findings of the previous chapters and concludes this thesis.

2. The Saldanha Bay - Langebaan Lagoon environment

Saldanha Bay and the Langebaan Lagoon are located approximately 100 km north of Cape Town, on the arid west coast of South Africa (figure 2-1). The system is essentially marine, as no perennial streams or rivers enter the bay. The yearly average precipitation rate in the area is approximately 300mm (Christie, 1981) with most of the precipitation concentrated over the winter months of May, June and July (Schulze, 1965).

Saldanha Bay:

Saldanha Bay is subject to the influence of the cold, nutrient-rich Benguela waters during the summer and sustains a rich and unique ecological environment. The ecology is characterized by numerous filter feeding organisms and supports a wide range of migrating birds including the endangered African penguin (CSIR, 1995).

Up to the 1970's, developments in the area were limited to small fishing communities. Attempts to develop Saldanha Bay remained unsuccessful until the Iron and Steel Corporation (ISCOR) decided to use the bay as a port for the export of the ore. The construction of the iron ore jetty and the causeway linking Marcus Island to the mainland separated Saldanha Bay into two smaller embayments: 'Small Bay' in the northern part of Saldanha Bay and 'Big Bay', located immediately north of the lagoon inlet. From the 1970's to the 1990's, Saldanha Bay was promoted as an industrial growth point by the government. During the 1980's a strategic oil storage facility was built on the east side of the bay, resulting in the regular visits of oil tankers into the bay. Despite the important increase of industrial activity in Saldanha, fishing remains the largest source of employment. The bay also provides an appropriate environment for the culture of shellfish and seaweed. Mariculture is practiced in Small Bay, with mussels having one of the fastest growth rates in the world (Du Plessis, 1994). Mussel farming is presently expanding to the northern section of Big Bay, where 300 hectares were recently leased to companies and individuals (CSIR, 1997).

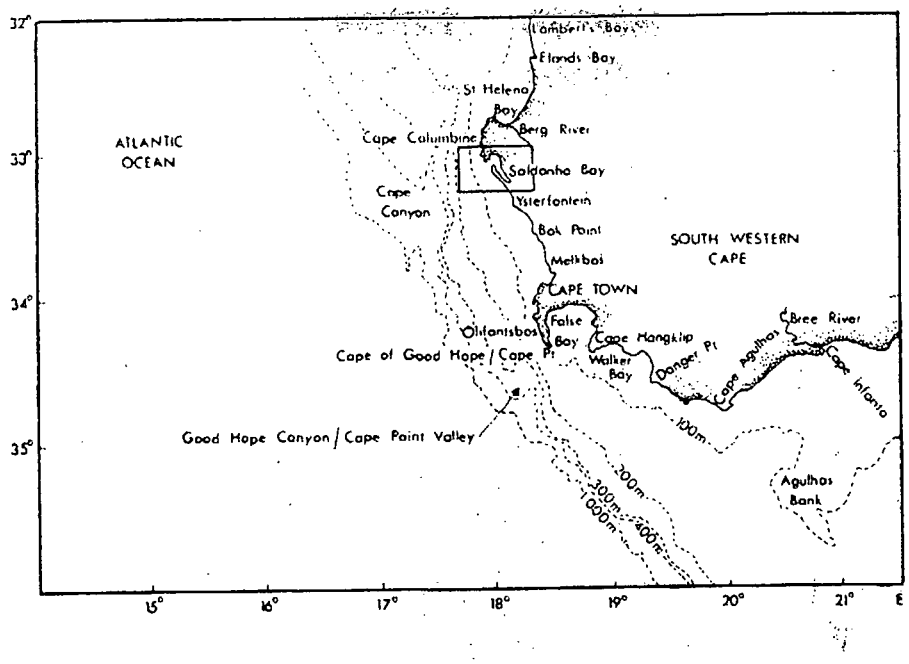

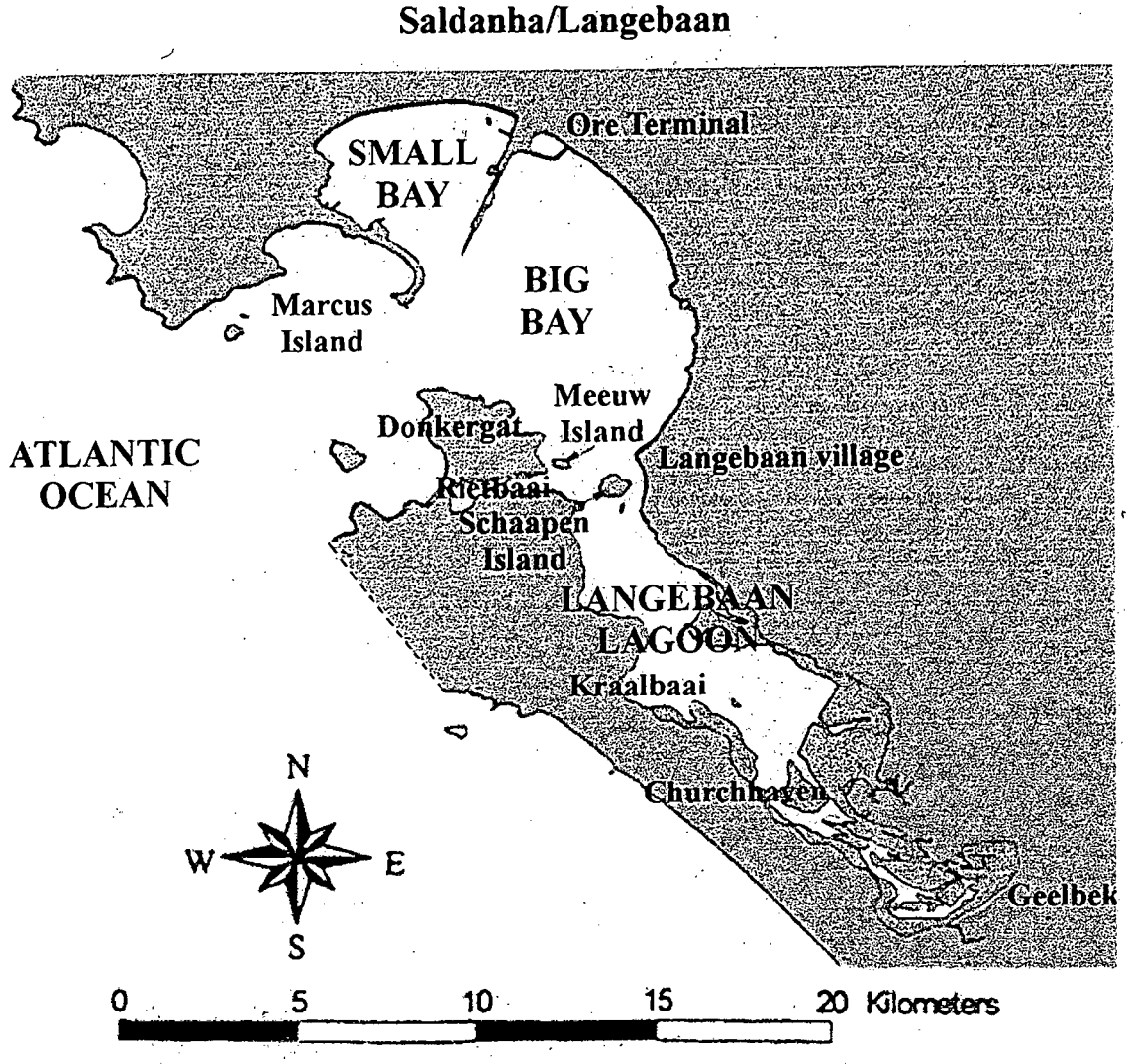

Figure 2-1: Location of the study area

The potential increase in industrial development in such a rich ecosystem created a need for scientists to undertake environmental studies in the bay. The circulation and the water properties of the bay system were first ascertained by Shannon and Stander (1977), prior to the construction of the iron ore jetty. Thermal data (Shannon and Stander, 1977) underlined the existence of three basic systems in the bay: the cold Benguela Current forming the western boundary, the bay system in the middle, and the warm Langebaan lagoon system. Over the last decade, further studies describing the patterns of temperature variation and flow motion in Saldanha Bay have been undertaken in anticipation of further development (CSIR, 1995; Weeks, 1990; Bilski, 1995; Monteiro and Brundrit, 1995; Spolander, 1995; Monteiro and Largier, 1999).

The wind and the tide are the main forces driving the flow circulation in Saldanha bay. Tidal currents are predominantly semi-diurnal and rarely exceed 0.15 $m.s^{-1}$ in Saldanha Bay itself (Flemming, 1977), except at the mouth where stronger tidal forcing is felt (Shannon and Sander, 1977).

Winds over the west coast of South-Africa are predominantly controlled by the anticyclonic motion round the South Atlantic high pressure system, the pressure field over the subcontinent, and the passage of eastward moving cyclones which cross the southern part of the continent (Shannon, 1985). Over the southern part of the Benguela, strong seasonal variations occur. During the summer months, the South Atlantic high pressure system intensifies and moves approximately 6° to the south (Preston-White and Tyson, 1988), while a well-developed low pressure is formed over the African subcontinent. The set up of the pressure field in the summer intensifies the southerly winds and drives a maximum upwelling in the ocean from September to March. In the southern Benguela, the passage of eastward moving cyclones (resulting from perturbations on the subtropical jet stream) induces wind relaxation or reversal and modulates the upwelling (Shannon, 1985). It seems that the approach of those cyclonic systems is associated with the formation of low pressure cells which form near Luderitz. Those coastal-trapped propagating low-pressure systems suppress upwelling locally and travel round the subcontinent as trapped waves (Shannon and Nelson, 1996). The cyclicity of coastal lows is of the order of 6 days (Jury et al., 1990). In winter, the South Atlantic pressure system moves back north and the pressure over the

southern west coast of Africa changes to a weak high. The influence of eastward moving cyclones is more strongly felt and, as a consequence, the frequency and intensity of winds with a westerly component become significant. In the Saldanha Bay-Langebaan Lagoon region, southwesterly winds (a local derivative of the south-east trade winds resulting from the topography of the bay) dominate in summer, while during winter, strong cyclonic northwesterly winds occur (Van der Merwe, 1990). Previous drogue studies (Weeks et al., 1991(a); Bilski, 1995) reveal that Saldanha Bay is a typical upwelling region during the summer months, with a wind driven surface layer and a bottom layer primarily driven by the tide. In winter, when the water column in Saldanha Bay is well mixed, the influence of the tide is relatively more important. In Saldanha Bay wind is the major mechanism controlling the flow, although the circulation at the mouth of the bay is mainly tidal (Shannon and Stander, 1977). Also to be noted is the presence of particularly strong tidal currents at the Langebaan Lagoon inlets.

The salinity in the bay is very similar to that of the ocean with a mean value of 34.9*psu* and little spatial variation (Shannon and Stander, 1977). In the winter months, the water column in Saldanha Bay is largely isothermal with typical temperatures of 13-14°C. During the summer, upwelling favorable winds drive the inflow of cold upwelled water (10-12°C) under warmer bay water (13-14°C). The subsequent warming of the surface water to temperatures of 18-20°C (Monteiro and Brundrit, 1990) leads to the development of stratification in the bay. The presence of a strong seasonal thermocline gives Saldanha Bay a near-estuarine hydrodynamic behavior. In the summer, winds drive a stratified shear flow whereby the out-flowing surface water is replaced by in-flowing bottom water (Weeks et al., 1991(b)). The bay-ocean density differences also drive cold dense bottom water into the bay (Monteiro and Largier, 1999). Stratification in the bay starts during the spring (August) and increases throughout the summer, temperature differences of 3-10°C observed between the surface and the bottom layer (Monteiro and Brundrit, 1995). To this seasonal stratification pattern, synoptic modulation of the thermocline can be superimposed. These synoptic modulation of the thermocline occur roughly every 6-7 days, as for wind events that drive the Benguela upwelling system (Monteiro and Brundrit, 1995). The occurrence of stratification in the bay has important consequences on dispersion, as greater stratification acts against vertical mixing.

The Langebaan Lagoon:

The Langebaan Lagoon is a shallow and sheltered water-body, attached to Saldanha Bay. In 1985, it became a protected area under the juristriction of the National Parks Board (Robinson, 1989). The southern part of the lagoon is bounded by marshes and sandflats which support a wide and varied flora and fauna. The southern part of the lagoon was proclaimed an area of international importance in terms of the Ramsar Convention (1975) as it supports more wading birds than any other marshland in South Africa. In the summer, up to 50 000 waders of 23 species live on the marshes, consuming at least 12 000 kg of organisms each year (Cooper, 1981). The lagoon also plays an important role as a nursery for the development of post-larval and juvenile fish, which take advantage of the abundant food source and the shelter from predators provided by the marshes. No commercial fishing is allowed in the lagoon. The Minister of Economic Affairs however, extended special permission to the Churchhaven fishing community to carry on fishing, thus preserving their traditional life-style. The lagoon contains approximately 5% of the volume of Saldanha Bay but covers approximately 40% of the surface area in the Langebaan/Saldanha Bay system. Langebaan Lagoon stretches for about 15km parallel to the coast and has a maximum width of 3.5km. Water enters and leaves the lagoon through the two 400m wide channels on either sides of Schaapen Island. The lagoon bed includes large intertidal flats, shallow subtidal flats and deeper drainage channels, giving the lagoon a mean depth of 1.35m at spring low tide and 3.19m at spring high tide (Arabonis, 1995).

The temperature and salinity vary to a much greater extent in the lagoon than in Saldanha Bay. In winter, the surface temperature of the lagoon differs little from that of Saldanha Bay with average values of 15°C (Shannon and Stander, 1977). Temperatures in the lagoon are affected by the state of the tide: at low tide temperatures are greater than at high tide. This is a consequence of the cooler Saldanha Bay water being advected into the lagoon during the flood tide. In summer, water is warmer in the lagoon as a result of solar heating on the shallow areas of the lagoon basin and the lagoon water hence constitutes a potential source of heat for Saldanha Bay. Measurements undertaken in 1975-1976, showed that the temperature gradient between the mouth and the southern part of the lagoon was greatest in January and would then decrease to reach a minimum in winter (Christie, 1981). The temperature ranges measured by Christie were 14.9-24 °C in January, 17.5-21 °C in

March and 13.5-15.3°C in August. Salinity profiles in the lagoon follow the same kind of pattern as temperature profiles with a marked increase from winter to summer. Salinity at the lagoon mouth is similar to that of the adjacent ocean with values in the order of 34.5-35*psu*. As one penetrates deeper into the lagoon, solar heating and strong southerly winds enhance evaporation and due to long residence times for water particles (Arabonis, 1995), the environment becomes hypersaline with salinity reaching typical values in excess of 37*psu* (Shannon and Stander, 1977; Christie, 1981). Extreme values of temperature and salinity were measured in the salt marshes with temperature and salinity reaching maximum of 30.5°C and 43*psu* in January (Christie, 1981). Drops in the lagoon salinity values can briefly occur as a result of precipitation in winter. The lagoon can be separated into three sections, each having defined temperature and salinity properties (Arabonis, 1995). At the inlet, the lagoon is essentially marine. At distances more than 2km from the mouth (but typically less than 6km), the lagoon behaves like a thermal estuary, with density decreasing as temperature increases with distance from the inlets. South of that region, the density starts increasing due to higher values of the salinity, giving the lagoon water characteristics similar to that of a hypersaline inverse estuary (Largier et al., 1997). The increase in temperature and salinity with distance from the lagoon mouth is particularly pronounced during the summer months, when solar heating is strongest.

Langebaan Lagoon circulation was studied by Shannon and Stander (1977) using drogues, dye-tracing techniques, drift cards and sea-bed drifters. Flemming (1977) drew some conclusions on the flow properties from current measurements and from the sedimentary structure of the lagoon basin.

Currents in the lagoon are primarily driven by the tide, the effect of the predominant northerly or southerly winds being to accelerate or retard the tidal flow. The disposition of the bedforms suggested a dominant north-south energy gradient and a secondary west-east energy gradient (Flemming, 1977). The tidal range observed at the mouth (Flemming, 1977), was equal to 1.35m and 0.5m for spring and the neap tides, respectively. In the southern part of the lagoon, the tidal range was reduced to values of 1.15m and 0.39m for the spring and neap tides, respectively. At the lagoon entrance, the onset of tidal currents appeared to be delayed by 20 minutes or more following occurrence of the tidal peak and

trough and (Shannon and Stander, 1977). Tidal currents in the lagoon decrease progressively with distance from the mouth. Flemming (1977) found that the currents were strongest during the ebb, with velocities 20% stronger than during the flood. His measurement showed maximum surface current velocity equal to $1.3m.s^{-1}$ and $1m.s^{-1}$ during the ebb, for the eastern and the western channels respectively. At the southern end of the lagoon and approximately 15km from the mouth, the ebb and flood currents dropped to $0.6m.s^{-1}$ and $0.45m.s^{-1}$ respectively. From current measurements and the consistent time lag between the water-level peak and the reversal of the current, Flemming deduced that there was a pronounced separation between the inflow and outflow paths of the tidal currents, with the eastern channel being the exit route for Langebaan Lagoon water. Data collected by Shannon and Stander (1977) showed different results. In their measurements, the current velocities were similar in the east and the west channels. The velocity they measured for the flow during the spring tides was up to $1m.s^{-1}$ in both channels. During the neap tides, current velocity decreased by 25% to 50%. They also found a double maximum in the surface current at the inlet and attributed it to some reflection or resonance effect in the bay or in the lagoon.

Estimates of the residence time and flushing characteristics of Langebaan water were made by Weeks (1990) and Arabonis (1995). Weeks (1990) calculated the removal time for pollutants assuming that the water column in the lagoon was completely mixed, and that the tidal prism was equal to the lagoon area times the tidal range. The resulting removal times of pollutants from the lagoon were 2 and 5 tidal cycles for the spring and the neap tide respectively. In the same study, the use of the spring high water mark for the area calculations in a system characterized by saltmarshes and numerous sandbanks and the assumption of complete mixing in the lagoon every tidal cycle, probably provided an upper estimate of the exchange between the lagoon and the adjacent bay. Arabonis (1995) used a one dimensional advection-diffusion model, in which residence and flushing times were calculated from observed salinity distributions. The model defined according to Largier et al. (1997), accounted for river inflow, precipitation and evaporation. The results gave a residence time of respectively 25 days near the lagoon head, 10 days in the mid- lagoon (Kraalbaai area), and 0 day at the lagoon mouth. Many assumptions were made in the derivation of the model. For example, the calculations were based on evaporation rates

measured over a very short period of 2 days and it was assumed that no fresh water was input into the system via groundwater seepage. Although many assumptions were made in the derivation of the model, this is a robust approach to define the scale for the residence and flushing times of the lagoon.

These previous studies have provided a basic understanding of the hydrodynamic and physical properties of Langebaan Lagoon, but there remains a lack of understanding of the mechanisms involved in the exchange between the lagoon and Saldanha Bay. Clear quantitative information on the flow speed or tidal excursion at the lagoon-bay interface is still lacking. The hydrodynamic properties of the flow at the lagoon inlets and the extent to which Langebaan Lagoon water affects Big Bay remain vague. Shannon and Stander (1977) suggested that the thermocline encountered on some occasions in Big Bay, was due to warmer lagoon water flowing over the colder bay water. This could have important repercussions on the water quality or on understanding eutrophication within the Saldanha Bay-Langebaan Lagoon system. Many conclusions about the nature of the circulation in the lagoon are speculative and still need to be confirmed.

3. Circulation in coastal lagoons

According to Kjerfve (1994), a coastal lagoon can be defined as:

> *" an inland water body, usually oriented parallel to the coast, separated from the ocean by a barrier, connected to the ocean by one or more restricted inlets, and having depths which seldom exceed a couple of meters. A lagoon may or may not be subject to tidal mixing, and salinity can vary from that of a coastal fresh-water lake to a hypersaline lagoon, depending on the hydrological balance ... "*

Coastal lagoons account for 13 % of all coastal environment (Barnes, 1980). They are generally highly productive systems, but are also often stressed by anthropogenic input or human activities (Kjerfve, 1994). Due to their shallow nature, coastal lagoons often constitute a source of heat for the neighbouring ocean or bay (Smith, 1994). Similar to estuaries, coastal lagoons experience forcing from the tides, the wind and the density variation in the water due to river run-off, evaporation or heating (Hansen and Rattray, 1966; Kjerfve, 1994; Sheng et al., 1996). The most important geomorphological factors influencing the water, salt and heat balance in coastal lagoons are inlet configuration and size, lagoon size, orientation of the lagoon relative to prevailing winds and water depth (Smith, 1994). While the lagoon proper is dominated by diffusive processes, advective processes generally prevail in the inlet channel (Kjerve and Knoppers, 1991).

The exchange between coastal lagoons and adjacent water bodies regulates the volumes of pollutants, dissolved or particulate nutrients and other water-borne materials being flushed in or out of the lagoon system. The exchange between coastal lagoons and adjacent water bodies is strongly influenced by the topography and is dominated by two factors (Black et al., 1981):

- the water level differences between the lagoon and the adjacent ocean or bay (imposed by astronomic and barometric tides, longer term changes in ocean water level and increases in the lagoon water level by river flow).
-the density difference between the lagoon and the adjacent water body (Hearn et al., 1991).

The flushing capacity and the overall ecology of the lagoon depend to a great extent on the

hydrodynamics at tidal inlets, and special focus should be put on those regions. It is still important however, that the circulation within the lagoon basin be known, because conditions at the lagoon entrance are influenced by the different forcing mechanisms imposed in the basin interior. For example, factors such as river run off, winds and tidal range will affect the gradients in water-level and density between the lagoon and the adjacent bay. Also, a knowledge of the circulation in the lagoon basin is essential to understand the fate of pollutants or other water-borne materials within the lagoon.

3.1 Circulation in the lagoon basin:

In coastal lagoons the forcing mechanisms dominating the circulation vary with location (Smith, 1994). Near the mouth of many estuaries and coastal lagoons, tidal forcing usually dominates. Other processes, while still perturbing the tidal signal measurably, are of secondary importance in explaining the total variance of the current records (Smith, 1985). Conversely, at the head of the lagoon, variations of fresh-water outflow may occur as well defined events and may dominate the negligible tidal and wind-driven current motions. Wind-driven motions may predominate in the middle reaches of the basin, where the tidal co-oscillations have been damped by friction and the effect of variations in freshwater outflow is reduced, the cross-sectional area being substantially greater than that of the river feeding the system (Smith, 1985). The astronomically forced tidal motions being the most obvious means of exchange between coastal lagoons and adjacent bay or ocean, we will first consider the factors influencing the water-levels within the lagoon basin. The influence of baroclinic forcing, local and non-local winds and low frequency remote forcing on the lagoon circulation will be considered subsequently.

Tidal waves propagating in coastal lagoons are reflected or dissipated by the boundaries. When the basin length is near 1/4 of the tidal wavelength (eg. Long Island Sound), near-resonance occurs such that the tidal amplitude increases while tidal current decreases from the ocean entrance toward the head. When the basin length is less than the 1/4-wavelength of tidal propagation (eg. Tampa Bay, Langebaan lagoon), water level in the lagoon fluctuates up and down simultaneously (in phase) (Sheng et al., 1996). DiLorenzo (1988)

has described the inlet modification of tidal motion in smaller basins, where the surface elevation varies uniformly in a 'Helmholtz' or 'pumping mode' response. The Helmholtz frequency, F_h, is defined by

$$F_h = \sqrt{\left(g\frac{A_c}{LA_l}\right)} \qquad \text{eq. 3-1}$$

where g is gravity, A_c is the mean cross-sectional area of the channel connecting the lagoon to the ocean, L is the channel length and A_l is the mean surface area of the lagoon. For low frequency ocean forcing (eg. less than $0.1F_h$), the rise and the fall of the lagoon surface will approximate that of the adjacent ocean closely. As the frequency of the ocean forcing approaches F_h, the morphology of the connecting channel becomes more important in determining the lagoon response. Previous studies on the tidal propagation in lagoons or estuaries showed that the tidal inlet acts as a hydraulic low-pass filter, reducing the tidal amplitude and inducing a phase-lag between the ocean and the lagoon (Mehta and Ozsoy, 1978; Pugh, 1979). The amplitude and phase of tidal constituents in the lagoon basin is dependent upon the width and the length of the inlet channel, the inlet cross-sectional area and the mean surface area of the lagoon basin (Mehta and Ozsoy, 1978; Spaulding, 1994). The effect of narrowing the entrance (which represents a decrease in F_h) between a coastal lagoon and the adjacent bay or ocean, will be to decrease the tidal range (Spaulding, 1994). For example, in choked lagoons which are characterised by a single long narrow entrance channel, tidal oscillations are often reduced to 5% or less compared to the adjacent coastal tide (Kjerfve, 1994). The extent to which the tidal component is attenuated is also dependent upon the forcing frequency, with higher frequency tidal constituents experiencing more severe attenuation (Spaulding, 1994; Wong, 1987).

The degree to which the lagoon entrance acts as a low-pass filter is very important in determining the forcing mechanisms which dominate the lagoon basin circulation, because the residual components due to the wind and the density gradient are both inversely proportional to the tidal amplitude (Prandle, 1985). When the tidal range in the lagoon is high, the propagation of the tide over a rapidly varying, shallow topography is often associated with strong nonlinearities in the current velocity field (Prandle, 1991). The non-linear interaction of the tide with the lagoon is reflected in the growth of harmonics and

compound tides of the principal astronomical constituents, with the M_4 tide usually being the largest harmonic formed when the M_2 is the largest imposed constituent (Dronkers, 1964). Nonlinearity generates residuals and higher harmonics and is responsible for features such as asymmetry between the ebb and the flood, occasional double high water occurrences and tidal pumping (in which an estuary exchanges water over a spring-neap cycle, complicating mass balance observations frequently made over a single semidiurnal period). Previous studies (Speer et al., 1991) revealed that tidal distortion, in systems such as coastal lagoons or shallow estuaries, results from two principal effects: 1) frictional interaction between the estuarine tidal current and the channel bottoms, 2) intertidal storage of water in flats and marshes. Systems dominated by the first effect have longer lags at low water than at high water and hence longer falling tide. As a result, they tend to develop stronger flood than ebb currents. In lagoons where the second effect dominates, longer lags occur at high water and as a result, the ebb currents are stronger than the flood currents. Tidally driven residual currents are usually one or two orders of magnitude less than the tidal currents themselves (typically a few $cm.s^{-1}$ compared with tidal currents of perhaps $1m.s^{-1}$) (Pugh, 1987). Tidal circulation is modified due to the effect of wind and density structure in the water.

The primary effect of the wind (despite enhancing vertical mixing) will be to set an upwind directed slope in the free surface of the lagoon. The resulting transport will be directed downwind in the surface layer of the water column, and upwind in the bottom layer or in the deeper channels of the lagoon. The slope set-up by local winds in the lagoon will be especially pronounced if the lagoon is elongated and the wind direction parallels the longitudinal axis of the lagoon. Previous study (Smith, 1994) suggested that even relative light winds of 5-10 $m.s^{-1}$ could generate slope in the free surface of the lagoon on the order of 0.5 $cm.km^{-1}$. According to Garvine (1985), the wind's influence on the sea-level variations inside a bay or lagoon, results mainly from remote atmospheric fluctuations acting over the adjacent shelf. The local wind thus has minimal consequences on the sea-level fluctuations within the lagoon, and can either contribute or act against the remote wind effect. Remote atmospheric fluctuations might produce coastal trapped wave or promote upwelling or downwelling over the adjacent shelf. The movement imposed on the

thermocline by coastal trapped waves or upwelling/downwelling events can become a source of baroclinic forcing at the lagoon entrance. The longitudinal density variations imposed between the oceanic boundary of the lagoon and the heads, which can be influenced by river input or high evaporation, might generate a buoyancy driven circulation in the lagoon basin. As demonstrated in laboratory experiments by Linden and Simpson (1986), the effect of gravitational circulation will only be significant when vertical mixing is sufficiently weak. In most lagoons, which are shallow and well mixed, the exchange along the lagoon is dependent on longitudinal dispersion (Holloway, 1996; Largier et al., 1997). In deeper and stratified lagoons, the density gradients existing between the basin waters and the intruding oceanic waters can significantly alter the tidal circulation. Transverse secondary circulation cells can be set-up, sometimes resulting in axial convergence (Nunes and Simpson, 1985). In lagoons or estuaries which are characterised by weak tidal currents and strong stratification, the circulation is primarily controlled by the density driven flows (Largier, 1992).

It is vital for the management of the ecosystem in the coastal lagoon that the circulation within the basin be known. Monitoring such systems however can not be done without a good understanding of the hydrodynamics at the lagoon entrance (Jay and Musiak, 1996), because it is in this region that nutrients, pollutants, sediments or other water-borne materials are exchanged. The following section will thus focus on the hydrodynamics of tidal inlets.

3.2 Hydrodynamic at the entrance of coastal lagoons:

In the inlets connecting coastal lagoons to the adjacent ocean or bay, tides are constrained by the surrounding geometry and strong horizontal gradients in the flow field are generated. Superimposed upon the back and forth motion of the tide through the inlets, there exists a tidal residual circulation. The Eulerian residual velocity can be defined as the velocity average, at each point over a tidal cycle. This definition has to be taken loosely, because no tidal cycle is identical to the one preceding or following it (Fisher et al., 1979). It is important, however, to know the order of magnitude of Eulerian residual currents, because

they have a large impact on the Lagrangian net transport of material and the exchange between different water bodies (Imasato, 1983). In Boston Harbour for example, it was found that the mean currents were dominated by the tide-induced residual flow over most of the harbour (Signell and Butman, 1992). Similarly, in Sarasota Bay (Florida), the spectral analysis of the long-term current data showed that 80% of the energy is associated with the tides (Sheng et al., 1996). Signell and Butman (1992) noted that the importance of Eulerian residual circulation on the Lagrangian transport changed with the scale of the residual circulation relative to the tidal excursion and the degree of tidal non-linearity. One way of assessing the importance of residual currents is to use the amplitude of higher harmonics in the current or sea-level data as a indicator of non-linearity (Speer et al., 1991).

Several of the key aspects of the tidal exchange process for bays with narrow entrances were first suggested by Stommel and Farmer (1952). During the flood water converges radially from the ocean into the lagoon channel. During the first stages of the ebb, the flow accelerates due to the set up of the pressure gradient and water converges radially from the lagoon toward the channel. As the ebb progresses, inertia causes the water to be expelled as a turbulent jet from the lagoon to the ocean (figure 3-1).

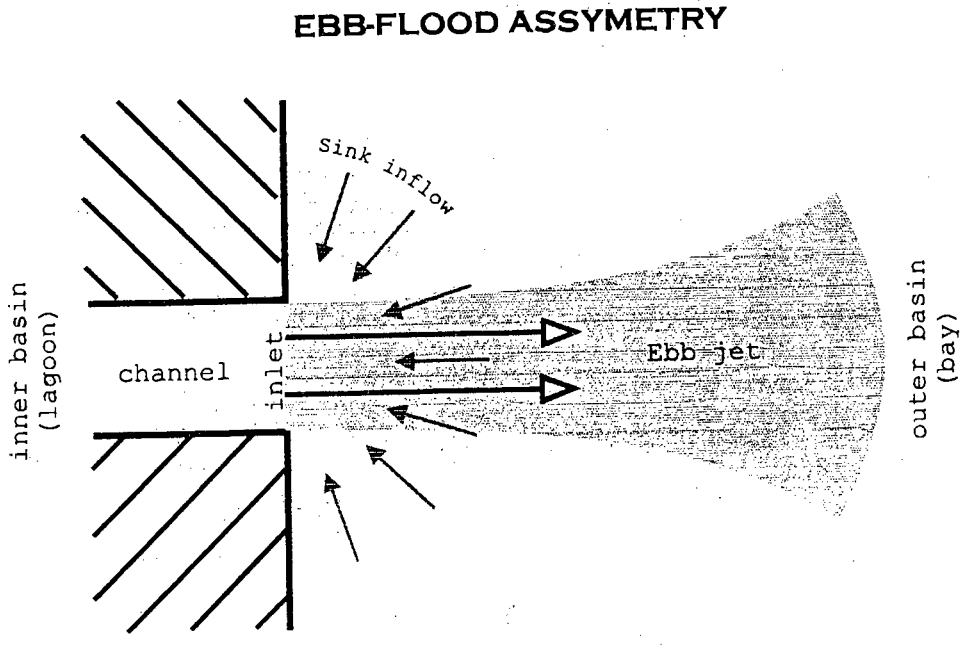

Figure 3-1: Schematic representation of the ebb and the flood flows at a tidal inlet

Averaging over a tidal cycle, the asymmetry between the ebb and the flood flows generates a residual circulation, with an inward flow (toward the lagoon) in regions surrounding the inlet and an outward flow along the inlet axis (figure 3-1). This process is often termed 'tidal pumping' (Fisher et al., 1979). Over a tidal period, the interaction of the tidal currents with the irregular bathymetry of the lagoon entrance, induces vortices and may also contribute to the tidal pump (Zimmerman, 1981). Detailed observations in San Diego Bay (Chadwick et al., 1997), have shown that the hydrodynamics at the mouth of the bay are governed by the ebb-flood asymmetry and suggest that tidal pumping can be the dominant mode of exchange for bays with large tides and narrow entrances.

The two narrow inlets connecting Langebaan Lagoon to Saldanha Bay are characterised by strong tidal currents and it is therefore likely that the lagoon effluent emerges into the bay as a turbulent jet. The water column at the lagoon mouth being generally well-mixed (Shannon and Stander, 1977), vertical circulation should be negligible in the vicinity of the lagoon mouth and it is expected that the tidal exchange will strongly depend on the ebb/flood asymmetry.

Previous studies (Ozsoy, 1977; Wilkenson, 1978) have shown that the inflow closely resembles an irrotational potential sink, provided that the bottom slope is gentle. In this case, the potential lines form semi-circular arcs with the velocities decreasing away from the mouth in proportion to x^{-1}, where x is the distance from the lagoon inlet. Since the properties of the inflow can easily be established, it is the nature of the jet that determines the effectiveness of tidal pumping.

A jet is produced when a large pressure gradient forces water through a narrow conduit, in which the fluid accelerates, to eventually emerge as a narrow axi-symmetric inertial flow (or jet), into a large body of the same or similar fluid (Tritton, 1988). At the boundary between the jet and the receiving fluid, there exists a strong discontinuity in velocity. Energy is dissipated through the jet boundary by a process called entrainment, by which the surrounding fluid is drawn into the jet due to the strong shear (Chadwick and Morfett, 1993). Associated with the entrainment of new fluid into the jet is the spreading of the

interface, a process by which new fluid drawn into the jet becomes turbulent. During the impulsive start of the jet formation, a vortex pair is shed off and then advected offshore, forming the frontal portion of the jet. Sometimes after the beginning of the ebb, a fully-developed turbulent jet is formed behind the frontal section (Joshi, 1982). Tidal jets are quasi-steady during a typical time scale much less than the tidal period, but which remains much larger than the time scale of turbulent fluctuations (Joshi, 1982). Tidal jets evolve in response to bottom friction, water depth, ambient currents and buoyancy forcing as they propagate into the neighbouring bay or ocean.

French (1960), who was the first to study tidal inlet hydrodynamics during both phases of the tide, used Tollmien's (1945) classical representation of a turbulent steady jet. In the region from the jet orifice to about six jet diameters, the shear layer is still 'eating away' at the constant velocity core of the jet flow (Fisher et al., 1979). Downstream of this core region, turbulent classical jets see their width expanding linearly and their maximum velocity decaying in proportion to $x^{-1/2}$, where x is the distance from the tidal inlet (Tritton, 1988). Later studies (Borichansky and Michailov, 1966; Taylor and Dean, 1974) revealed the exponential dependence of jet expansion and velocity decay with distance offshore. These findings however, were still oversimplistic in that important factors were neglected. Indeed, Borichansky and Michailov assumed that the axial momentum of the jet remained unchanged by bottom friction, while Taylor and Dean neglected the lateral entrainment due to turbulent mixing. More research, based on the assumption that the flow is self-similar, simultaneously account for the effect of key factors such as lateral mixing, bottom friction, variable bathymetry (Joshi, 1982) and even ambient currents (Ozsoy and Unluata, 1982). The evolution of buoyant jets over a sloping bottom was considered by Safaie (1979). Mehta and Joshi (1988) analysed the unsteady behaviour of a buoyant jet by combining a steady turbulent jet with an unsteady frontal region.

In many of these descriptions, tidal jets are separated into a zone of flow establishment (ZOFE) and a zone of established flow (ZOEF). The ZOFE is characterised by intermittent vorticity fluctuations, with eddies of all sizes influencing the shape of the interface and a centerline velocity equal to the initial velocity. In the ZOEF, the motion is self similar, that

is, at any cross section the time averaged properties of the jet can be expressed in terms of a maximum value measured at the jet centerline (Fisher et al., 1979). In the ZOEF, the jet width continues to expand and the jet centerline velocity decays (figure 3-2). Ozsoy (1977) probably conducted one of the most thorough analyses on tidal jets in a situation where buoyancy forcing was negligible. Ozsoy's analysis included the effect of bottom friction, offshore bathymetric changes, turbulent mixing and entrainment.

The motion for a self-similar, quasi-steady non-buoyant plane jet (Ozsoy and Unluata, 1982) can be expressed in terms of the depth and time-averaged Navier-Stokes (eq. 3-2) and continuity (eq. 3-3) equations.

$$\frac{\partial hu^2}{\partial x}+\frac{\partial huv}{\partial y}=-\frac{f}{8}u^2+\frac{1}{\rho}\frac{\partial}{\partial y}F_{yx} \qquad \text{eq. 3-2}$$

$$\frac{\partial hu}{\partial x}+\frac{\partial hv}{\partial y}=0 \qquad \text{eq. 3-3}$$

where: u and v are the depth and time averaged velocities

h is the water depth

F_{yx} is the depth-averaged turbulent shear stress acting laterally on the jet

f is the friction factor on the sea-floor

The properties of a self similar plane jet are often expressed in terms of normalised co-ordinates :

$$\xi=\frac{x}{b_0}\ ,\ \mu=\frac{fb_0}{8h_0}\ ,\ H(\xi)=\frac{h}{h_0}\ ,\ \xi_s=\frac{r}{b_0}\ ,\ B(\xi)=\frac{b}{b_0}\ ,\ U(\xi)=\frac{u_c}{u_0}\ ,$$

where b_0 , h_0 , and u_0 are respectively the half width, depth and depth-averaged velocity at the inlet, u_c is the centerline velocity of the jet, r is the length of the core region and μ is a non-dimensional number accounting for the effect of both friction and bottom slope. Ozsoy (1977) adopted the similarity profile $\frac{u}{u_c}=F(\zeta)$ defined by Ambramovich (1963) with respect to the normalised co-ordinate $\zeta=\frac{|y|}{b(x)}$ where

$$F(\zeta)=\begin{cases}0 & ;\ 1<\bar{\zeta}\\ \left(1-\overline{\zeta^{1.5}}\right)^2 & ;\ 0<\bar{\zeta}<1\\ 1 & ;\ \overline{\zeta<0}\end{cases} \qquad \bar{\zeta}=\frac{\zeta-r/b}{1-r/b} \qquad \text{eq. 3-4}$$

Ozsoy (1977) then obtained two ordinary differential equations (eq. 3-5 and 3-6) from which the jet properties could be determined.

$$\frac{d}{d\xi}\left(\overline{I_2}HBU^2\right)=-\overline{I_2}BU^2 \qquad \text{eq. 3-5}$$

$$\frac{d}{d\xi}\left(\overline{I_1}HBU\right)=\alpha HU \qquad \text{eq. 3-6}$$

I_1 and I_2 are both constants of integration. At the jet boundary, the velocity u and the shear force F_{yx} vanish, but there remains a lateral entrainment velocity $v_e=\alpha\times u_c$, where α is the entrainment factor and u_c is the centerline velocity (figure 3-2).

Experimental and theoretical studies (Savage and Sobey, 1975; Gadgil,1971) demonstrated that the momentum loss induced by bottom friction resulted in a more rapid expansion of the jet. Similarly, a decrease in bottom depth induces fast spreading rates of tidal jets. When the water column depth increases, the jet contracts due to mass conservation, with a centerline velocity remaining constant. Ozsoy and Unluata (1982) revealed that even very slight modifications of the sea-bed depth could significantly alter the properties of the jet. In his model, Ozsoy combined the effects of friction, bathymetry changes and entrainment on the jet hydrodynamics. He found that changing the relative order of magnitude of those 3 parameters, dramatically affected the behaviour of the jet. Contraction of the jet as a result of increasing depth, could counteract the effect of bottom friction. Ozsoy and Unluata (1982) also found that when the increase in depth balanced the effect of bottom friction, the tidal jet expanded linearly, only differing from the classical jet by a faster velocity decay. When flowing into cross currents, tidal jets are deflected sideways and their expansion is reduced.

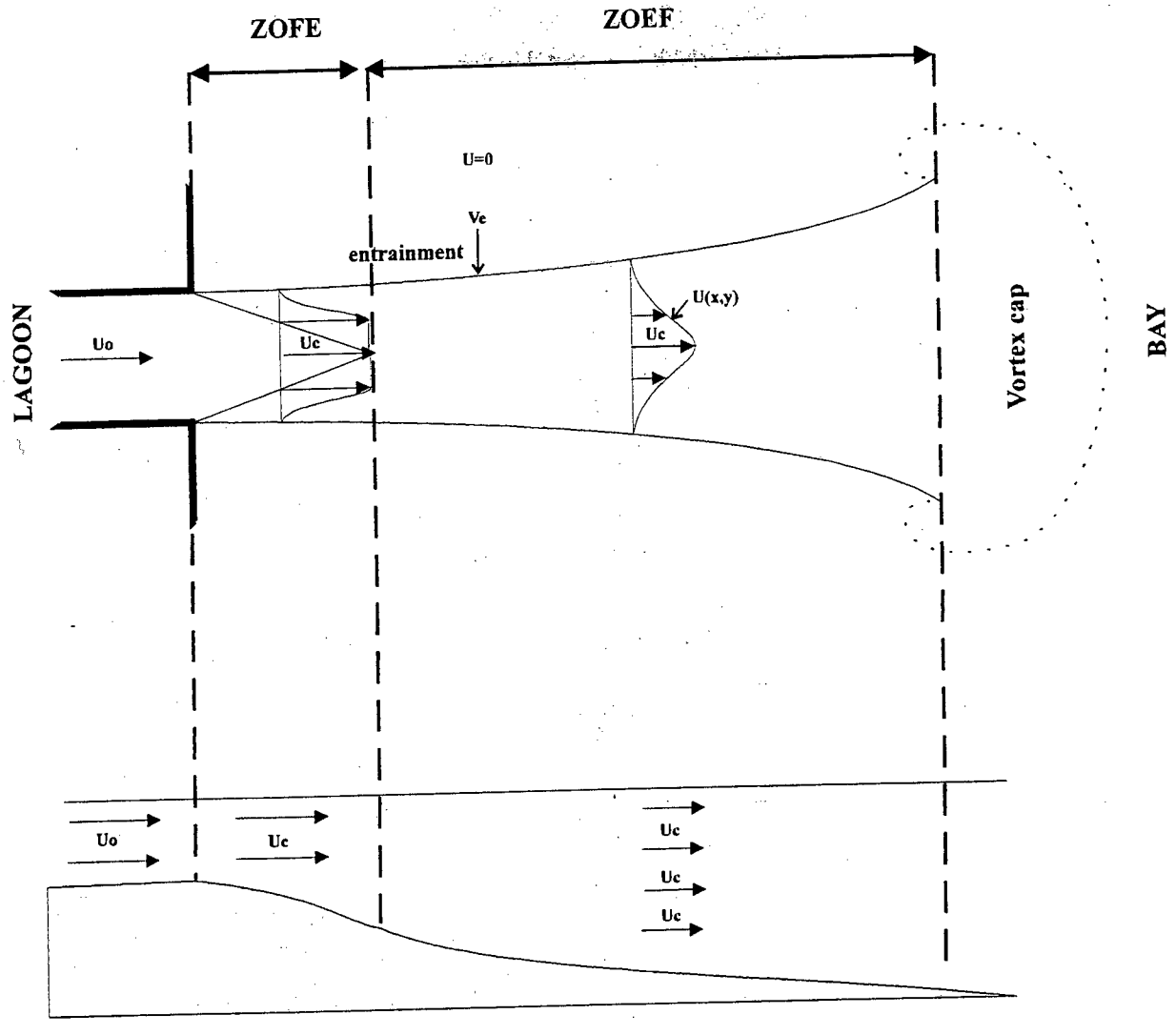

Figure 3-2: Schematic representation of the horizontal and vertical structure of the flow in a bottom frictional jet. adapted from Ozsoy (1982).

Assuming that the jet fluid is lower in density than the receiving fluid, a buoyant force exists, which may cause the jet to lift off from the bottom. Similarly to water entrained at the lateral boundaries of the jet, vertical entrainment is generated between the bottom boundary of the jet and the surrounding fluid (Hearn et al., 1990). Vertical entrainment however, differs from lateral entrainment in that it is damped out by the stratification. As buoyant jets lift off, their half-width increase due to the shallower depth of the lifted interface (Chadwick et al., 1997). Several criteria have been suggested to predict the point at which the jet lifts off (Hauenstein, 1983; Safaie, 1979; Hearn et al., 1990).

Dimensional analysis showed that buoyant jets can be characterised by two dimensionless

numbers for sufficiently high Reynold numbers, namely the source densimetric Froude number F_0, and the discharge aspect ratio A_s (Safaie, 1979. Chadwick et al., 1997). Those two numbers can be expressed as:

$$F_0(h) = \frac{u_0}{\sqrt{g' h_0}} \qquad \text{eq. 3-7}$$

$$A_s = \frac{h_0}{2b_0} \qquad \text{eq. 3-8}$$

where g' is reduced gravity associated with the density difference between the basins.

$$g' = g\frac{\Delta\rho}{\rho} \qquad \text{eq. 3-9}$$

The jet lifts off from the bottom when the buoyancy force becomes comparable in magnitude with the inertia force, that is, when F_0 approaches one (Tritton, 1988). Experiments conducted by Safaie (1979) on turbulent buoyant jets over a sloping bottom revealed the strong dependency of the flow pattern on the source densimetric Froude number. Safaie concluded that the characteristics of the jet were determined by the buoyancy spread, the spread due to the formation of large-scale vortices and the spread due to turbulent mixing. Provided that the buoyancy effects do not greatly influence the rate of lateral spread (Wolanski, 1986), a vortex pair, similar to that sketched in figure 3-2, is shed at the start of the buoyant jet formation and moved offshore, forming the frontal portion of the jet. Observations of river plumes (Luketina and Imberger, 1987) and surface buoyant jets (Mehta and Joshi, 1988) have shown that most of the vertical mixing occurred near the front of the jet. Luketina and Imberger (1987) found that the buoyant jet at the entrance of Koombana Bay (Australia) had a frontal section characterised by a strong roller. The roller had a well defined rotating core. Water at the surface moved toward the leading front, where it plunged to a depth equal to twice the thickness of the jet and entrained the underlying ambient water, forming a mixing layer in the lee of the roller, immediately underneath the overflowing water. In previous analyses, buoyant jets have been approximated as a composite of a steady turbulent jet with an unsteady frontal region (Middleton, 1975). It is important to be able to predict how and when tidal jets separate from the sea bed because in the vicinity of tidal inlets, the circulation and the mixing induced by buoyant jets differs from that induced by a bottomed attached jet. Chadwick et al. (1997) found that the structure of the tidal-residual flow and the residual transport at the mouth of

San Diego Bay, were strongly influenced by the vertical exchange resulting from the jet lift off.

Several studies have underlined the complexity of modelling the mixing and exchange of waters between tidal inlets. Awaji et al. (1980), used a Lagrangian approach to further examine the processes affecting tidal exchange in the vicinity of tidal inlets. In his study, Awaji revealed that the large Stokes drift of water particles associated with rapid changes in the phase and magnitude of the principal tidal constituents, contributed substantially to the tidal exchange. The steep spatial variations in the tidal constituent properties are associated with strong horizontal velocity shear and result in the water particle having a 'broken' ellipse path - the difference in the starting and ending positions of water particles being some measure of tidal dispersion. In his model, Awaji found that the tidal residual circulation also played an important role, although secondary, in the water exchange. In a later model, Awaji (1982) added turbulence. The presence of turbulence resulted in an increase of the areal extent to which water particles were exchanged. Other 2-dimensional modelling studies (Signell and Butman, 1992; Ridderinkhof and Zimmerman, 1990) showed that velocity variations occurring on a length scale of the tidal excursion length, were most relevant to the tidal dispersion process. Kapolnai et al. (1996) added 3-dimensionality and stratification to the previous analysis and found that the residual flow near the inlet was significantly altered by stratification. Kapolnai's study also revealed that the presence of the plume served to increase the offshore extent of the flood withdrawal area.

The exchange of water between a basin and the neighbouring ocean or bay is generally expressed in terms of the tidal exchange ratio (TER) with

$$TER = \frac{V_0}{V_f} \qquad \text{eq. 3-10}$$

where V_0 is the volume of new bay water entering the lagoon during the flood tide and V_f is the total water volume entering the lagoon on the flood tide. If one assumes that no freshwater is input into the lagoon basin, then V_f is equal to the tidal prism (P), or intertidal, volume. Assuming that the surface area of the lagoon does not vary significantly over a tidal cycle, the tidal prism becomes

$$P = A_l \times 2\eta_0 \qquad \text{eq. 3-11}$$

where A_l is the surface area of the lagoon and η_0 is the tidal amplitude.

We may note that if the volume of water drawn into the lagoon during the flood, V_{inflow}, equals that expelled from the lagoon during the ebb, $V_{outflow}$, we have

$$V_{outflow} = V_{inflow} = P \qquad \text{eq. 3-12}$$

The difficulty lies in determining a value for V_0 Fisher et al. (1979) showed that if the total salt and water contents of the lagoon are to remain constant, the TER could be determined through a knowledge of the average salinity of the ebb and flood flows. The TER then becomes

$$TER = \frac{S_f - S_e}{S_o - S_e} \qquad \text{eq. 3-13}$$

where S_f is the average salinity of the water entering the lagoon on the flood tide, S_e is the average salinity of water leaving the lagoon on the ebb tide and S_o, is the salinity in the neighbouring bay or ocean. In more recent work, Chadwick et al. (1997) derived an empirical equation for the tidal exchange ratio, for systems where tidal pumping dominated the exchange. Chadwick et al. assumed that the exchange was controlled by the overlap between the ebb jet and the flood sink and found that the TER could be expressed as

$$TER = 1 - \frac{L_{sink}}{L_{jet}} \qquad \text{eq. 3-14}$$

Where L_{sink} is the radius of the flood withdrawal zone and L_{jet} is the offshore lengthscale of the ebb jet. During the flood, water is drawn uniformly from the offshore region according to an irrotational potential sink. Consequently, the offshore lengthscale of the flood withdrawal zone may be estimated based on a knowledge of the tidal prism (Chadwick et al., 1997) as

$$L_{sink} = \sqrt{\frac{P}{phw}} \qquad \text{eq. 3-15}$$

where h is the mean water depth of the withdrawal zone and w is the fraction of a complete circular sink occupied by the withdrawal zone. If one considers, as in Stommel and Farmer (1952) that the ebb jet width can be approximated by the inlet width, then a lengthscale for the ebb jet would be

$$L_{jet} = \frac{P}{h \times b} \qquad \text{eq. 3-16}$$

where h is the mean depth below the ebb jet and b is the inlet width.

Another parameter which can be useful to assess the influence of a coastal lagoon on adjacent water bodies is the tidal excursion, as tidal excursion and tidal dispersion typically occurs on the same scale (Zimmerman, 1986). The tidal excursion represents how far a water parcel is advected away from the inlet in a tidal period and can be obtained theoretically or through measurements.

In this section, we have underlined the importance of the ebb/flood asymmetry and the associated tidal pumping mechanism in driving the tidal exchange. The exchange of water at the vicinity of tidal inlets is seen to result principally from the strong horizontal shear in the velocity field, although the tidally induced residual circulation still contributes significantly to the exchange. Understanding the hydrodynamics of tidal inlets gives us valuable insight into the nature of the flow but one should bear in mind that real flows are usually more complex in shape. Rapidly varying bottom topography at tidal inlets generates local vorticity and non-linearity within the flow, making it difficult for scientists to accurately model the circulation. In addition, the tidal hydrodynamics and the exchange at tidal inlets, while being affected by the circulation in the lagoon interior, might also be influenced by external parameters, such as the wind or the input of different water types into the system. This results in a very complex system and often, measurements in these environments are under-resolved in space and time (Signell and Butman, 1992). For a reasonable estimation of the tidal exchange it is therefore best to couple high-resolution measurements with a strong understanding of the inlet hydrodynamics.

4. Method

4.1 Measurements:

The aim of the fieldwork was to define the parameters affecting water circulation, to describe and explain water movements in the vicinity of the lagoon-bay interface and to further our understanding of the hydrodynamic properties in the lagoon basin. The greater insights gained on the nature of the flow between Langebaan Lagoon and Saldanha Bay and within the lagoon proper, would subsequently enable us to determine the exchange of water occurring between the bay and the lagoon. Direct observations of water type, current velocity, water-levels and wind speed were obtained for this purpose.

The position of the instruments and sampling stations were obtained with a Magellan 4000 differential global positioning system (GPS). Unfortunately, due to some technical problem with the GPS, we were unable to use the differential capacity of the instrument. As a result, the GPS was subject to random errors due to 'selective availability' and positions may be displaced by as much as 100m. Visual sightings were used in order to obtain more precise and reliable positions. The positions of the instruments is represented in figure 4-1 and the schedule of instrument deployment appears in figure 4-2.

4.1.1 Currents:

Current measurements were obtained with a 1200 KHz Workhorse Acoustic Doppler Current Profiler (ADCP) from RD Instruments and two drifters made available by the Sea Fisheries Research Institute (SFRI). In addition to the Eulerian current velocity acquired from the Workhorse ADCP in each of the inlet channel, two cross-section views of the inflow were obtained on the 6th of March 1997 with a boat-mounted ADCP which belonged to the Council for Scientific and Industrial Research (CSIR). The position of the ADCP cross-section views appears in figure 4-3.

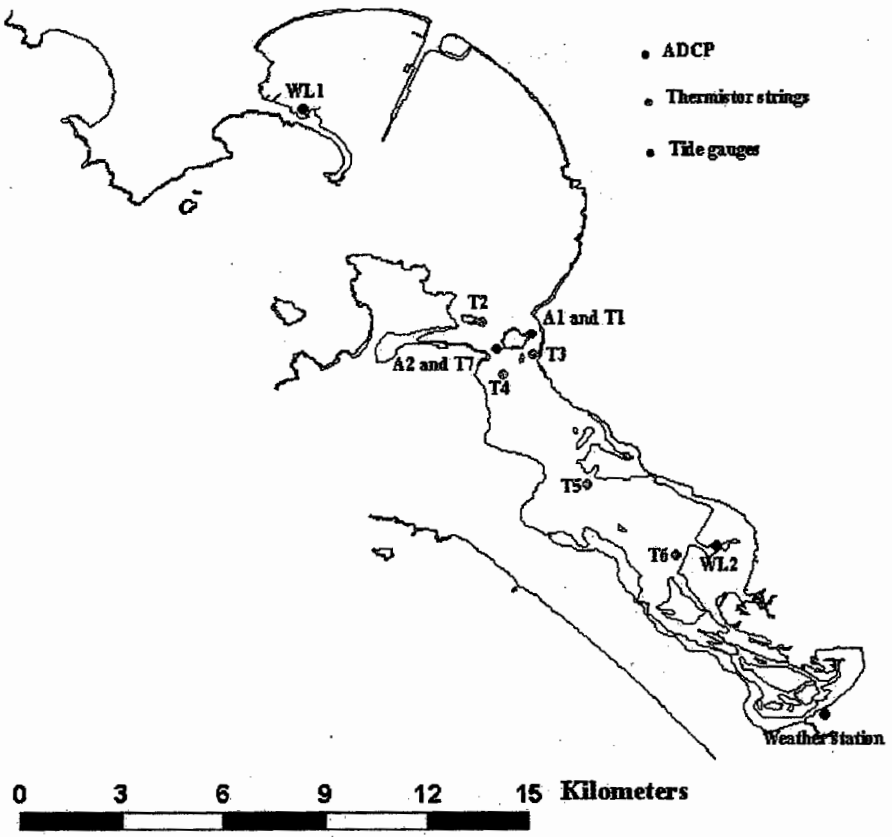

Figure 4-1: Position of the instruments during the survey. The different strings of thermistors deployed during the experiment are labelled T1 to T7. The moored ADCP is labelled A1 to A2, while the tide gauges are labelled WL1 for the Saldanha Bay tide gauge and WL2 for the lagoon tide gauge.

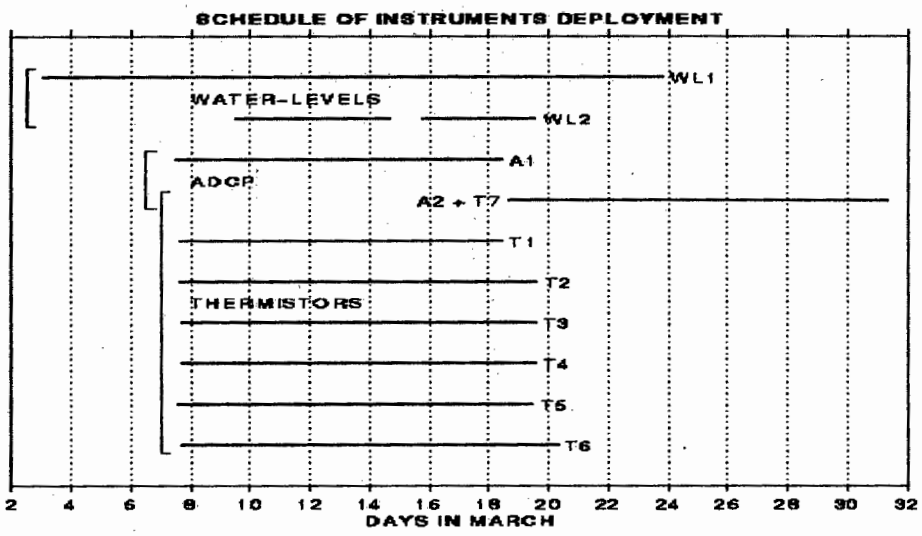

Figure 4-2: Schedule of instrument deployments.

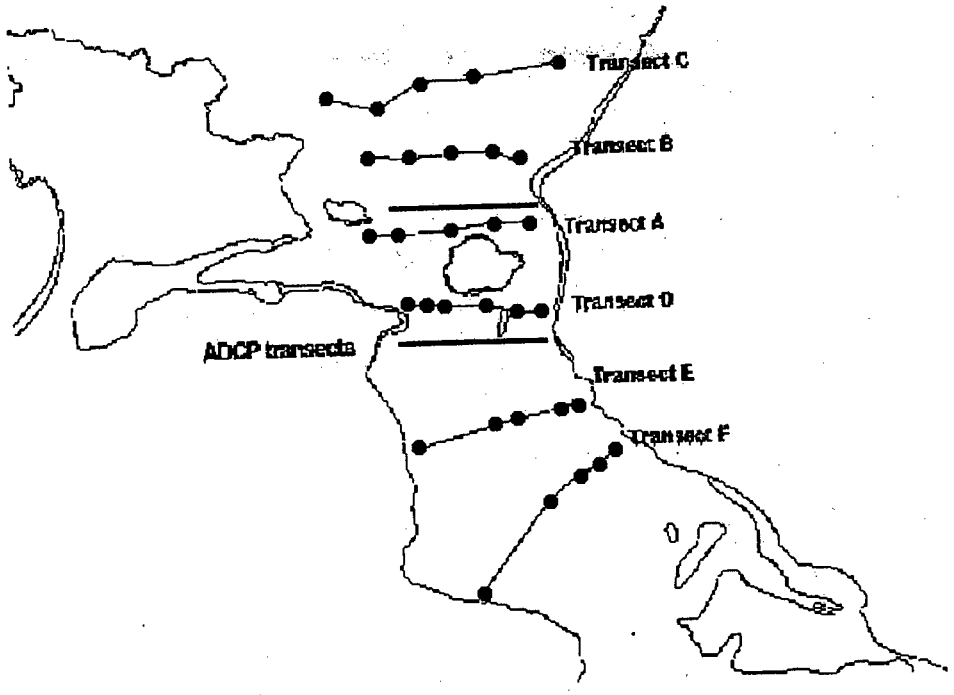

Figure 4-3: Location of the CTD and ADCP transects. The thick lines represent the ADCP transect. CTD transects are labelled A to F and individual profile positions are shown as dots.

The ADCP works by emitting sound pulses through the four beams located on its transducer head. The Doppler shift (apparent increase or decrease in the frequency of sound), between the sound pulse that is emitted and that which is returned to the instrument can be correlated to the current, thus providing a measure of the flow strength and direction. Data is recorded over the whole water column except in the immediate vicinity of the instrument, where emitted and reflected sound can not be differentiated accurately.

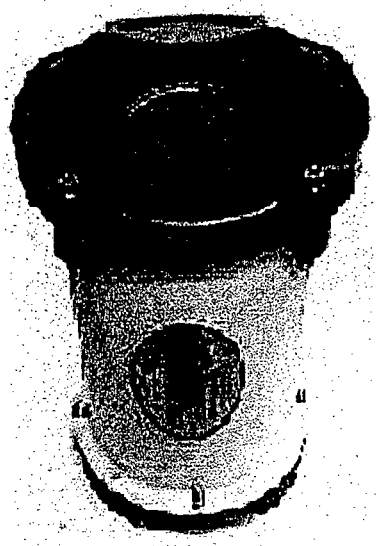

Figure 4-4: Workhorse ADCP

The instrument set up remained the same throughout the whole length of the experiment. The ADCP was moored on the lagoon bed and sampled at bin intervals of 50 cm, at a frequency of 1200 kHz with 45 pings per ensemble. Data was blanked after transmission within the first

1.76m, meaning that the distance to the first bin was located 2.32m from the ADCP transducer head. Some data is also lost at the air-sea interface due to the strong reflection of the sound pulses. The sampling interval was 4min, in order to represent short term fluctuations as well as oceanographic events with longer periods. The data output consisted of the horizontal velocities and directions of the currents. The velocity error was also obtained to give us an estimation of our measurement accuracy. The velocity error is a measure of data 'reasonableness' determined from the three orthogonal velocity components. The position and the time of deployment of the ADCP are represented in figure 4-1 and 4-2. The duration of the deployments allowed us to get the current velocity for both neap and spring tidal cycles, in each of the inlet channels. For both deployments, the position of the ADCP was chosen to correspond to the point of maximum depth in that channel: 16.5m and 8.5m in the east and west inlets respectively. This location was chosen as maximum flow is expected to occur in the deepest section of the channel, and also because mooring the ADCP in greater depths mitigates the loss of near-bottom data as a result of blanking.

Lagrangian surface currents were measured with drifters (sketched in figure 4-5). Drifter deployments provide information on current velocities and flow pathways. Also, when left to drift throughout the ebb or the flood, drifters can give some indication on the length of the tidal excursion. The main objective behind the deployment of the drifters was to determine how water particles at the Langebaan Lagoon-Saldanha Bay interface were advected in and out of the lagoon system. For all deployments, one drifter was dropped in each of the inlet's channel, with the aim of comparing the east and the west channel surface current velocities. The drifters were used in two ways during the fieldwork. Firstly, on the 13th and 14th of March, drifters were released at the beginning of the ebb tide and were left to drift throughout the outflow. The long drifts provide an estimate of the length of the ebb tide excursion. Similar information was gained on the flood tide excursion, on the 11th and the 20th of March. Secondly, on the 15th, 16th and 17th of March, drifters were used in conjunction with CTD transects undertaken on the ebb. These repeated short duration deployments provide information on the characteristics and the position of one parcel of water leaving the lagoon at a particular time, and how this changed

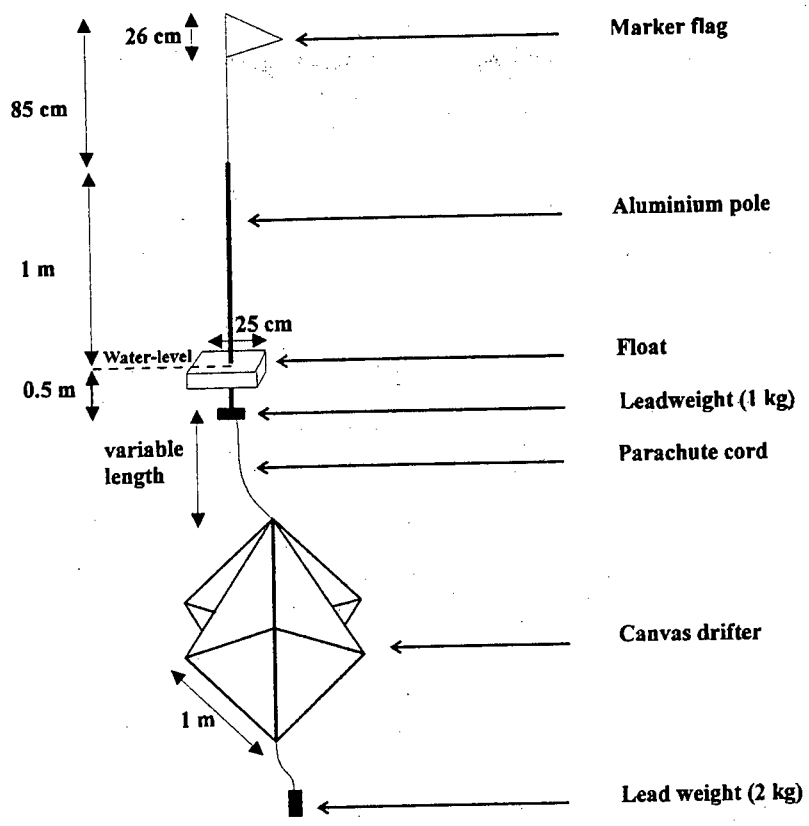

Figure 4-5: Schematic diagram of a typical assembled drifter for use in current tracking.

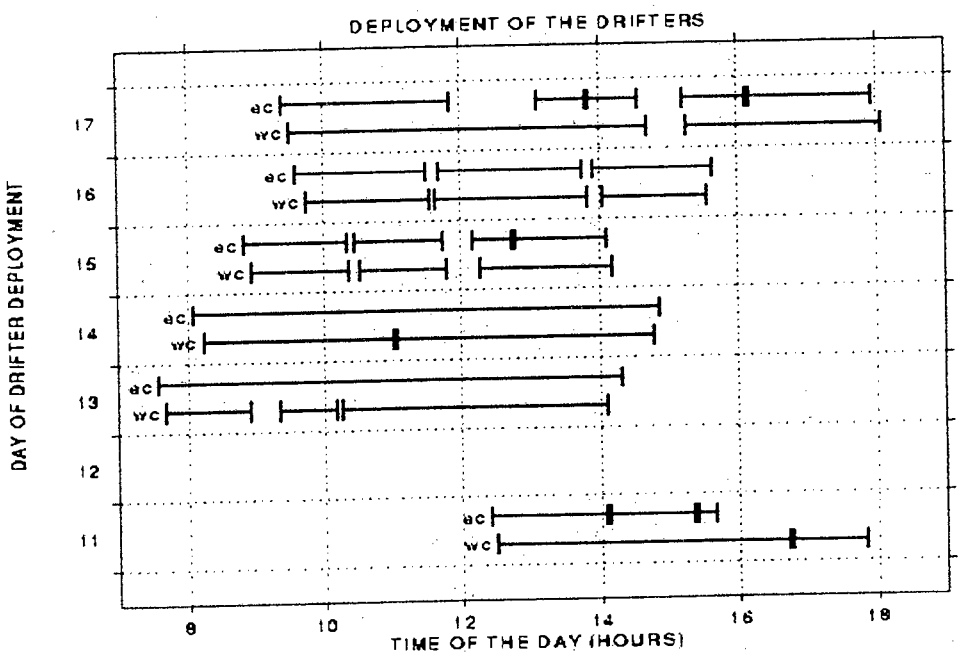

Figure 4-6: Schedule of drifter deployments. The black horizontal lines on this plot represent the time at which the drifters were in the water. The short vertical lines appear every time the drifter is put in, or taken out of the water column. ec stands for deployments in the east channel, while wc stands for deployments in the west channel.

over the tidal cycle. The properties of each of the drifters deployment is summarised in the figure 4-6. In strong wind conditions, the above-water parts of the drifter are subject to wind drag, which causes the drifter to slip through the water, introducing error in the estimation of the true water current velocity. This error is small, but over time it may result in the drifter not always following the same parcel of water. Errors in the velocity measurement will also result from the grounding of the drifters in shallow regions. Frequent monitoring of the drifters limited that type of error and grounding events were clearly logged.

4.1.2 Waterlevels:

Water levels in Saldanha Bay were measured every minute and were obtained from a Sonar Research and Development tide monitor (SRD) which belongs to the hydrographic department of the South-African Navy (figure 4-7). In the lagoon, water-levels were obtained by measuring the pressure fluctuation in the water column with an Ocean Sensor CTD (OS200).

The SRD tide Monitor obtains the distance from the transducer to the sea surface by measuring the time elapsed between transmission and reception of an acoustic pulse. This time is converted to distance using a calibration velocity obtained from the fixed range target measurement. This distance is subtracted from the TIDE LEVEL which is then averaged over the selected period, displayed on the four digit display, printed on the graph, and transmitted by whatever telemetry method is selected.

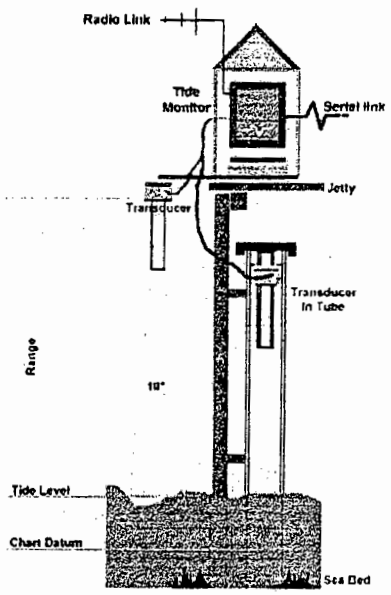

Figure 4-7: Schematic representation of the SRD Tide Monitor.

The SRD tide monitor measures distances to within 0.05% of a 75cm range thus giving an accuracy of 0.375mm.

In the lagoon, the OS200 provided us with pressure measurements (in decibars) every 4 minutes, with an accuracy 0.5% of sampled range.

4.1.3 Temperature, salinity and density:

Temperature, salinity and density measurements were obtained with temperature recorders and a Seacat CTD profiler (SBE 19) from Seabird Electronics. The Seacat CTD measures the temperature to an accuracy of 0.01°C. The conductivity accuracy is 0.001S/m, while the accuracy for the pressure is equal to 0.15% of the full sampled range.

Sixteen temperature recorders (thermistors) were deployed at selected locations (figure 4-1). Thermistors were put in both channels in order to monitor the temperature of water entering or leaving the lagoon. In the east channel, 7 thermistors were deployed over the whole water column and at the location of the ADCP to explore the nature of stratified flow. The rest of the thermistors were spread out in the lagoon and reflected the temperature characteristics of the whole system. From the 19th to the 31st of March, another string of 4 thermistors (T7) was deployed in the western channel with the ADCP. The thermistors collected data at 10min intervals and recorded the water temperature with an accuracy of 0.1°C.

CTD surveys were conducted to gain some understanding of the temperature, salinity and hence density throughout the lagoon and within the southern section of Big Bay. During the spring and the neap tide cycles, longitudinal CTD surveys were completed in the lagoon. Two of these longitudinal CTD surveys were undertaken on the same day: one at high tide and the other at low tide. The CTD stations on the 8th (spring tide) and the 17th of March (neap tide) are plotted in figure 4-8. In addition, a fine scale grid survey was undertaken in the vicinity of the lagoon mouth for the inflow and the outflow. These data were collected to specify the type of water flowing in or out of the lagoon and to see the small scale structure of the inflow or outflow. The positions of the CTD transects across the lagoon mouth are given in figure 4-3. Table 1 summarises the time at which CTD transects were started.

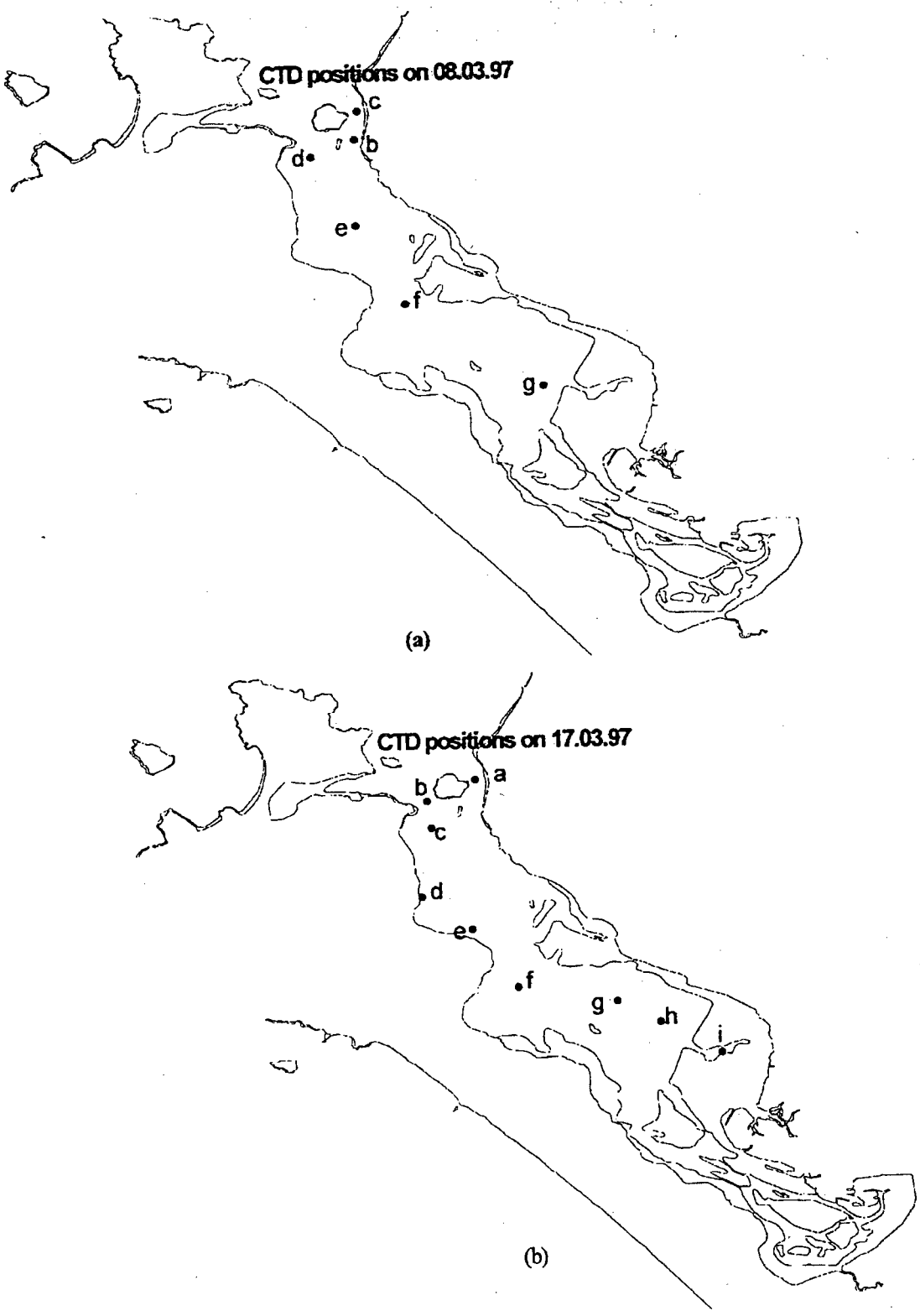

Figure 4-8: Longitudinal CTD profiles undertaken into the lagoon during the spring tide (a) and the neap tide (b).

Date	Transect A	Transect B	Transect C
9.03.97	7:37am 8:35am 9.35am 13.42pm	8:00am 8:50am 14:40am	8:15am 9:15am 10:02am
15.03.97	9:20am 10:50am 12:30pm 15:50pm	10:00am 11:25am 13:10pm	
16.03.97	10:00am 12:00pm 14:10pm	10:30am 12:40pm 14:40pm	11:10am 13:30pm 15:15pm
17.03.97	13:30pm 15:30pm 17:02pm	14:07pm 15:55pm 17:42pm	16:30pm
	Transect D	**Transect E**	**Transect F**
	10:00am	10:40am	11:25am

Table 1: Schedule of CTD deployment.. This table summarises the time at which CTD transects were started. Each transect taking approximately 15min to complete.

4.1.4 Meteorological data:

Hourly values of atmospheric data were obtained for the month of March, from the South-African Weather Bureau weather station located in Geelbek (figure 2-1). The parameters measured were air temperature, wind speed and direction, percentage of humidity in the air and air pressure. The atmospheric data are used for the correction of the sea-level data and a better understanding of the impact of the wind on the lagoon. A time-series plot of the wind in February and March at the Cape Colombine weather station (figure 2-1) was obtained from Van Ballegooyen (CSIR).

4.2 Method for the correction and analysis of the data

4.2.1 Corrections applied to the data:

Waterlevels:

During the fieldwork, pressure values obtained from the Saldanha and the Langebaan lagoon tide gauges were constantly affected by atmospheric pressure fluctuations. In our analysis, it was therefore necessary to remove the assumed static effect of the atmospheric pressure from the raw sea-level data to obtain the true level of the water. Hourly atmospheric pressure values were available from the Geelbek weather station. In order to apply the correction to sea-level data with 1 or 4min intervals, the atmospheric pressure was interpolated linearly from one hour to the next. For atmospheric pressure of 1013 hPa, zero correction is applied. The inverse barometer adjustment was implemented according to the *Unesco (1983) algorithms for computation of fundamental properties of seawater*.

ADCP current data:

On plotting the raw data, it was obvious that erroneous 'spikes' were found in the velocity records. Those were removed simply by assuming that any current with a magnitude greater than $1.5 m.s^{-1}$ was an outlier and should be removed from the time-series, as the maximum tidal currents flowed at approximately $1 m.s^{-1}$. The second step in processing the current velocity data was to calculate the acceleration between two successive sampling intervals. When the middle point acceleration exceeded three times the standard deviation, we would consider that value to be unreliable and subsequently remove it from the record. Eventually, gaps in the data were filled using a linear interpolation method, the longest gaps not exceeding 12 minutes. In order to remove the remaining outliers and to 'clean' the data further, we decimated the data to 16min intervals, using a 30-point lowpass filter from the MATLAB toolbox. However this provided little benefit, hence the original sampling interval of 4 min was retained. The noisiest current measurements occurred near the surface (farthest away from the ADCP) and during the period of strongest flow. This probably resulted from side lobe interference, or from the ADCP sound pulses occasionally propagating out of the water due to the low-water level occurring at

low tide. At mid-depth or closer to the instrument (located on the sea-bed), data noise was significantly reduced. After correction of the data, the currents were rotated along the principal axis component of the tidal ellipse.

CTD temperature, salinity and density data:

In region of strong temperature gradient, 'spiking' occurred in the CTD records due to a mismatch of the temperature and conductivity sensors. To remove the salinity, density and temperature spikes a running mean filter was applied to the data records.

A variety of data analysis techniques are used in this thesis. This section provides a background for the methods of data analysis. Time-series analysis is a large and broad subject and one can refer to one of many books for a complete overview of the subject (eg. Bendat and Piersol, 1971; Otnes, 1978).

4.2.2 Spectral analysis:

Data analysis consists of separating oceanographic signals from noise. The definition of noise varies accordingly to the type of physical parameter that we aim to analyse. For example, if we decide to look at oceanographic signals within a specific frequency band, data outside of that frequency range becomes noise. When manipulating the data, we use a property often attributed to random or pseudo-random data, called ergodicity. The ergodicity theorem states that for the right kind of process (one that is stationary, among other more general requirements), we are able to determine statistical properties with time averages.

The spectral structure of the data can be obtained through the use of Power Spectral Density functions (PSD). The goal behind the use of PSD, is to detect specific frequency signals buried in wide-band noise and to determine the energy associated with certain frequency ranges. PSD can be defined via correlation functions, finite Fourier transform, or filtering-squaring-averaging operations (Bendat and Piersol, 1971). In this study, PSDs were obtained with the MATLAB toolbox, according to the Welch 's average periodogram method. Welch's method consists in finding the Fourier transform of samples of the process and taking the magnitude squared of the

result. The PSD estimate consequently obtained is called the periodogram. The accuracy of the periodogram estimate depends on the property of the window used. For a record of length N and sampling intervals Δt, a window of length m will imply that the PSD is estimated at frequencies $\frac{1}{2m\Delta t}$, $\frac{2}{2m\Delta t}$, ..., $\frac{1}{2\Delta t}$. The Nyquist frequency, $\frac{1}{2\Delta t}$, determines the maximum frequency resolved for the data record. As m gets larger, the window narrows and the bias decreases, but the variance of the resulting estimator increases. This concept is illustrated by figure 4-9.

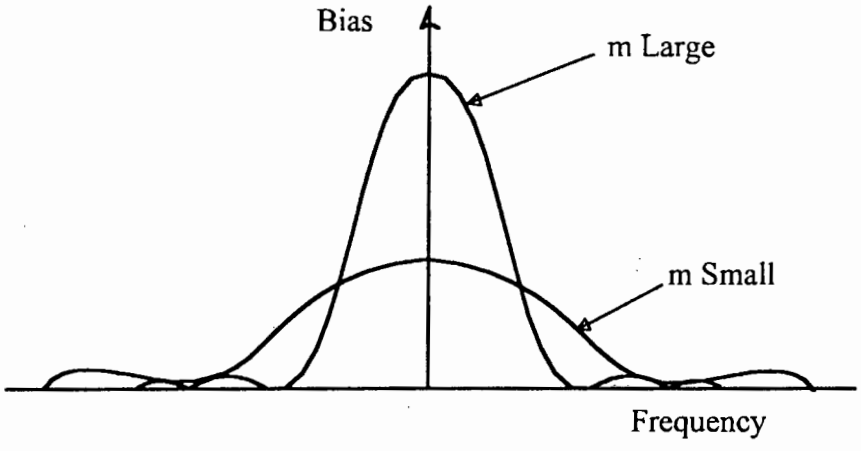

Figure 4-9: Spectral window for different values of m as from Bendat and Piersol (1971).

Errors can also result from discontinuities arising at the beginning and end of the records to be analysed. Those type of errors are minimised by using windows with tapers and faders. Eventually, the PSD estimate variance can be reduced even further by overlapping sections of the record. For a suitable window, overlap rates of about half the section length were found to significantly lower the variance of the estimate. A Hanning window was used for all our analysis. Due to short time period of the record, the window length, m, had to be approximately equal to the record length. Indeed, smaller values of m resulted in a very poor resolution in the frequency range. The PSD plots obtained during our analysis were therefore mainly used to reveal the range of frequencies affecting our oceanographic signals, only providing a rough estimate of the energy associated with a particular frequency. The PSD estimates were scaled

according to the window property and plotted as a function of frequency. Both the x and y scales are logarithmic, with frequency units in cycles per minute.

4.2.3 Filtering:

Once the dominant signals are identified in the spectrum, it is of interest to remove one or several of those constituents from our records. For example, the Langebaan lagoon system is influenced by tidal forces to such an extent, that it often becomes difficult to distinguish variations in the data induced by oceanographic phenomenon with lower frequencies. The impact of synoptic events with period 2 to 5 days on the lagoon becomes more obvious once the main tidal constituents are taken out of our signal. The removal of the tidal signal from the data is achieved by applying a lowpass filter to the time-series. If the cut-off frequency is ω_0, an ideal digital lowpass filter will have magnitude (or gain) 0 at all frequencies higher than ω_0, and magnitude 1 at all frequencies lower than ω_0. The filtering, or frequency response function is

$$H(\omega) = G(\omega)e^{i\phi(\omega)} \qquad \text{eq. 4-1}$$

where $G(\omega)$ and $\phi(\omega)$ are the respective gain and phase of the filter. By using a Fourier transform, we can express the input data in the form of the sum of a series of sinusoidal functions. The Fourier transform applied over a split moving window, will hence allow us to damp or retain certain frequencies in the input data using $H(\omega)$. If $y(t)$ is the output function with *t* being the time variable, we then have:

$$y(t) = IFT(H(\omega).X(\omega)) \qquad \text{eq. 4-2}$$

where IFT denotes the inverse Fourier transform operation, ω is the frequency and $X(\omega)$ is the Fourier transform for the input function $x(t)$. The inverse Fourier transform of $H(\omega)$ is the impulse response function, also called the weighting function $h(t)$. The function $h(t)$ assigns weights to the input points of each window, which act to damp data points with frequencies above ω_0.

The short length of the data constrains us to have as narrow a bandwidth as possible to avoid excessive data loss. It is also a necessary requirement for the filter to have a sharp amplitude cut-off near the half-power point. The quarter-power filter cut-off was set up to 36hr, thus removing semi-diurnal and diurnal constituents from the input data. Different filters were used according to the type of data considered (figure 4-10).

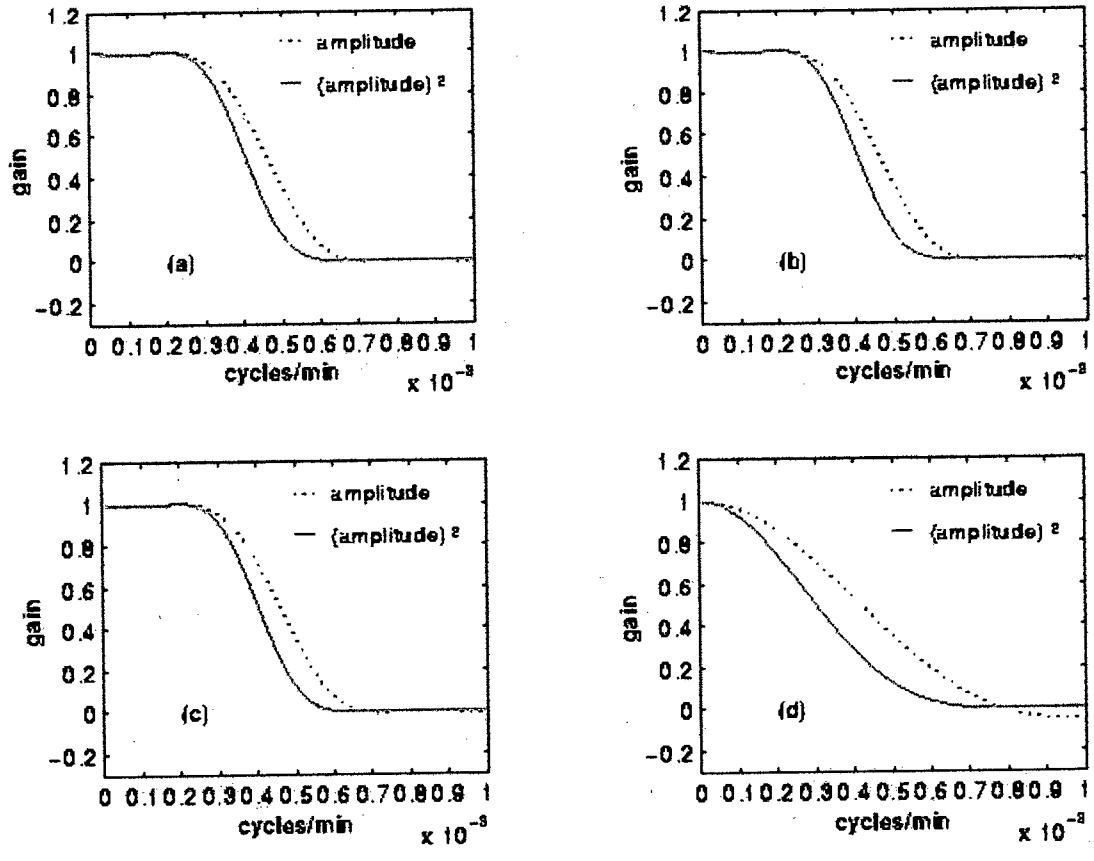

Figure 4-10: Plots of the lowpass filters amplitude and gain for the water-level, current, and temperature data. The filter was the WHOI (PL33/64) as used in CODE (1985). All the data was lowpassed with a quarter power filter cut-off of 36 hours, except for the water-level in the lagoon which was lowpassed with a 30hr quarter power filter cut-off. (a) shows the filter response for the water-level record collected in the Langebaan lagoon. (b) shows the filter response for the water-level record collected in Saldanha Bay. (c) shows the typical filter response for current velocity records collected at the lagoon mouth. (d) shows the typical filter response for temperature records collected with the thermistors.

The computation of the low-passed time-series was realised with a MATLAB program written by R. C. Van Ballegooyen. For sampling intervals of 4min, that is for the current data and the lagoon water level data, the PL64 filter (as used in CODE, 1985) was much more suitable than the cosine-Lanczos filter and gave improved lowpassed data outputs. Although Van Ballegooyen (1995) showed that the PL64 filter was not efficient in removing the diurnal components O1 and Q1 from the data, this is not very significant with the present data, as there is very low energy in these frequency bands for the Saldanha-Langebaan system.

4.2.4 Harmonic analysis:

Through spectral analysis, one is able to define the range of frequencies having a significant role in shaping the data record. If one wants to further the spectral analysis by looking for tidal constituents (determined by planetary motions) of precise frequencies, a harmonic analysis is required. Harmonic analysis is a very valuable tool in understanding the hydrodynamic of a system. Indeed, it allows one to represent the data with a few significant numbers, related to physical reality, and independent of the time at which observations were made. Changes in the magnitude of a signal can in fact be thought of, as the interactions of constant tidal constituents. For example, the interaction of the M_2 and the S_2 tidal constituents will generate spring-neap variations in a tidal signal. The basis of harmonic analysis is to treat the signal as the sum of a finite number of harmonic constituents, whose angular speed and phases are determined from the astronomical arguments. Sea-levels can then be represented by a tidal function T, fitted to the records and expressed by:

$$T(t) = z_0 + \sum_N h_n f_n \cos[\sigma_n t - g_n + (A_n + b_n)] \qquad \text{eq. 4-3}$$

where N is the number of constituents, z_0 is the elevation of the mean sea-level above tidal datum, H_n and g_n are the tidal constituent amplitude and phase, σ_n is the constituent frequency, f_n is the astronomical argument (it can be regarded as a constant during one particular year (Rozenthal and Grant, 1989)), A_n and b_n are phases angles that reference the cosine argument to a universal origin in time and space. The only values for the astronomical arguments and phases in the vicinity of the study site, are those derived by Rozenthal and Grant (1989) for Saldanha Bay. f_n, A_n and b_n would then be the assigned the same value for either

the Langebaan lagoon or the Saldanha bay system . Considering that we only wish to determine the constituents within that particular system, we can reduce the tidal function to

$$T(t) = z_0 + \sum_N H_n \cos(\sigma_n t - g_n) \qquad \text{eq. 4-4}$$

The number of constituents to be used in the analysis depends on the length of the data. In general, the longer the record, the greater the number of constituents. The standard criterion used to choose the constituents is the Raleigh criterion (Pugh, 1987). It requires that only constituents separated by at least a complete period from their neighbouring constituents over the data length, be included in the analysis. For example, for constituents with frequencies σ_j and σ_k (in radians), the length of data required will be

$$L = \frac{2\pi}{\sigma_j - \sigma_k} \qquad \text{eq. 4-5}$$

In our analysis, the 6 tidal constituents used were: K_1, O_1, M_2, S_2, M_4, and M_6. The time-series were preliminary lowpassed with a 40 hours quarter power point and a PL64 filter. Then, the tidal function was fitted to the residual (high-pass) data using a least square procedure. This requires that the square of the difference between the observed and the computed values, is minimum when summed over all the recorded values. The accuracy of the tidal fit was estimated by computing the residual and the standard error. The standard error due to a random background noise of variance σ^2 in the elemental band around a constituent frequency being $\sigma/\sqrt{2}$ for the amplitude.

A similar approach was used for the harmonic analysis of currents. The two scalar components U (across the channel) and V (along the channel) of the current data were subjected to separate harmonic analysis by least square fitting. The harmonic expression of the U and V component of the flow is given by:

$$U(t) = U_0 + \sum_N U_n \cos(\sigma_n t - g_{un}) \qquad \text{eq. 4-6}$$

$$V(t) = V_0 + \sum_N V_n \cos(\sigma_n t - g_{vn}) \qquad \text{eq. 4-7}$$

where U_0 and V_0 are the mean velocities and the parameters (U_n, g_{un}) and (V_n, g_{vn}) define the current ellipse for the tidal constituent n. Through the harmonic analysis of currents one can:

detect a local tidal circulation, verify whether the circulation reflects a net current or if asymmetry between the inflow and outflow is induced by bathymetry, correlate the tidal currents with the tidal changes in sea-level and thus, provide some authentic and physically proven information about the predictive part of the signal. The analysis of currents is however more perilous than that performed on sea-levels. Indeed, in coastal environments, strong horizontal gradients in the flow occur, associated with either the complex geometry of the system or the state of the tide. Hence, currents may show little coherence in the horizontal, compared to sea-level measurements which are coherent over large distances.

5. Results

5.1 Description of the results

5.1.1 Temperature, salinity and density:

A strong vertical homogeneity of the lagoon temperature was observed at all sampling locations. Temperature in the lagoon basin increases with distance from the mouth. Temperatures were between 10.5°C and 22°C, with the coldest waters found at the lagoon entrance during the inflow and the warmest waters encountered in the most southern locations of the lagoon. Transient vertical stratification was sometimes observed at the lagoon inlets during flood tides. The stratification encountered at the beginning of the inflow at the lagoon entrance was more pronounced in the west inlet, where temperature differences between the surface and a 5m depth often reached 1°C (with a maximum of 4°C). In the east inlet differences between the surface and the bottom layer in the eastern channel seldom exceeded 0.2°C (with a maximum of 1°C) (figure 5-1 (a)).

Lateral variations of temperature were encountered in the vicinity of the lagoon inlets, with colder water on the western side of the lagoon. The west inlet displayed surface temperature on average 1°C colder than that in the east inlet (figure 5-1). CTD cross-sections showed that the temperature difference between the two inlets extended to the region surrounding the lagoon mouth. On the 17th of March, the temperature gradient existing between the western and the eastern part of the lagoon, could be noticed as far as transect C (2km into the bay) to the north and as far as transect E (2km into the lagoon) (figure 5-2).

Temperature at specific locations in the lagoon varied strongly with the state of the tide. On the inflow, bay water entered the mouth bringing cool water into the lagoon. During the ebb, warm water draining from the shallows and the salt marsh area was advected toward the lagoon inlet. In the vicinity of the lagoon mouth, cold water was found throughout most of the tidal period. Temperature only increased briefly at the end of the ebb, when the

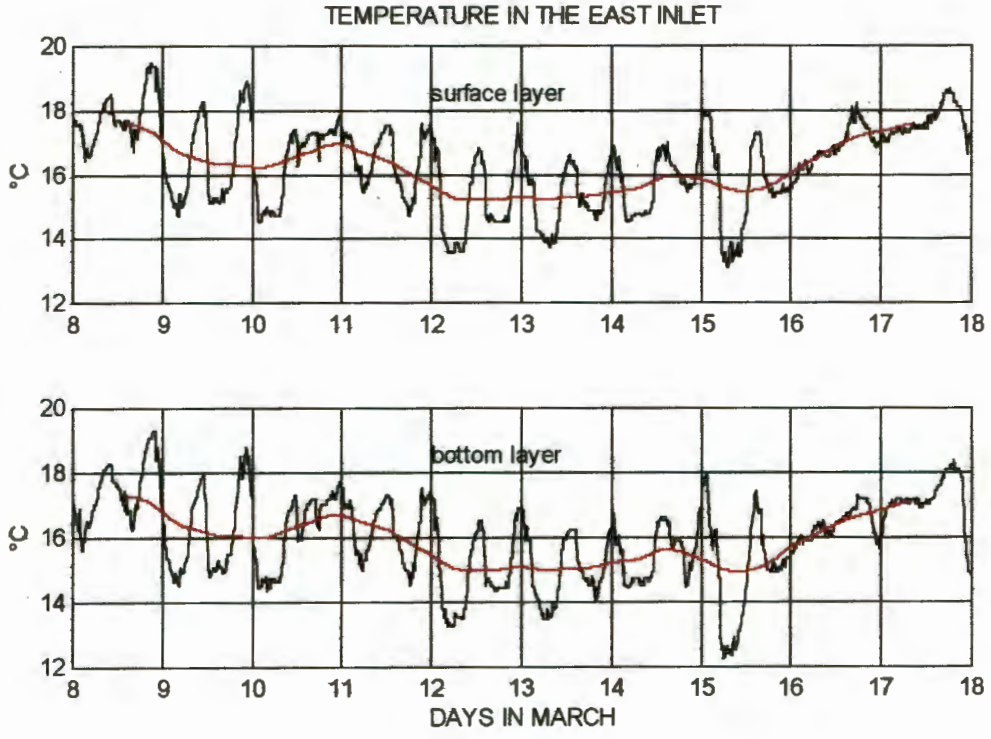

(a)

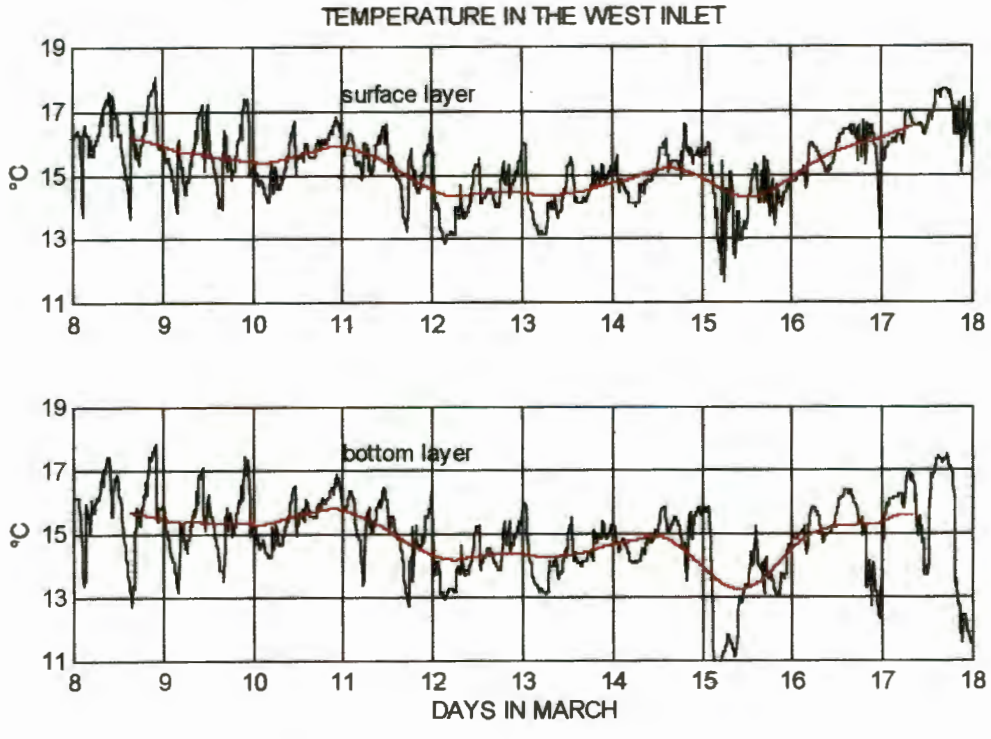

(b)

Figure 5-1: Time-series of the temperature at the east inlet (a) and at the west inlet (b). The red line is the lowpassed time-series. In the east inlet, the surface thermistor is 1.5m below the surface while the bottom thermistor is 3m above the seabed. In the west inlet, the surface thermistor is 2m below the surface while the bottom thermistor is 3.5m above the seabed.

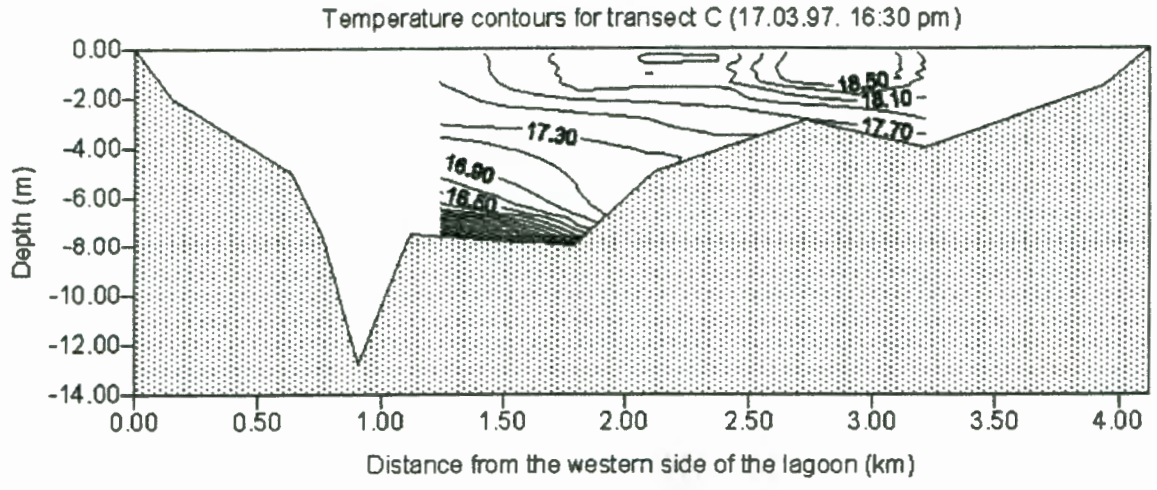

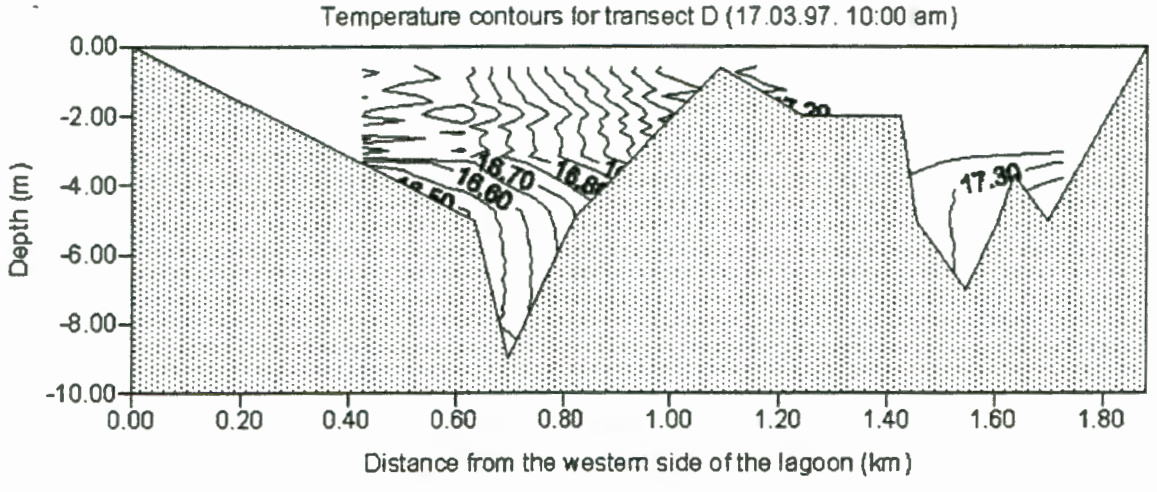

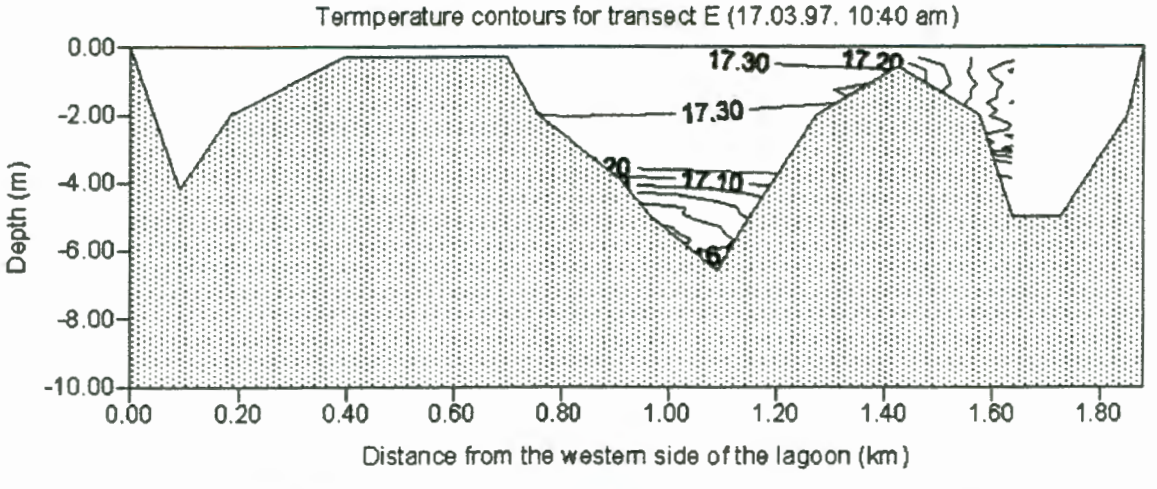

Figure 5-2: Temperature contours drawn from CTD data collected on the 17.03.97. The positions of the CTD transects appears in figure 4-3. Contour intervals are 0.2°C for transect C and 0.1°C for transects D and E.

warmer water from the middle lagoon reached the mouth. Similarly, water in the southern part of the lagoon (station T6) stayed warm throughout most of the tidal period, but became colder as outer lagoon water moved in on the late flood tide. Typically, temperature at a station varied by approximately 4°C during a tidal cycle (figure 5-3).

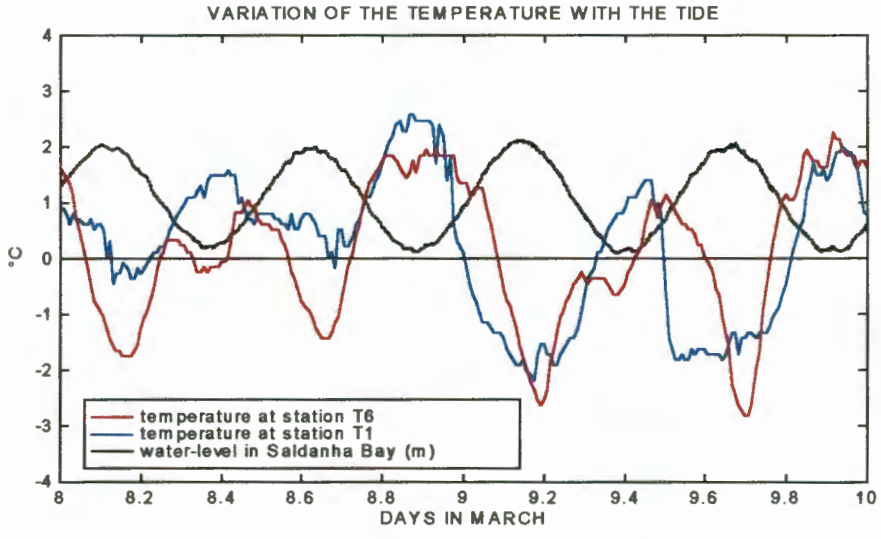

Figure 5-3: Tidal fluctuations from the mean for the lagoon temperature plotted alongside tidal variations in the Saldanha Bay waterlevel. Station T1 was located at the Langebaan lagoon entrance, while station T6 was in the southern part of the lagoon (see figure 4-1).

Maximum temperature fluctuations during a tidal period were found to occur at station T5 (Kraalbaai). At this location, variations of 6°C between the ebb and the flood were frequent (figure 5-4). Also, in contrast to water bodies located near the lagoon mouth or head, water in the vicinity of station T5 never stayed warm or cold during a long portion of the tidal cycle. This large tidal variation is explained by the maximum longitudinal temperature gradient observed in the vicinity of Kraalbaai (figures 5-5 and 5-6).

Tidal variations of temperature depended on the longitudinal gradient within the lagoon basin. When the water in Saldanha Bay was warmer, reduced tidal variations were seen in the lagoon. In plots of low-passed temperature one can see that the 11th and the 16th to the 18th of March were warmer periods and also periods of reduced tidal variation (figure 5-1 and 5-4). On those days, the temperature only varied by approximately 1°C during a tidal cycle, instead of the usual 3°C to 4°C. Similarly, large tidal variations in the temperature were associated with cooler periods. Cold bay water and large temperature variations were

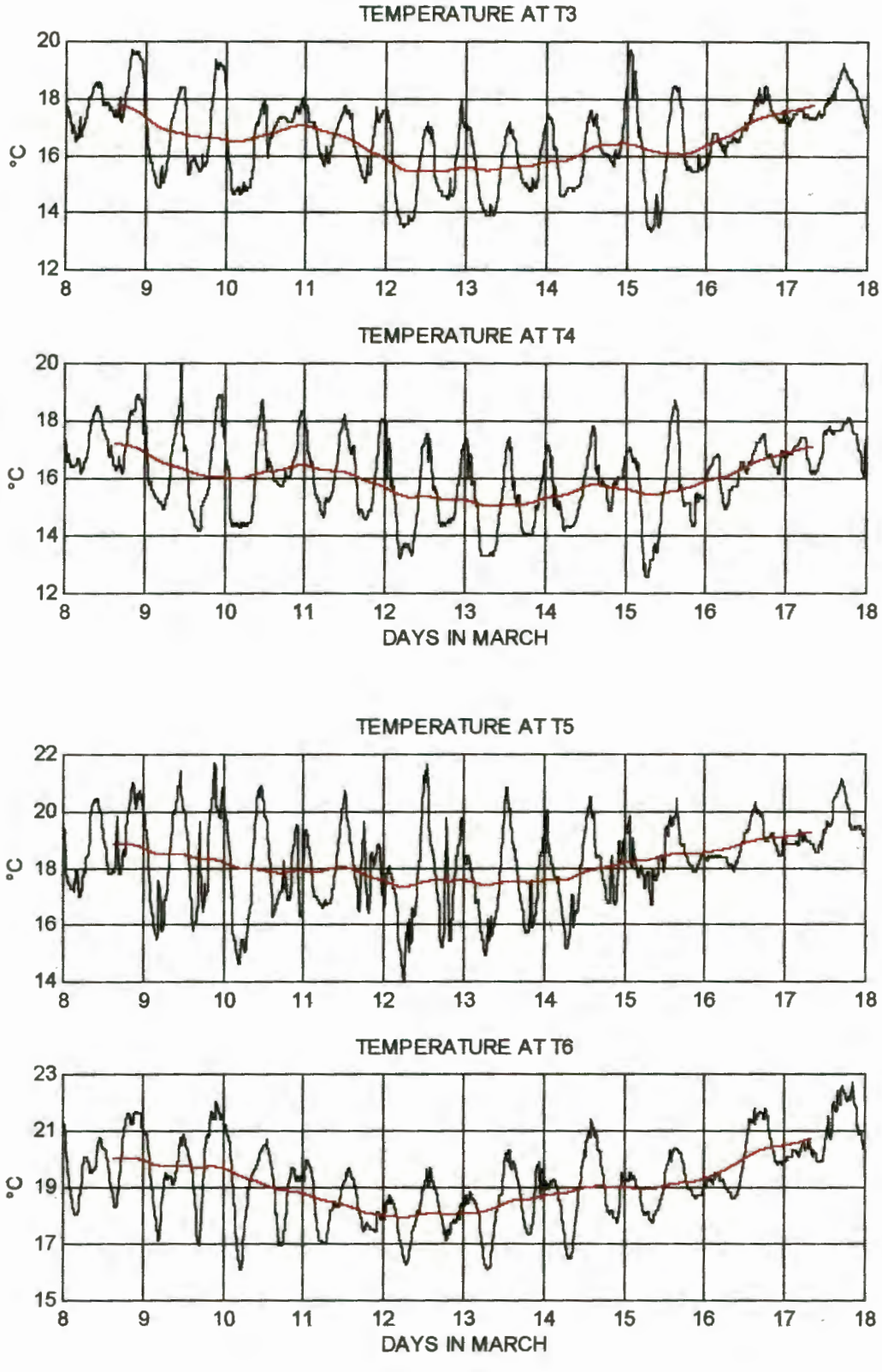

Figure 5-4: Time-series of the temperature at stations T3, T4, T5 and T6. The red line represents the lowpassed time-series. See figure 4-8 for station locations.

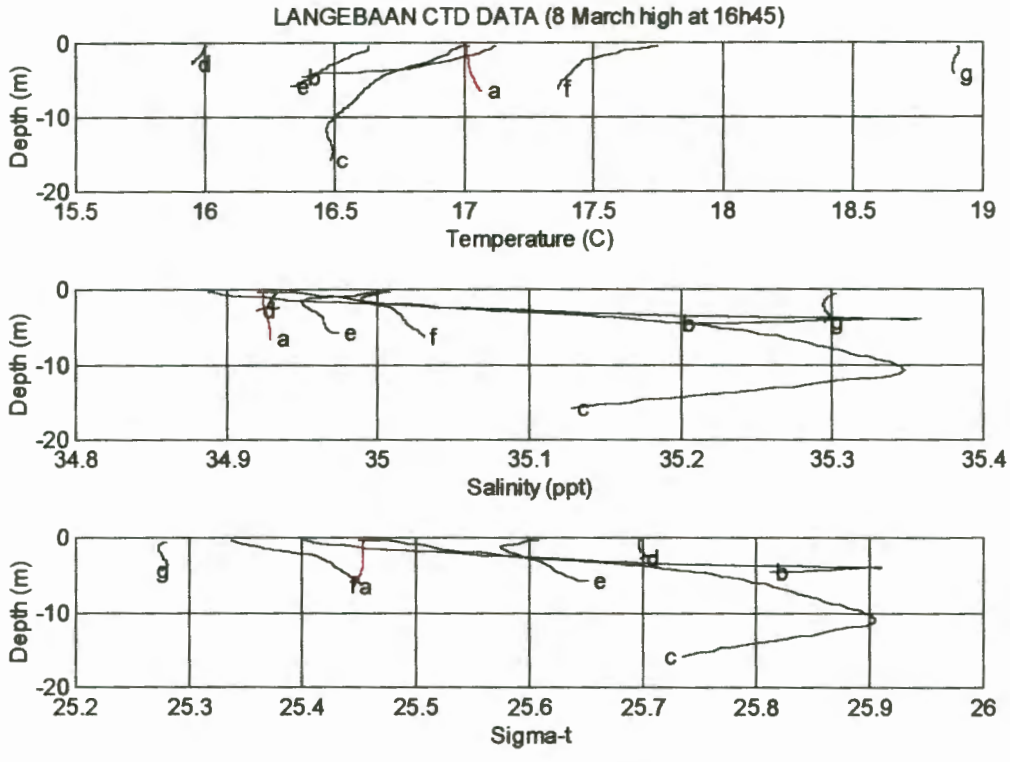

(a)

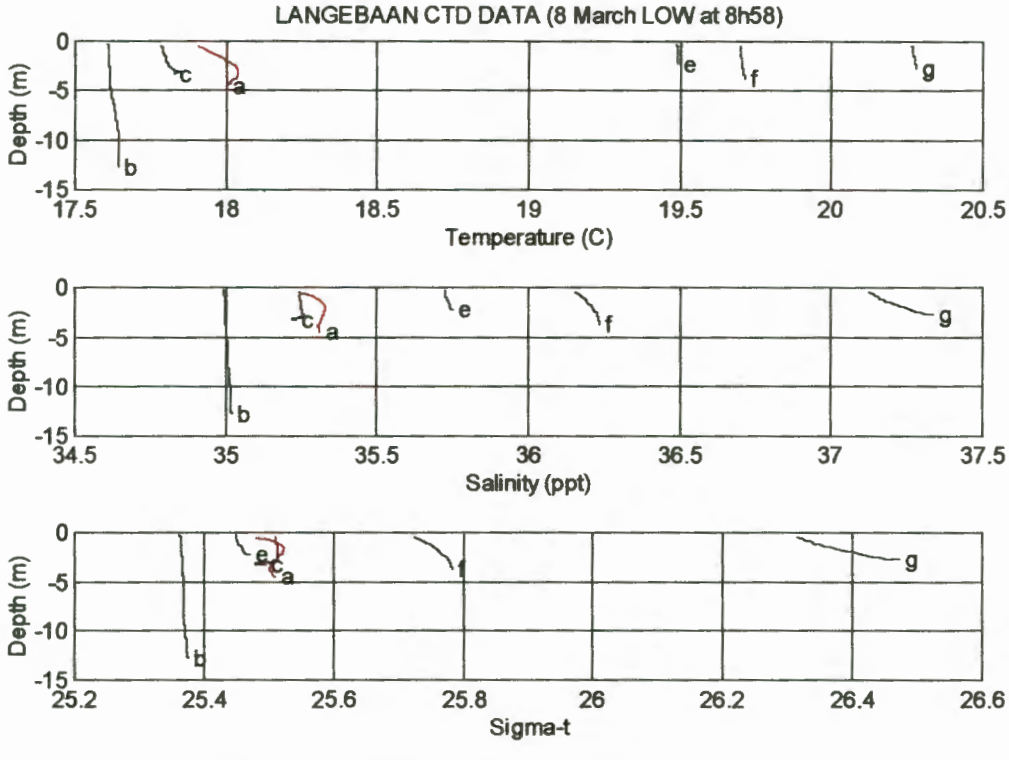

(b)

Figure 5-5: CTD profiles taken in the lagoon on the 8.03.97 (spring tide). Plot (a) represents the data obtained at high tide. Plot (b) represents the data obtained at low tide. CTD stations are named from b (near the lagoon mouth) to i (farthest into the lagoon). See figure 4-8(a) for station locations.

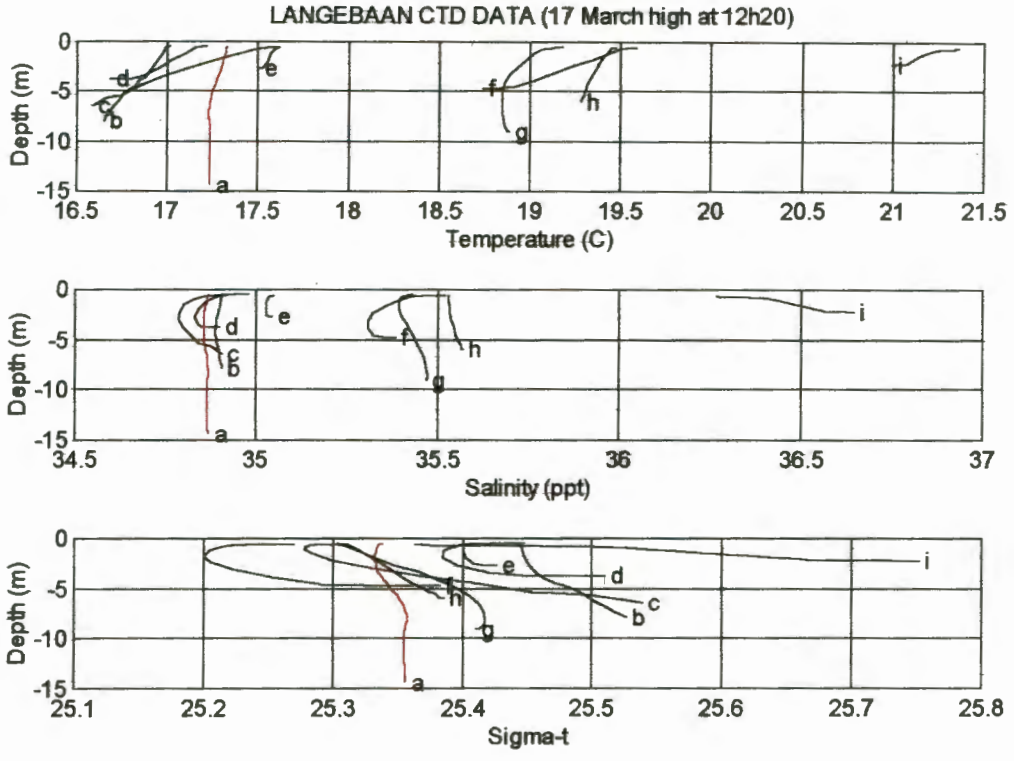

(a)

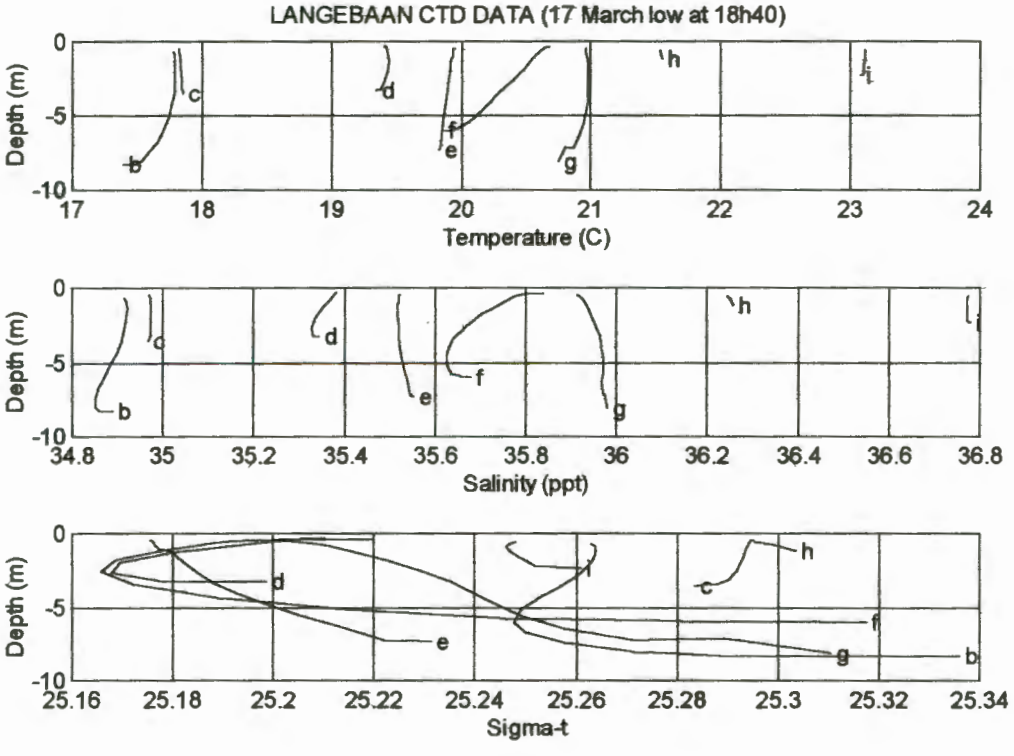

(b)

Figure 5-6: CTD profiles taken in the lagoon on the 17.03.97 (neap tide). Plot (a) represents the data obtained at high tide. Plot (b) represents the data obtained at low tide. CTD stations are named from b (near the lagoon mouth) to i (farthest into the lagoon). See figure 4-8(b) for station locations.

observed on the 15th of March at transects A, B and C and at thermistors positioned north of Kraalbaai. On the 26th of March, a large variation in temperature was also observed for thermistors located in the western channel (figure 5-7).

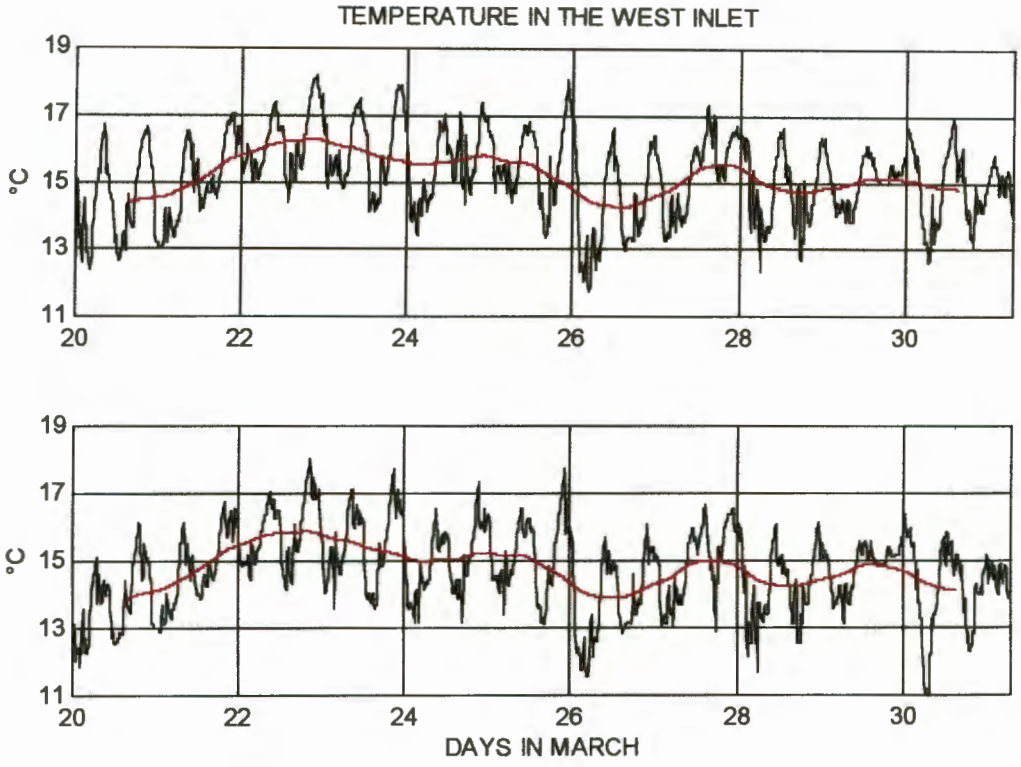

Figure 5-7: Time-series of the temperature at the west inlet..The red line is the lowpassed time-series. In the east inlet, the surface thermistor is 1.5m below the surface while the bottom thermistor is 3m above the seabed. In the west inlet, the surface thermistor is 2m below the surface while the bottom thermistor is 3.5m above the seabed.

Fluctuations in the low-passed temperature signal were greater and more frequent for regions located north of Kraalbaai, that is regions directly influenced by bay water. Over the two week sampling period, lowpassed temperatures were maximum on the 8th and the 18th of March and minimum from the 11th to the 15th of March. On the 9th of March, the unusual presence of a cold tongue of water (14-14.5°C) was observed on the eastern shore of transect C (figure 5-8). That day, the temperature gradient between the eastern and the western sides of the lagoon inlet was reversed: water along the eastern side of the lagoon mouth was coldest. It is not possible to say how far into the lagoon this reversed temperature gradient would have been observed, since no transects were undertaken into the lagoon. We expect that this situation was only encountered in the vicinity of the lagoon

entrance because, as mentioned at the beginning of this chapter, lateral temperature gradients do not occur farther inside the lagoon.

Although water temperature depends primarily on distance from the mouth and displays a tidal rise and fall, some regions have slightly different patterns of temperature variations compared to their surroundings. The most striking example is that of the western inlet. Temperature for thermistors located in the western channel and at the lagoon mouth, was subject to supertidal temperature fluctuations. Within the more noisy signal displayed by thermistors located in the western inlet, it was possible to notice the regular occurrence of a warm pulse of water at the beginning of the outflow (figure 5-9). This warm pulse probably resulted from tidal trapping in Rietbaai. The intensity of the pulse of warm water was highly variable (from 0.5°C to over 2°C magnitude). The increase in temperature was sudden, indicating the passage of a thermal front.

The salinity distribution was assessed from the two CTD surveys undertaken on the spring and the neap tides. Salinity hardly varied with depth. The maximum vertical gradients measured in the east and west inlets, were equal to 0.5*psu* and 0.4*psu* respectively. In a similar way as for the temperature, salinity increased as we progressed into the lagoon (figures 5-5, 5-6 and 5-10). Near the mouth, the water column was characterised by a salinity similar to that of the ocean (about 35*psu*). The CTD stations located farthest from the mouth were characterised by salinities greater than the ocean values (hypersalinity occurred). Near the lagoon mouth salinity remained constant throughout the tidal cycle, whereas for stations farther into the lagoon, salinity increased during the outflow. During the length of the fieldwork salinity varied within a 34.8-37.4*psu* range, with the highest values measured on the spring low tide towards the south end of the lagoon.

The density structure of the lagoon water was mostly due to temperature rather than salinity variations. Typical tide-induced variations in density were 0.18 Sigma-t in the surface layer of the east inlet on the 8th of March and 0.15 in the west inlet on the 17th of March.

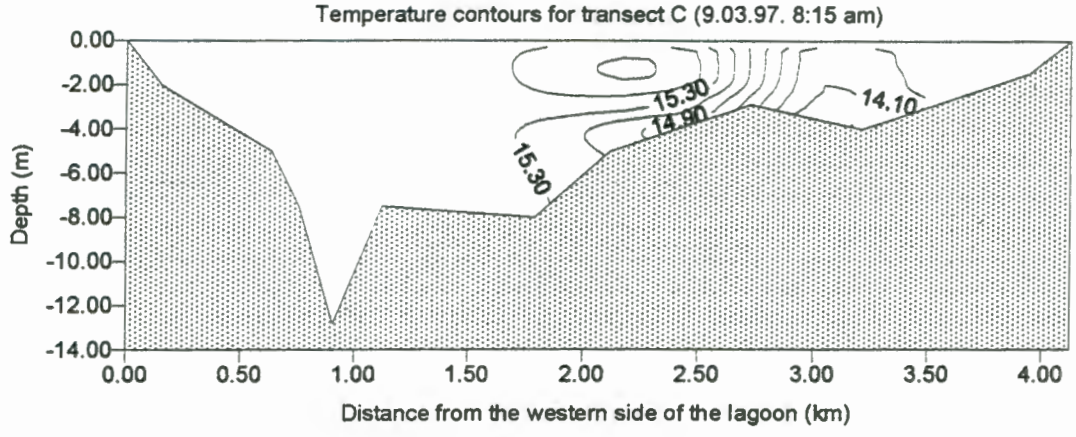

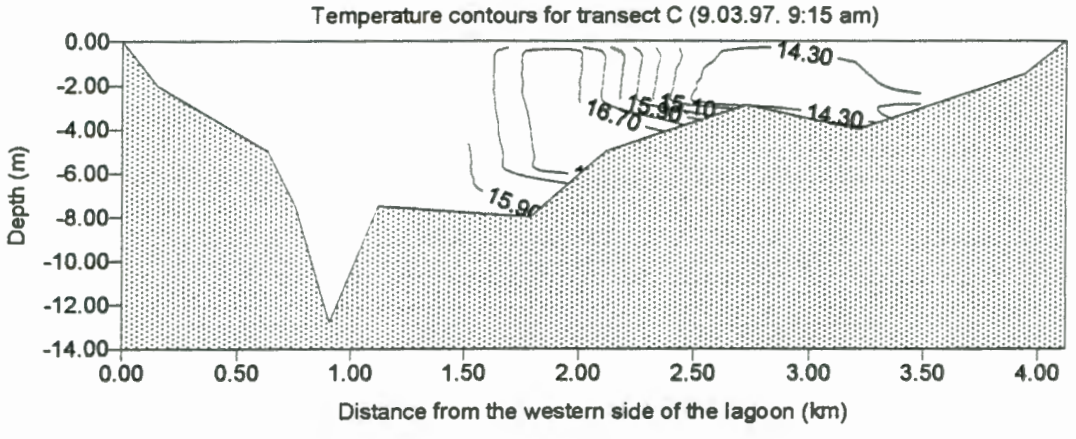

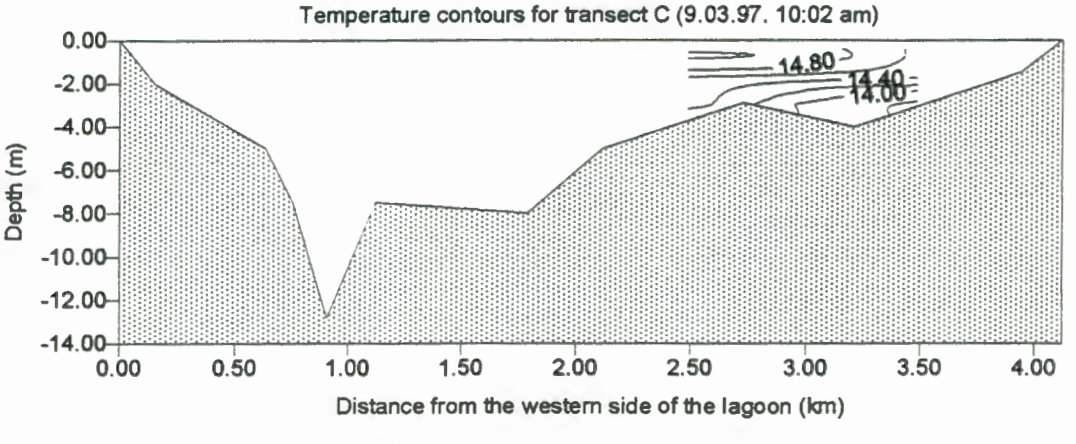

Figure 5-8: Temperature contours obtained at transect C on the 9.03.97. The unusual presence of a cold tongue of water is observed on the eastern shore of transect C. Some data was lost for the last transect C, resulting in a poor spatial resolution.

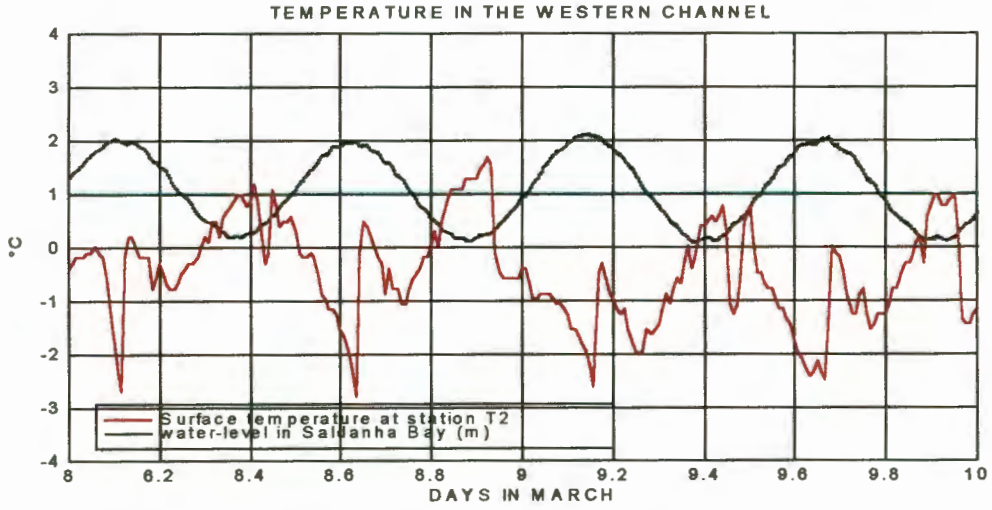

Figure 5-9: Temperature fluctuations due to the tide in the west inlet of the lagoon. A pulse of warm water occurred at the beginning of the outflow.

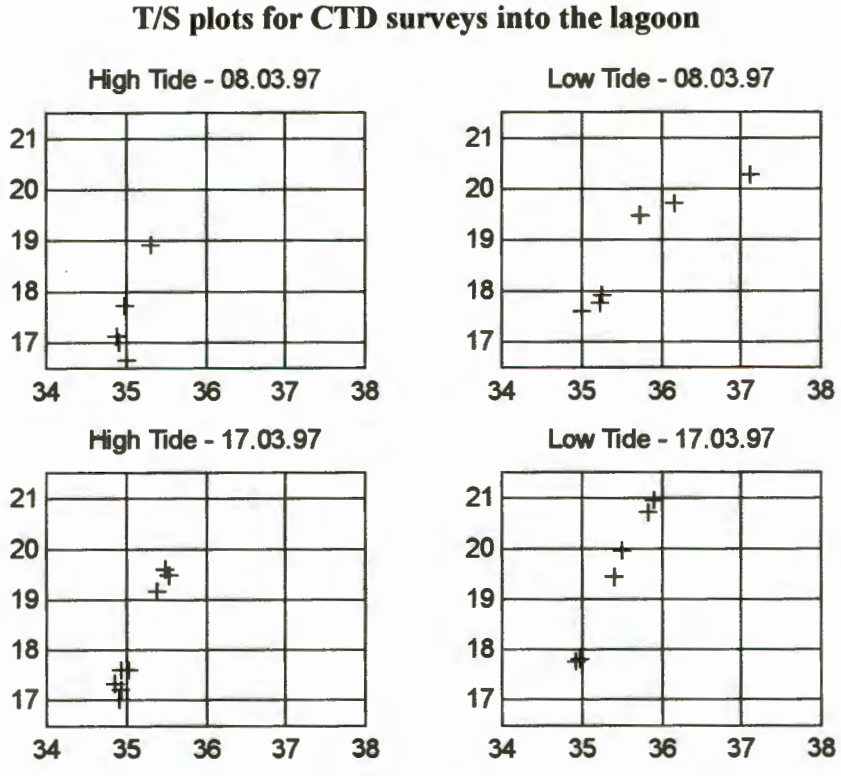

Figure 5-10: Surface (1m) Temperature and Salinity plots for the CTD surveys undertaken on the 8.03.97 (spring) and 17.03.97 (neap).

5.1.2 Wind and currents:

Wind:

During the month of March, south-easterly winds were predominant. The wind data obtained from the Geelbek weather station exhibits a very strong diurnal signal. The wind was minimum at dawn, increased through the mid to late morning and reached a maximum at about 17:00pm (late afternoon), before decreasing again. The across-lagoon wind was generally less than 5m.s^{-1}. The maximum velocity reached by the along-lagoon wind on the 25th of March was equal to 11.6 m.s^{-1} and resulted from a combination of a local diurnal component and a synoptic low-pass component (each attaining strength of about 5m.s^{-1}). The wind variations for the Geelbek weather station are represented in figure 5-11.

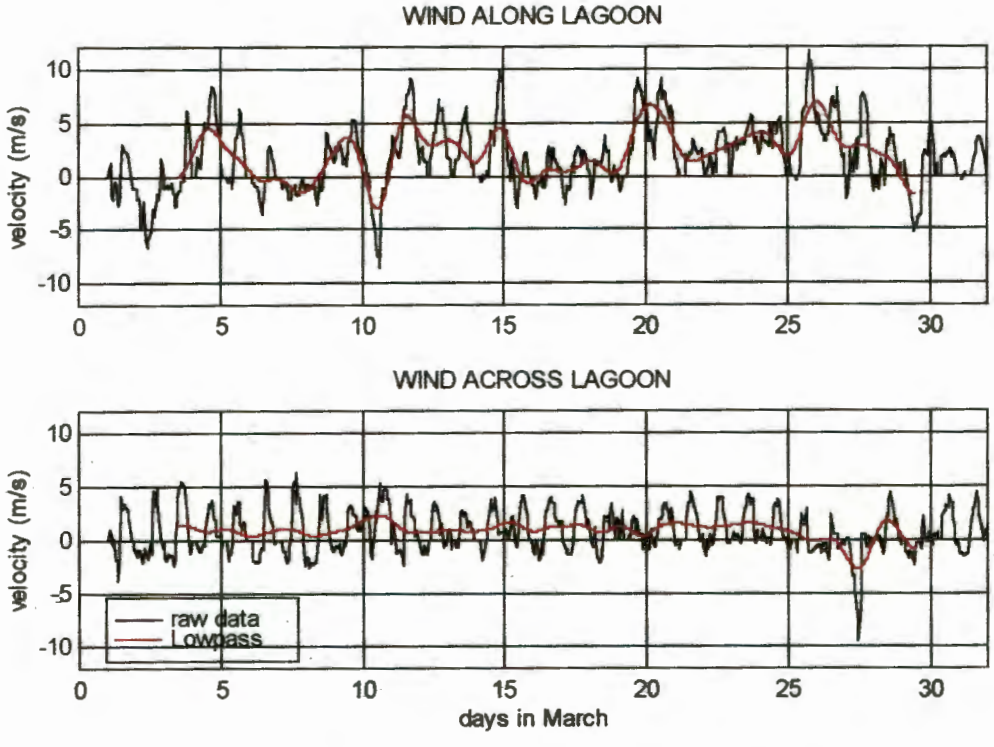

Figure 5-11: Timeseries for the wind data obtained from the Geelbek weather station (see figure 4-1 for location). The along-lagoon axis, tilted at an angle of -20° from north, was chosen to follow the topography.

Time-series of the wind at Cape Colombine were obtained (figure 5-12). Cape Colombine is located approximately 20km north of Saldanha Bay and is subject to atmospheric forcing acting over the adjacent ocean. The intensity of the wind at Cape Colombine significantly exceeded

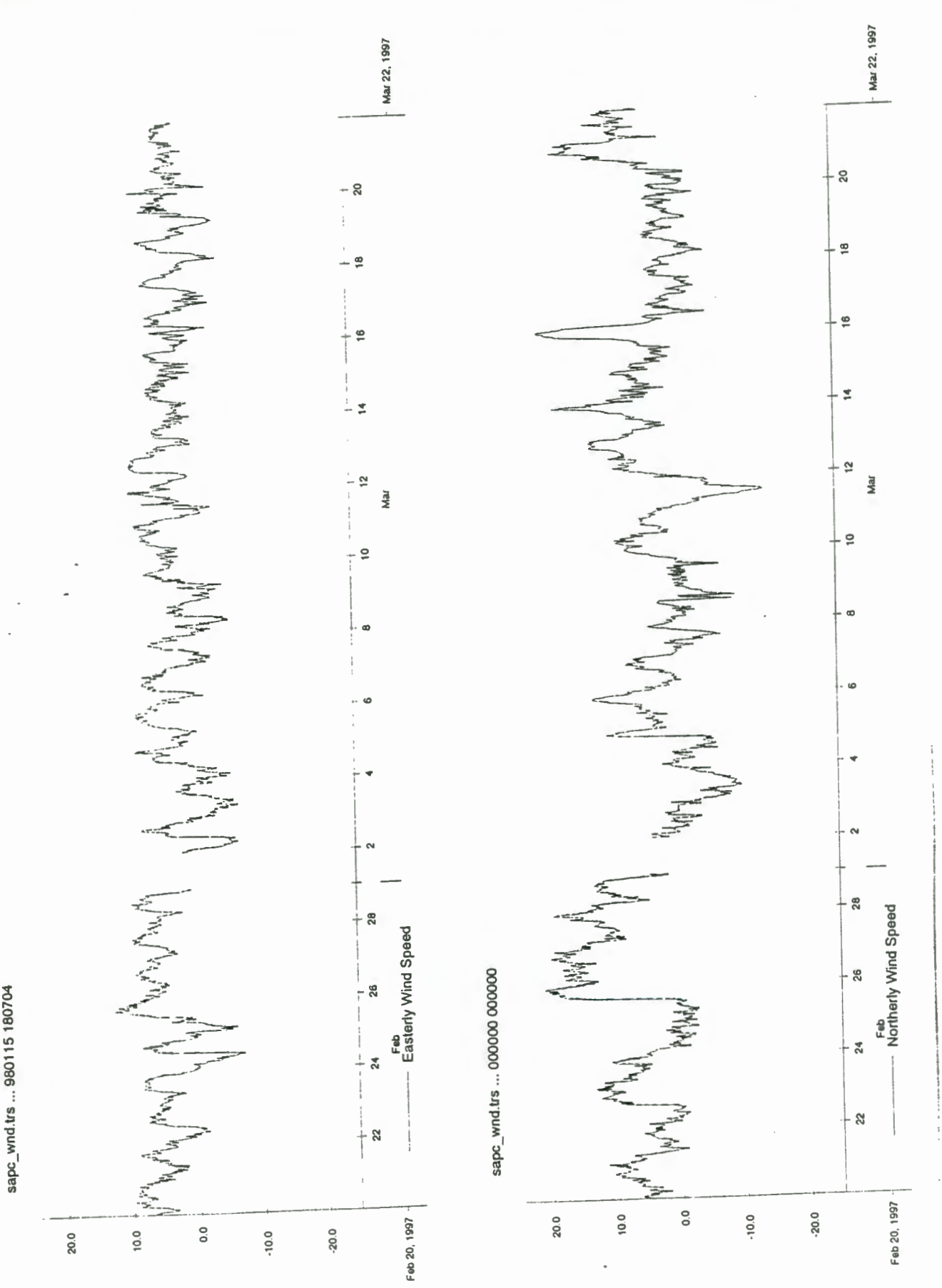

Figure 5-12: Time-series for the easterly and the northerly components of the wind velocity at Cape Colombine (figure 2-1) for the months of February and March 1997. The plot was obtained from Van Ballegooyen (CSIR).

that measured at Geelbek. The north-south component of the wind often reached velocity of about 20cm.s^{-1}, while the west-east component of the wind generally remained less than 10m.s^{-1}. Synoptic wind variations were observed at Cape Colombine. In March 1997, the strongest southerly winds occurred between the 10th and the 12th of March and the strongest northerly winds were observed on the 16th of March.

Tidal waterlevels and excursions:

The Saldanha Bay-Langebaan Lagoon system is a micro-tidal environment. In Saldanha Bay and in Langebaan Lagoon, the tidal ranges during the spring and neap cycles were respectively equal to 2m and 0.6m. There seemed to be no significant attenuation of the tidal range as the tidal wave propagated into the lagoon (figure 5-13). During the spring cycle, the tide lag between Saldanha Bay and the lagoon was equal to 48min at high tide and 1hr15min at low tide. During neaps, lags between the high and low waters in both the lagoon and the bay are significantly reduced (figure 5-13). Calculations of the lags between the onset of the inflow and the outflow in the bay and in the lagoon showed that the Langebaan Lagoon tide lags the tide in Saldanha Bay by an average of 49mn during the spring cycle, and by an average of 16mn during the neap cycle. The tidal curve showed no apparent ebb/flood asymmetry and was dominated by the sinusoidal variations associated with the semi-diurnal tide (figure 5-13 and 5-14(a)).

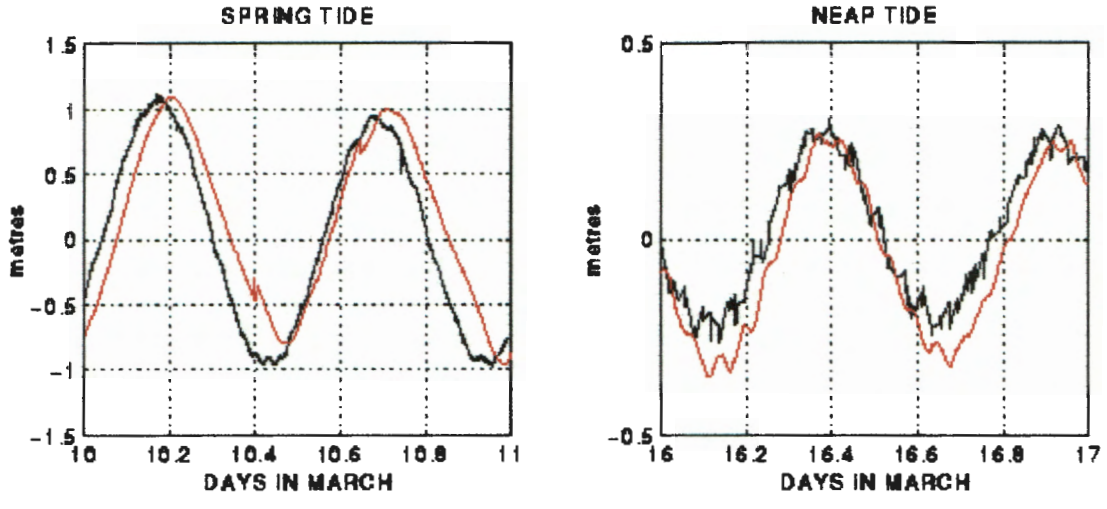

Figure 5-13: Water level variations in Saldanha Bay (black) and Langebaan Lagoon (red) during the spring and the neap tides. The lags between the tides in Saldanha Bay and in Langebaan Lagoon are greatest during the low spring tide and lowest during the high neap tide.

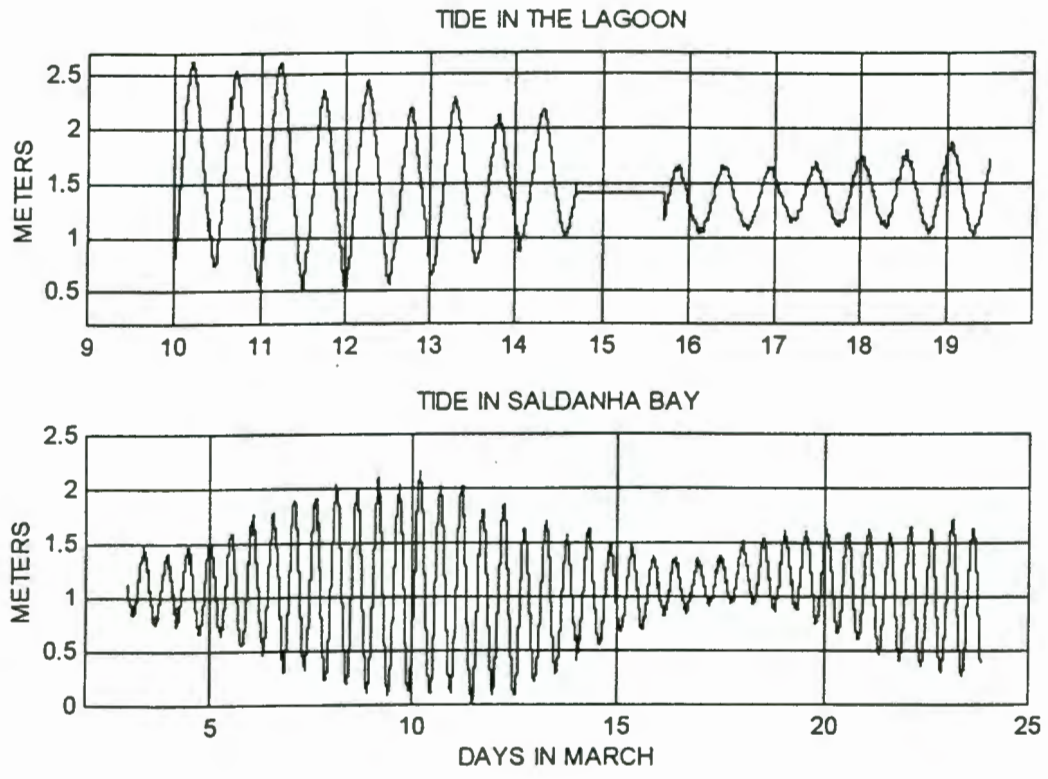

(a)

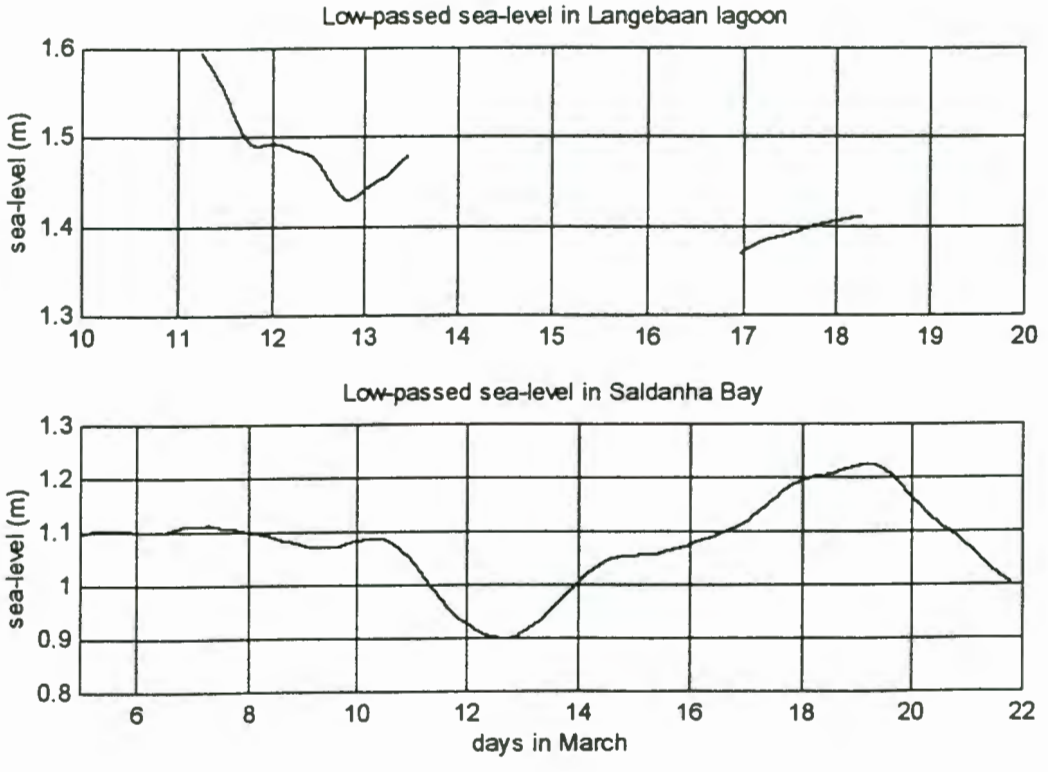

(b)

Figure 5-14: (a) Time-series for the water-level in Saldanha Bay and Langebaan Lagoon. (b) Lowpassed time-series of waterlevel using the WHOI PL33/64 filter. The quarter power filter cut-off was set to 30 hours for the lagoon data, and 36 hours for Saldanha Bay data.

Drifter data obtained on the 13th and the 14th of March gave us an estimate of the tidal excursion at the mouth (figure 5-15), that is, how far a specific parcel of water present at the lagoon inlets flows in or out of the lagoon during the ebb or the flood. On the 13th of March, the drifters released at the start of the ebb in the eastern and the western channels of the lagoon, covered distances of approximately 4.8km (1.5km from the mouth of Saldanha Bay) and 4.3km respectively. Considering that the drifter released in the western channel was picked up by the Navy, we can assume that, had it followed its natural path, the drifter would have travelled even farther from the lagoon mouth. Only a limited number of drifter deployments were undertaken during the inflow, because the focus of this thesis is to understand the nature of the flow out of the lagoon. Also, it was soon realised that the quality of the data obtained during the inflow drifter experiments was going to be poor, as the irregularity of the bathymetry caused frequent grounding of the drogues. The movements of isotherms and isohalines obtained from the CTD data, provided us with a better estimation of the flood tidal excursion into the lagoon. On the 8th of March (spring), the tidal range was equal to 1.73m and we found that the water present at the inlet at low tide, had moved 8km into the lagoon during the inflow (figure 5-5). On the 17th of March (neap), water present at the inlets only propagated approximately 4km into the lagoon during the flood (figure 5-6).

The subtidal waterlevel fluctuations (frequencies lower than those associated with the semi-diurnal tides) seemed to be similar in the lagoon and the bay. The low passed water-level time-series (figure 5-14 (b)) did not correlate with the wind at the Geelbek weather station. However, a strong relationship was observed between the wind at Cape Colombine and subtidal variations of the waterlevel in the bay and in the lagoon. Drops in the bay and the lagoon waterlevels corresponded to periods of southerly winds at Cape Colombine. Similarly, northerly winds induced a rise of the waterlevel in the bay. During the neap cycle the shape of tidal curve was irregular. The supertidal variations (frequencies higher than those associated with the semi-diurnal tides) apparent on the tidal curve probably resulted from non-linearity induced by bottom friction. Waterlevel in Saldanha Bay was subject to short term fluctuations (with periods of about 4 minutes) to a greater extent than the waterlevel collected into the lagoon.

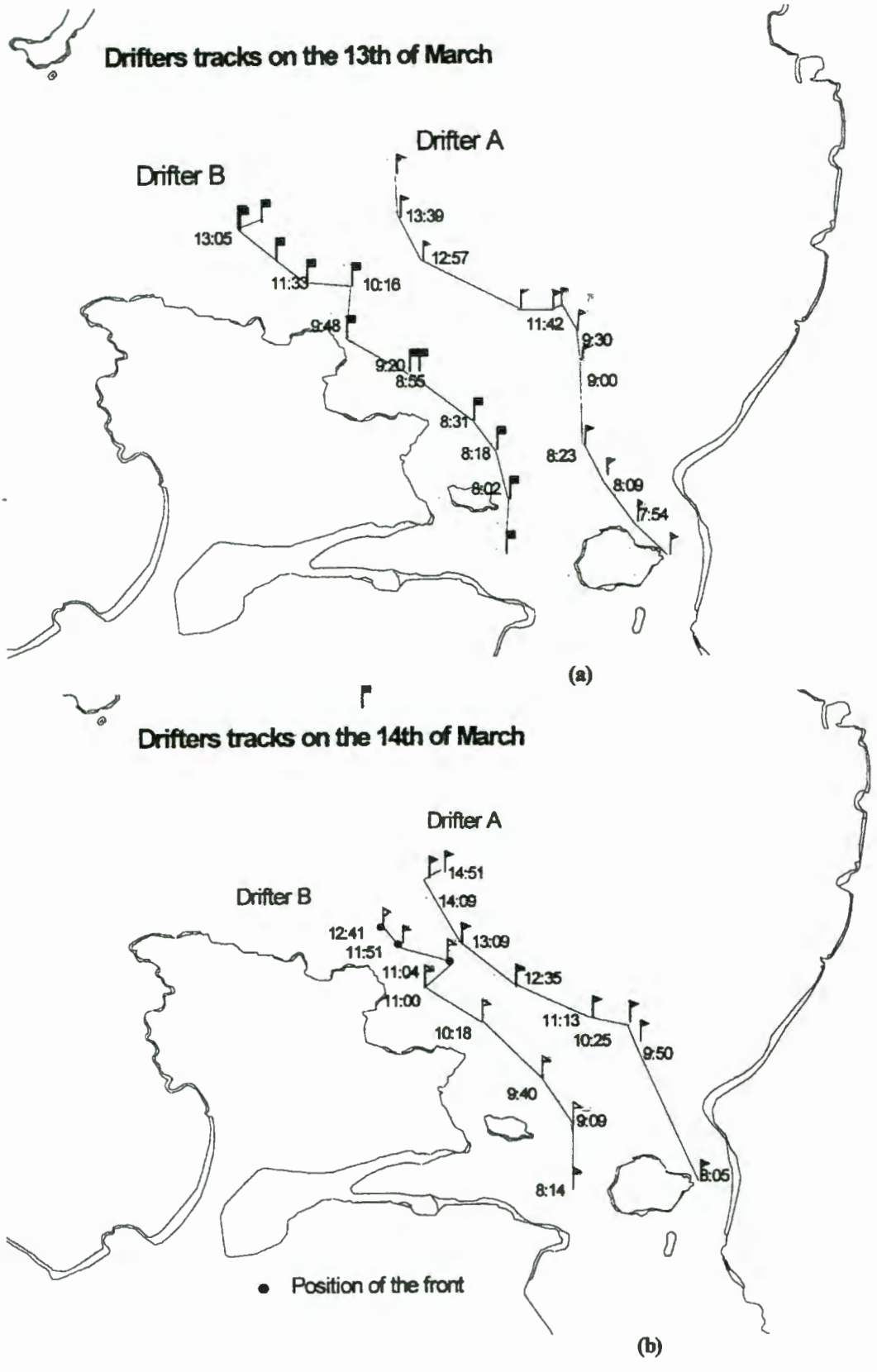

Figure 5-15: Path followed by the drifters on the outflow of the 13th and on the 14th of March 1997.

Currents:

Current velocities depended strongly on the state of the tide. The tidal inflow into the lagoon was greater at mid-tide, when the waterlevel difference between Saldanha Bay and the lagoon was maximum. Similarly, the outflow was greatest at mid-tide during the ebb (figure 5-16).

In the eastern channel, the water started flowing out of the lagoon on average 53min after the high tide in Saldanha bay. The inflow of water into the eastern channel was found to start on average 27min after the low tide in Saldanha Bay. The reversal of the current also slightly lagged the reversal of the pressure gradient (figure 5-16).

Along-channel current velocity often reached values of $1m.s^{-1}$, while the across-channel velocity was typically less than $0.2m.s^{-1}$. For both channels there was hardly any variation of the current velocity with depth (figure 5-17 and 5-18). The current was of similar order of magnitude in both channels and was aligned with the channel bathymetry (figures 5-19 and 5-20). In the east channel the flow at the ADCP was strongly unidirectional, occurring along an axis oriented approximately -35° from North. In the western channel, the current

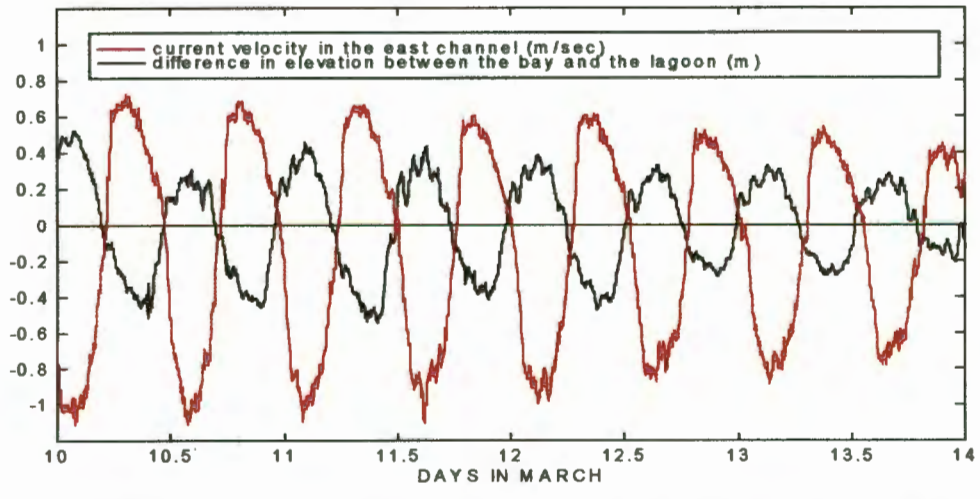

Figure 5-16: Variation of the along channel current velocity in the east channel (bin depth = 5.18m), alongside the difference in waterlevels in Saldanha Bay and the lagoon. The maximum pressure gradient in the lagoon is associated with the greatest currents. Positive values for the waterlevel data indicate that the waterlevel in Saldanha Bay is greater than in the lagoon. For the current data, positive values are indicative of a flow from the lagoon to the bay.

measured at the ADCP revealed the different direction taken by the flood and the ebb flow. Still, we chose to align the current data with the direction of the major axis component (-46° to the north in this case), which resulted in a westward across-shore flow on the plots of the timeseries (figure 5-18).

Comparisons between the ADCP current velocity (at a bin depth of 2.18m) and the drifter velocity (surface currents) were made for the eastern inlet, in order to underline how the strength and the trajectory of the flow varied as we moved away from the Langebaan Lagoon inlets. On the flood, drifters remained confined to the channel in which they were dropped (figure 5-21). It was found that, when water was advected into the lagoon, the velocity loss was small as long as water remained within the lagoon channel. As soon as drifters were advected away from the channel, their velocity strongly decreased (figure 5-22). During the inflow, currents within the channel and inside the lagoon had the same order of magnitude as those found at the ADCP location. On the outflow and at the lagoon entrance, the water issuing from the east and west inlet respectively, flowed in a north-westerly and north direction (figure 5-23). Farther away from the lagoon, the flow direction was predominantly north-westerly. On the outflow, the drifter velocity compared well with the ADCP velocity in the region surrounding the inlets. However, 1.5km downstream of the east channel ADCP location, the drifter velocity was much weaker than the ADCP current velocity in the inlet. The drifter velocity decreased more with distance from the ADCP. On the 13th of March, approximately 2km away from the eastern inlet, the surface current was 60% of the current present at the same time at the ADCP (figure 5-24). On the 14th of March, a similar difference between the ADCP and the drifter current velocity occurred 1.5km away from the eastern inlet.

One interesting feature coming out of our results is that for both channels, the ebb and the flood velocities differed. In the eastern channel, the strength of the flow was greater during the flood than during the ebb, while the reverse was true for the western channel. The asymmetry between the ebb and the flood velocities, generated a residual circulation with a net inflow at the eastern inlet and a net outflow at the western inlet. This pattern was clearly apparent when looking at the low-passed time-series of the current velocities (figures 5-25 and 5-26). Both low-passed time-series of the along-channel current records, underlined the

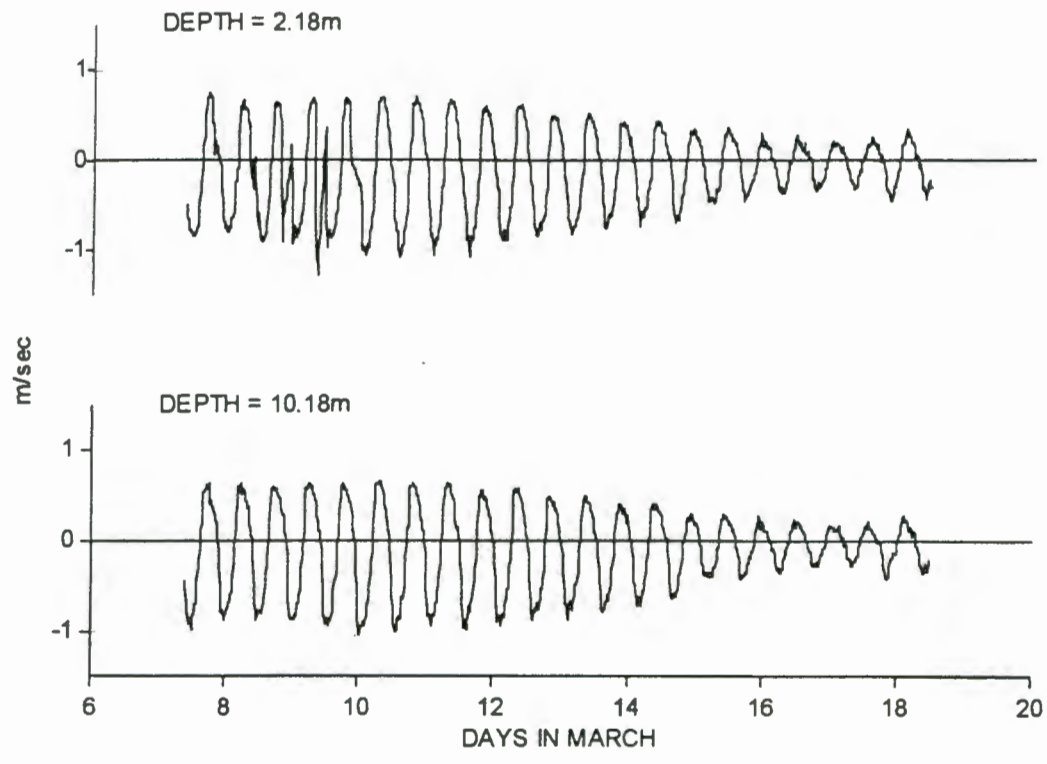

(a)

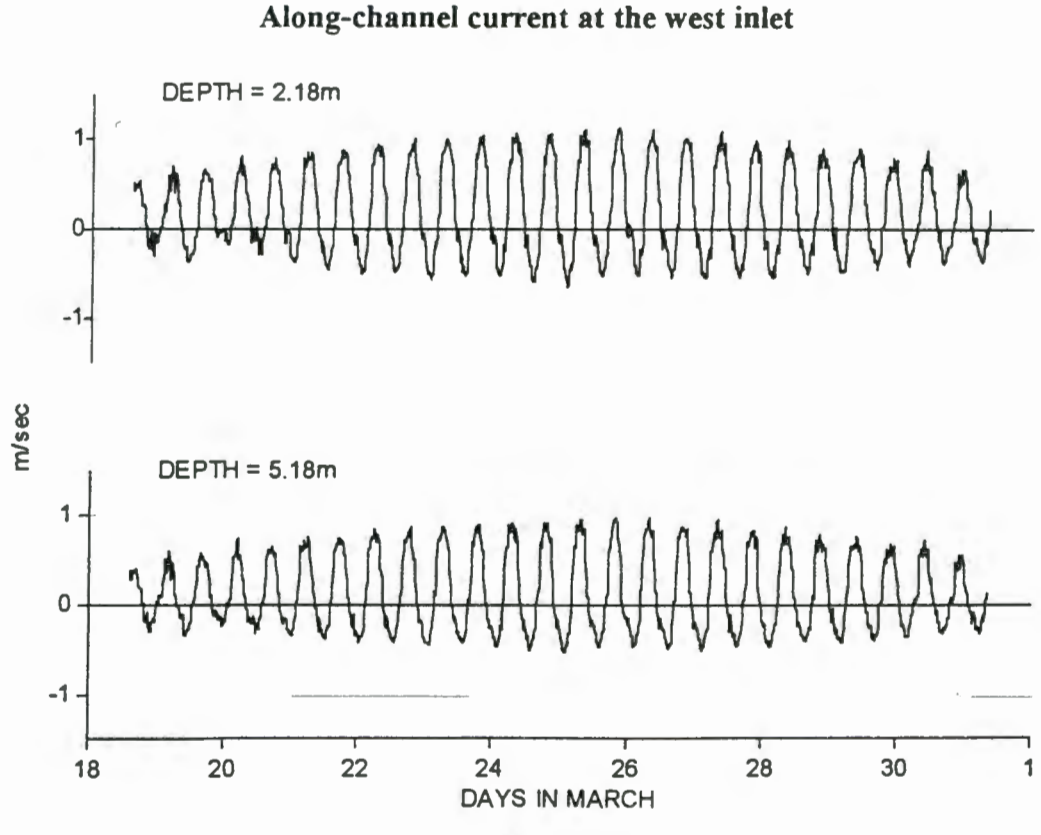

(b)

Figure 5-17: Time-series of the surface and near-bottom along-channel currents, at the east inlet (a) and at the west inlet (b).Positive values indicate a flow out of the lagoon.

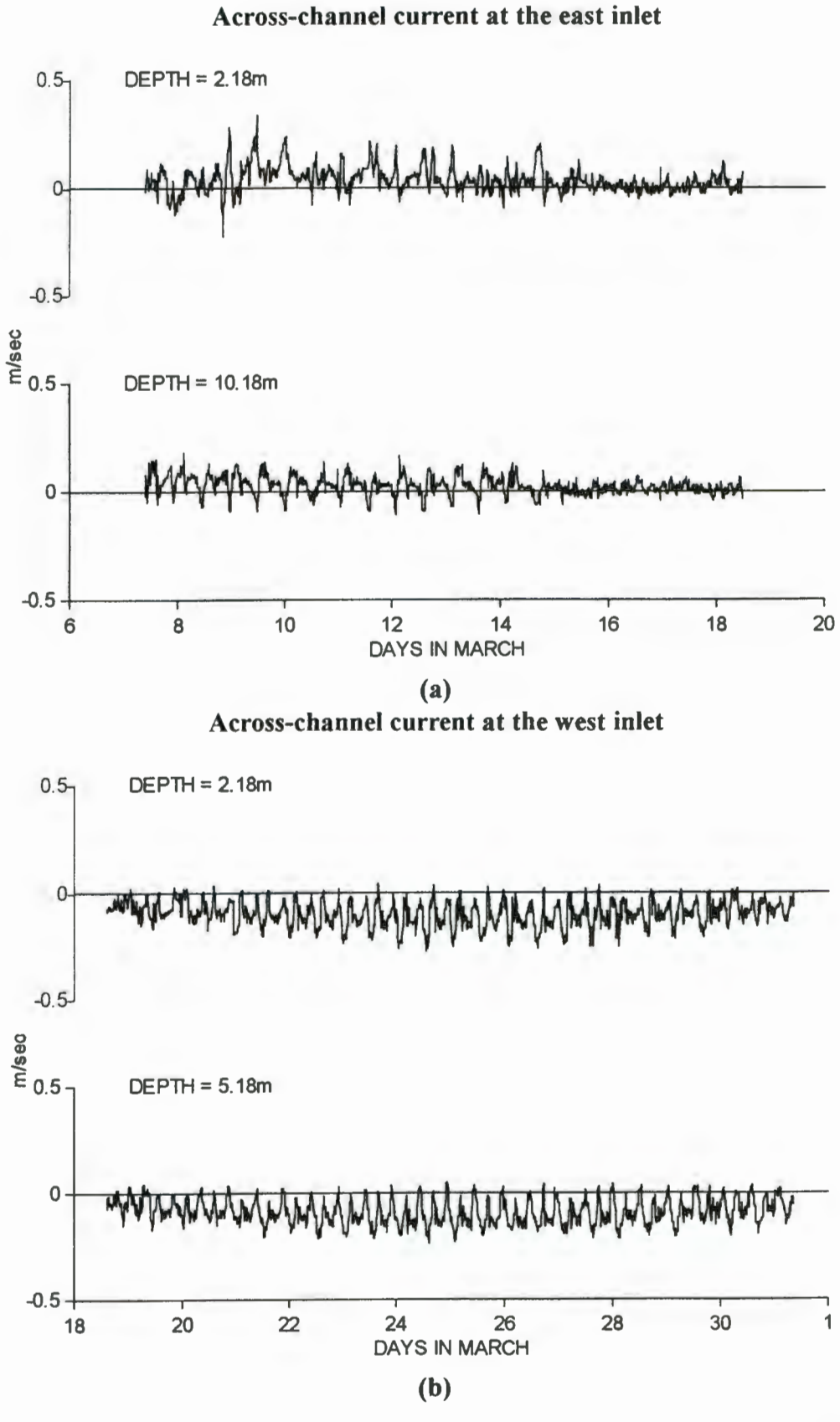

Figure 5-18: Time-series of the surface and near-bottom across-channel currents, at the east inlet (a) and at the west inlet (b). Positive values indicate a flow toward the east.

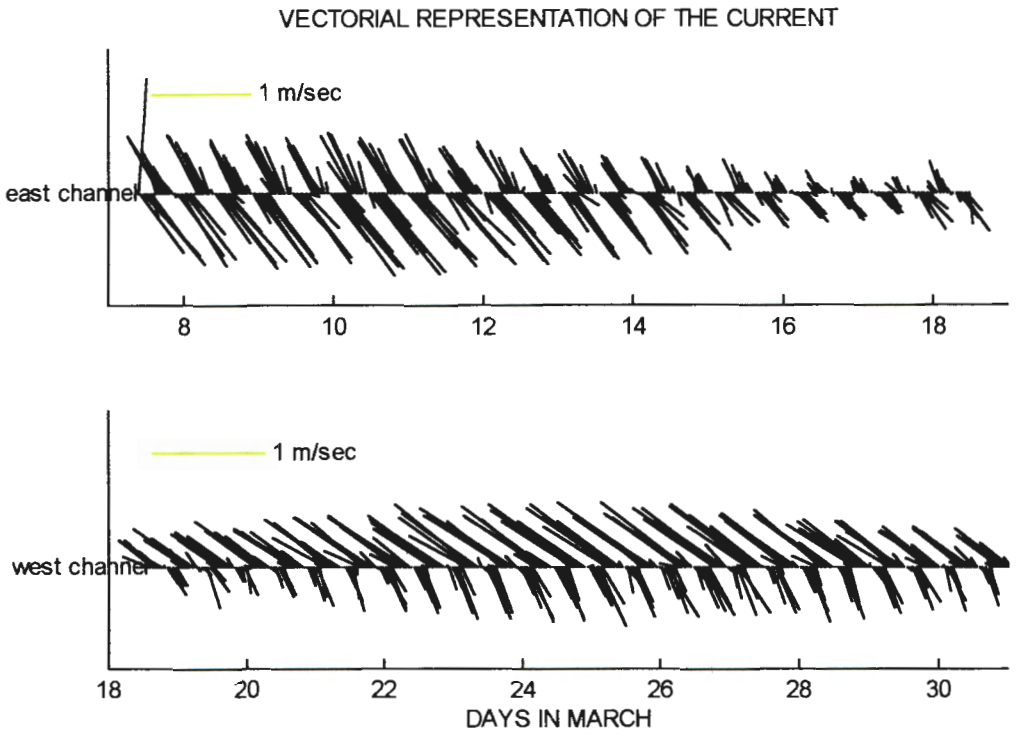

Figure 5-19:Vectorial representation of the current in the east and west channels of the lagoon inlets.

presence of a tidal residual flow, with Saldanha Bay water entering the lagoon via the eastern channel and exiting through the western channel.

In both channels, the residual current frequently attained a velocity of about 0.2 $m.s^{-1}$. In the east inlet, the low-passed time-series of the along channel current was related to changes in the tidal range with greater residual velocity during periods of spring tides. In the east channel, the lowpassed signal could also be related to waterlevel variations in Saldanha Bay. Drops in waterlevels corresponded to decreases in the amount of bay water transported into the lagoon. For example, from the 10^{th} to the 12^{th} of March, the waterlevel dropped over the bay and the lagoon and the flux of Saldanha Bay water into the east inlet decreased (figure 5-25). After the 12^{th} of March, the waterlevel rose in Saldanha Bay and the strength of the residual flow at the east inlet of the lagoon decreased (less water from Saldanha Bay was transported into the lagoon through the east inlet).

These current data exhibit strong variations with the tidal range. During the spring cycle and at the east inlet, the along-channel current at the ADCP location had a typical velocity of

1m.s^{-1} on the flood and 0.7m.s^{-1} on the ebb. On the neap tide, the along-channel velocity at the ADCP was reduced to values of 0.4 m.s^{-1} and 0.25 m.s^{-1} for the flood and the ebb respectively. In the western inlet, velocities at the ADCP during the spring tide were equal to 1 m.s^{-1} and 0.6 m.s^{-1} s for the outflow and the inflow respectively. On the neap cycle, ebb and flood velocities were reduced to about 0.6 m.s^{-1} and 0.4 m.s^{-1} respectively. The across channel flow was minimal during the neap tide and remained small compared to that of the along-channel flow.

Drifter experiments showed greater horizontal velocity divergence between the eastern inlet and the inner lagoon during periods of high tidal range (table 2). On the inflow of the 11th of March, the current decreased by 35% between the ADCP location and a point 3.2km into the lagoon. Past that point, the currents within the channel were not significantly attenuated. On the inflow of the 17th and the 20th of March, there was no significant decrease in the flow strength as the water was advected along the lagoon channel (table 2). Also, the ebb/flood asymmetry apparent on the ADCP current data, was reduced during the neap tide.

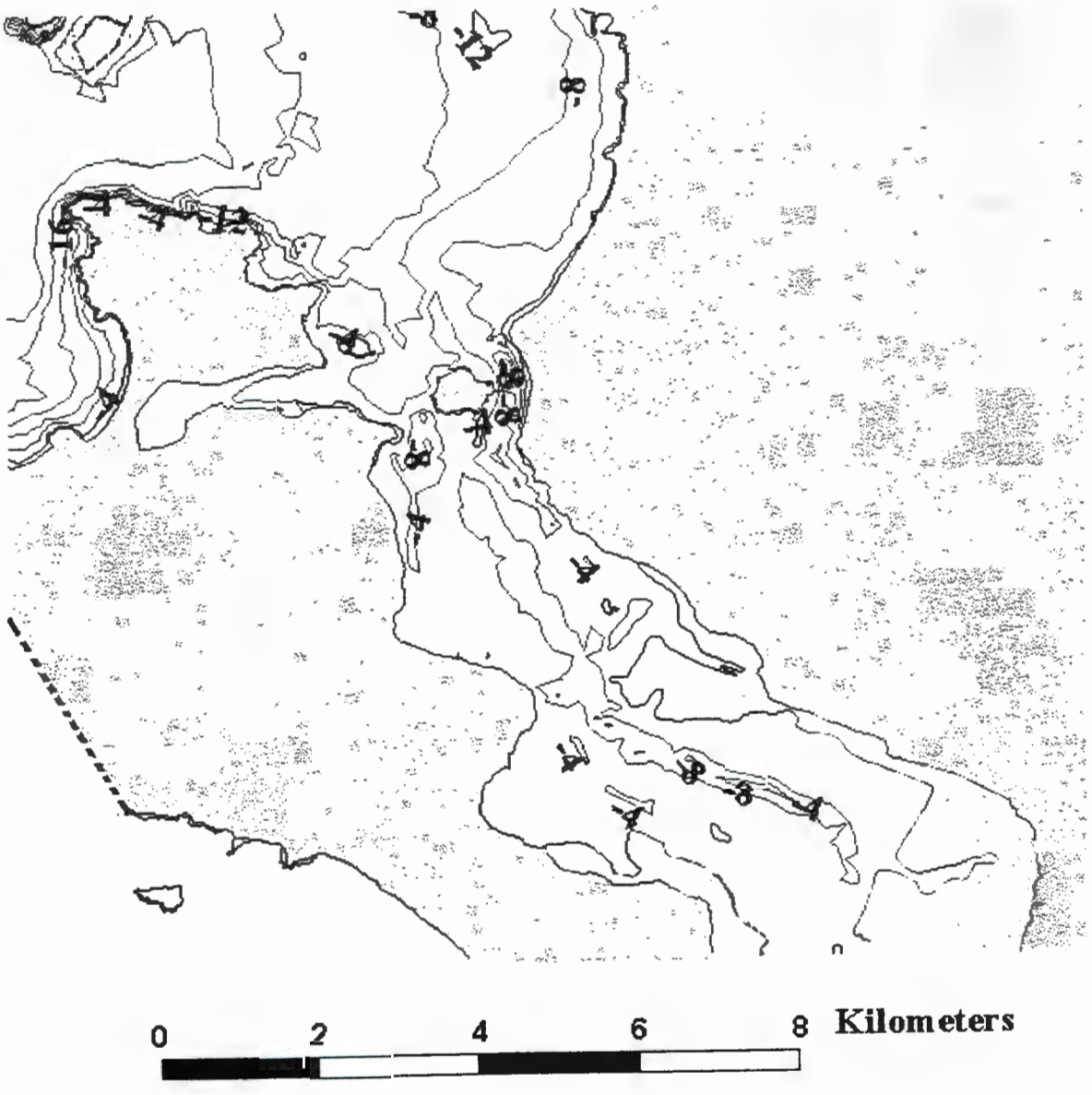

Figure 5-20: Bathymetry of Langebaan Lagoon.

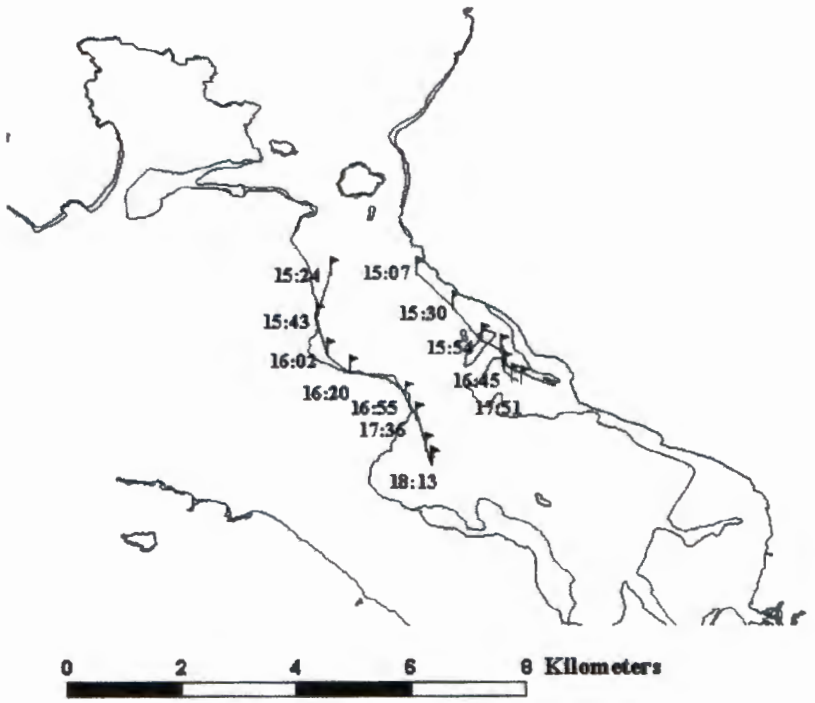

Figure 5-21: Path followed by the drifters on the inflow of the 11.03.97.

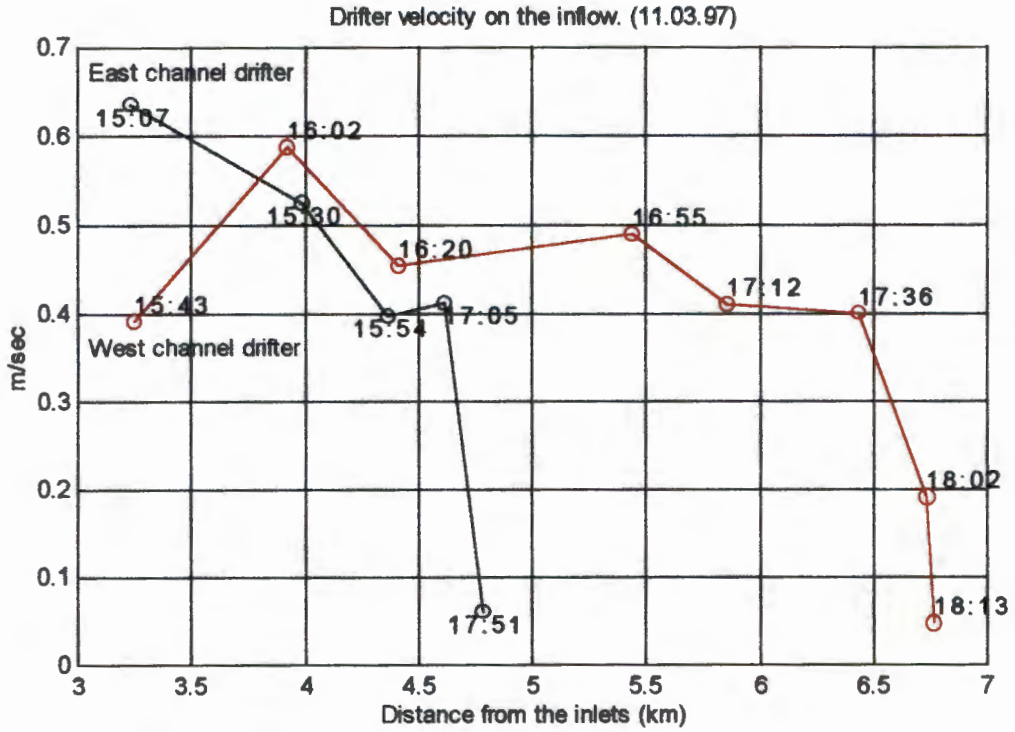

Figure 5-22: Variation of the drifter velocity on the inflow of the 11.03.97. The velocity for drifters located within the lagoon channels is plotted in a solid line. For drifters which have been advected away from the channel, the velocity is plotted in a broken line.

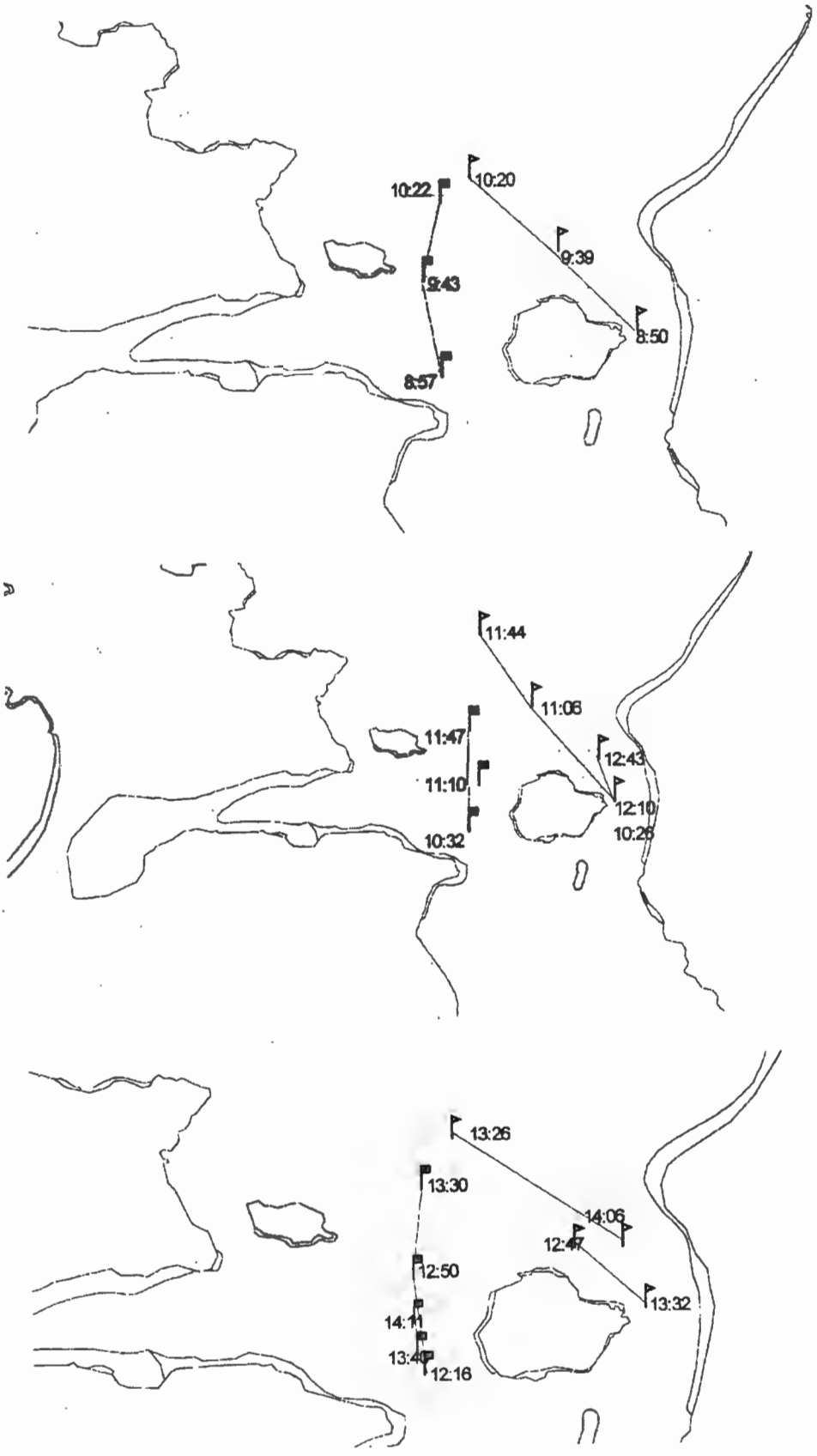

Figure 5-23: Paths followed by the drifters on the outflow of the 15.03.97.

Comparisons between drifter and ADCP current velocities on 13.03.97

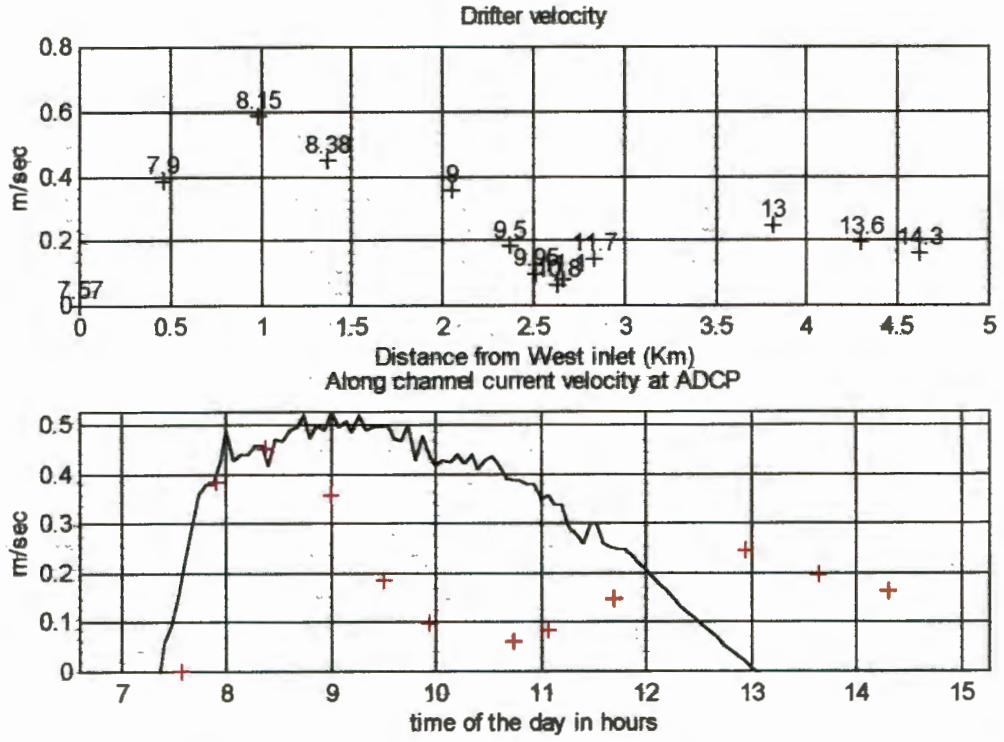

Figure 5-24: In the upper panel, surface currents speed (obtained from the drifter) is plotted as a function of distance from the east inlet. Data points are labelled with the time (in decimal hours) at which the current velocity calculation was computed. In the lower panel, the surface current measured at the ADCP in the east channel (bin depth of 2.18m) is as plotted a function of time. The drifter velocity (red crosses) are repeated in this time-series plot.

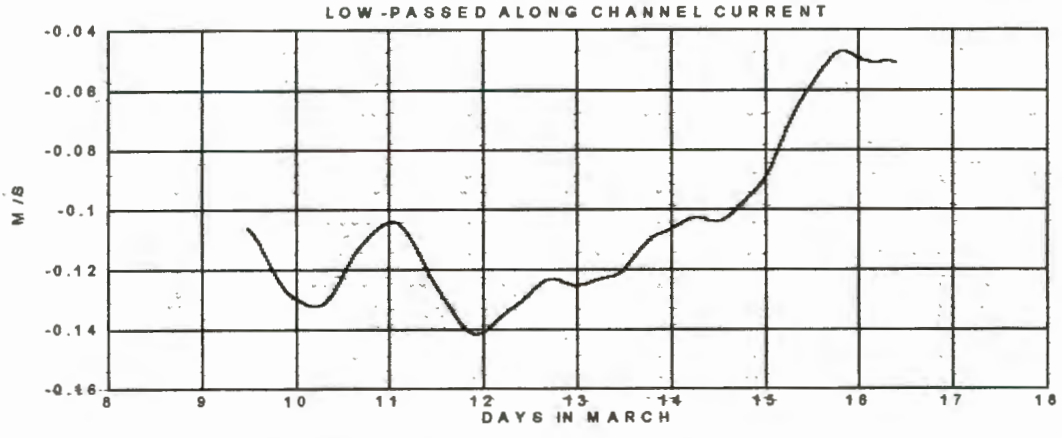

Figure 5-25: Low-passed timeseries for the along-channel component of the flow in the east channel at a bin depth of 5.18m. Negative current velocity indicates a flow into the lagoon.

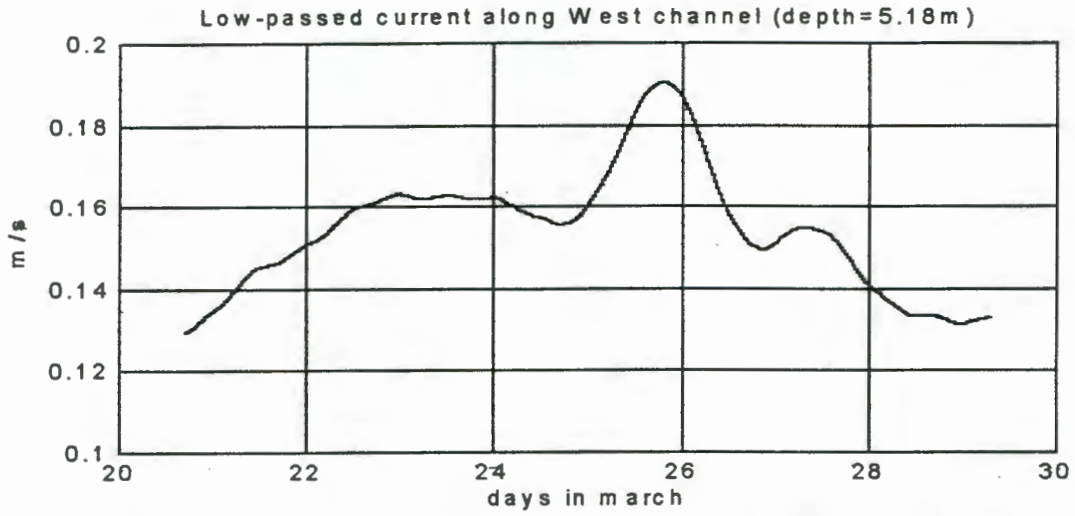

Figure 5-26: Low-passed timeseries for the along-channel component of the flow in the west channel at a bin depth of 5.18m. Positive current velocity indicates a flow out of the lagoon.

Table2:

Drifter velocity during the inflow

The velocity was calculated between two successive positions of the surface drifting buoys. Positions at which drifters grounded were not included in the calculations.

11.03.97

East channel:			West channel		
Time (hr)	**Distance (km)**	**Velocity (m/s)**	**Time (hr)**	**Distance (km)**	**Velocity (m/s)**
15:07			15:24		
15:30	0.8763	0.635	15:43	0.4458	0.391
15:54	0.7546	0.524	16:02	0.6704	0.5881
16:10	0.3824	0.3983	16:20	0.4884	0.4552
16:45			16:55	1.0299	0.4904
17:05	0.2477	0.4128	17:12	0.419	0.4108
17:51	0.1652	0.0598	17:36	0.5772	0.4009
			18:02	0.2984	0.1913
			18:13	0.031	0.047

17.03.97

East channel			West channel		
Time (hr)	**Distance (km)**	**Velocity (m/s)**	**Time (hr)**	**Distance (km)**	**Velocity (m/s)**
09:24			09:31		
10:22	0.9583	0.2754	10:15	0.995	0.3769
11:08	0.3784	0.1371	10:56	0.424	0.1724
11:51	0.1932	0.0749	11:42	0.1278	0.0463

20.03.97

East channel			West channel		
Time (hr)	**Distance (km)**	**Velocity (m/s)**	**Time (hr)**	**Distance (km)**	**Velocity (m/s)**
11:49			12:04		
13:00	1.0796	0.2534	12:44	0.7013	0.2922
13:34	0.1589	0.0779	13:30	0.681	0.2467

Drifter velocity during the outflow

13.03.97

East Channel			West channel		
Time (hr)	**Distance (km)**	**Velocity(m/s)**	**Time (hr)**	**Distance (km)**	**Velocity(m/s)**
07:34			07:41		
07:54	0.4352	0.3627	08:02	0.5568	0.4419
08:09	0.5171	0.5746	08:18	0.5121	0.5334
08:23	0.3724	0.4433	08:31	0.3587	0.4599
09:00	0.8341	0.3757	08:55	0.7503	0.5210
09:30	0.3478	0.1932	09:20	0	0
09:57	0.1668	0.103	09:48	0.6478	0.3856
10:45	0.1504	0.0522	10:16	0.5402	0.3215
11:04	0.0781	0.0685	11:33	0.7019	0.1519
11:42	0.2798	0.1227	12:03		
12:57	0.971	0.2158	13:05		
13:39	0.4987	0.1979	13:30		
14:19	0.4117	0.1715	14:06		

14.03.97

East Channel			West Channel		
Time (hr)	**Distance (km)**	**Velocity(m/s)**	**Time (hr)**	**Distance (km)**	**Velocity(m/s)**
08:05					
09:50	1.5913	0.2526	08:14		
10:25	0.2248	0.107	09:09	0.6861	0.2079
11:13	0.3308	0.1149	09:40	0.5816	0.3127
12:35	0.7605	0.1546	10:18	0.8228	0.3607
13:09	0.6554	0.3213	11:00	0.6115	0.2427
14:09	0.7632	0.212	11:51	0.4951	0.1618
14:51	0.1504	0.0597	12:41	0.2144	0.0715
mean		0.1746	mean		0.2262

15.03.97

East channel			West channel		
Time (hr)	**Distance (km)**	**Velocity(m/s)**	**Time (hr)**	**Distance (km)**	**Velocity(m/s)**
08:50			08:57		
09:39	0.752	0.2558	09:43	0.6978	0.2528
10:20	0.7622	0.3098	10:22	0.5664	0.242
10:26			10:32		
11:06	1.0847	0.452	11:10	0.4225	0.1853
11:44	0.7797	0.342	11:47	0.5006	0.2255
12:10			12:16		
12:43	0.4084	0.2063	12:50	0.5579	0.2735
12:47			13:30	0.5247	0.2186
13:26	0.8746	0.3737	13:40		
13:32			14:11	0.1896	0.1019
14:06	0.3719	0.1823			

16.03.97

East channel			West channel		
Time (hr)	**Distance (km)**	**Velocity(m/s)**	**Time (hr)**	**Distance (km)**	**Velocity(m/s)**
09:35			09:45		
10:17	0	0	10:21	0.2135	0.0988
10:50	0.1343	0.052	10:54	0.1154	0.0583
11:29	0.6608	0.2824	11:33	0.231	0.0962
11:41			11:37		
12:22	0.9149	0.3719	12:26	0.3354	0.1141
13:08	0.7625	0.2763	13:12	0.5121	0.1856
13:45	0.3892	0.1753	13:50	0.3678	0.1613
13:55			14:03		
14:26	0.3239	0.1741	14:30	0.1104	0.0681
14:58	0.0836	0.0435	15:01	0.0516	0.0278
			15:33	0.1123	0.0585

17.03.97

East channel			West channel		
Time (hr)	**Distance (km)**	**Velocity(m/s)**	**Time (hr)**	**Distance (km)**	**Velocity(m/s)**
13:52			13:11		
14:53	0.8497	0.3454	13:55	0.2224	0.0842
15:13			14:42	0.3144	0.1115
15:38	0.3932	0.2621	15:15		
16:10			15:41	0.5228	0.3352
16:45	0.4456	0.2122	16:13	0.1454	0.0757
17:25	0.1807	0.0753	16:50	0.1911	0.0861
17:56	0.0778	0.0418	17:29	0.1259	0.0538
			18:05	0.1748	0.0809

5.2 Results of the statistical analysis:

5.2.1 Spectral analysis of data:

Due to the short length of the data series, the power spectral analysis was used mainly as a means to illustrate the range of frequencies affecting the signal. Power spectrum density (PSD) plots revealed the strong predominance of the semi-diurnal frequencies. Away from the semi-diurnal band, the waterlevel data was affected by events with period longer than that of the M_2 constituent. The waterlevel and current PSD reveal the same basic features (figure 5-27). On the currents PSD plots, oceanographic events with frequencies located outside the semi-diurnal band seem to bring similar amount of energy into the signal. This illustrates the relative importance of high frequency phenomenon in shaping the velocity profiles.

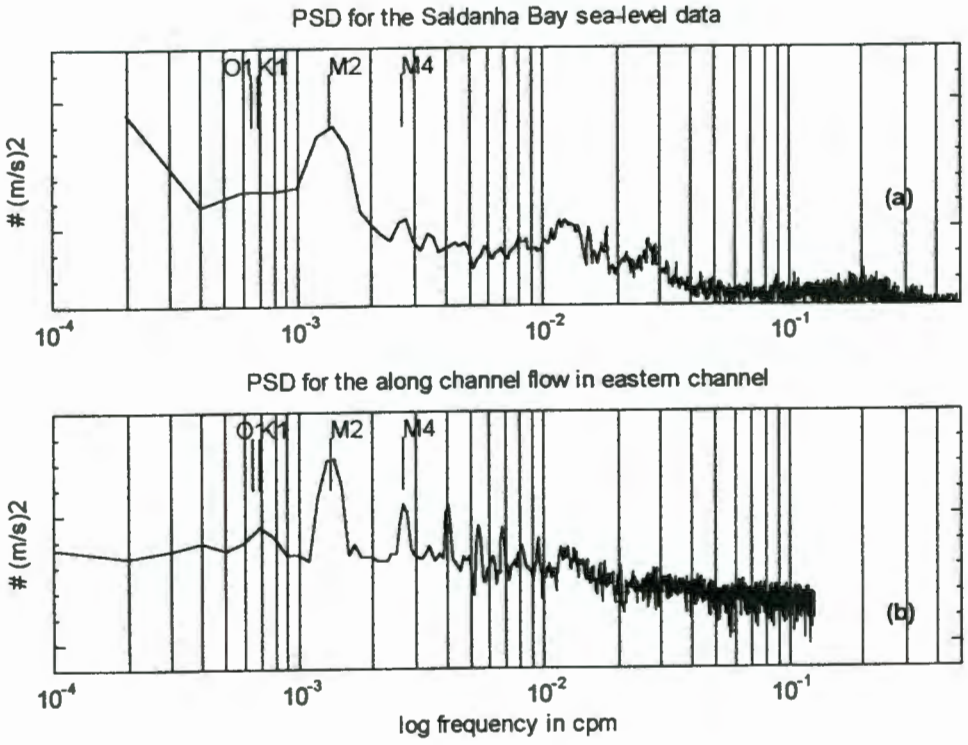

Figure 5-27: (a) Power Spectrum Density plot for the Saldanha Bay waterlevel record. (b) Power Spectrum Density plot for the along-shore component of the flow in the east inlet channel, at a bin depth of 5.18m. Both PSD plots were obtained for a frequency range of 7 days.

5.2.2 Harmonic analysis:

The results of harmonic analysis (Figure 5-28, 5-29 and 5-30) confirmed the fact that the circulation in Langebaan Lagoon is dominated by semi-diurnal forcing. Although the harmonic fit (Figure 5-28 and 5-29) closely approximates the data records for the Saldanha Bay tide and the East inlet along-channel current, it can be seen from the plots of the residuals (Figure 5-30) that the results from the harmonic analysis are significantly biased. Due to the short length of the data records, the estimation of the phase-lags between different tidal constituents was inaccurate and the separate contribution from the K_1 and O_1, M_2 and S_2 constituents could only be resolved for the Saldanha Bay tidal record. The residuals signal in Figure 5-30 shows large amount of energy at semi-diurnal periods, illustrating the fact that the phase-lags estimated through the harmonic analysis are inaccurate. Also, the substantial attenuation of the S_2 tidal constituent from Saldanha Bay to Langebaan Lagoon shows that the harmonic analysis failed to resolve the separate contribution of the K_1 and O_1, M_2 and S_2 tidal constituents in Langebaan Lagoon. According to the Raleigh criterion however, the data records were long enough to identify single semi-diurnal and diurnal species. Therefore, the 9cm amplitude attenuation of the M_2 tidal constituent from Saldanha Bay to Langebaan Lagoon, should account for the decrease in amplitude experienced by the tidal wave as it progresses from the bay to the lagoon.

In this section, the measurements obtained during the field survey of March 1997 brought us valuable insights into the processes controlling the velocity field or the temperature distribution within the Langebaan lagoon. Were it based solely on observations, our understanding of the system would be very limited since measurements can only be obtained at a few selected locations in a system exhibiting strong spatial variability. For a more accurate description of the Langebaan-Saldanha system, the following three chapters will combine previous theoretical work on coastal lagoons to our results.

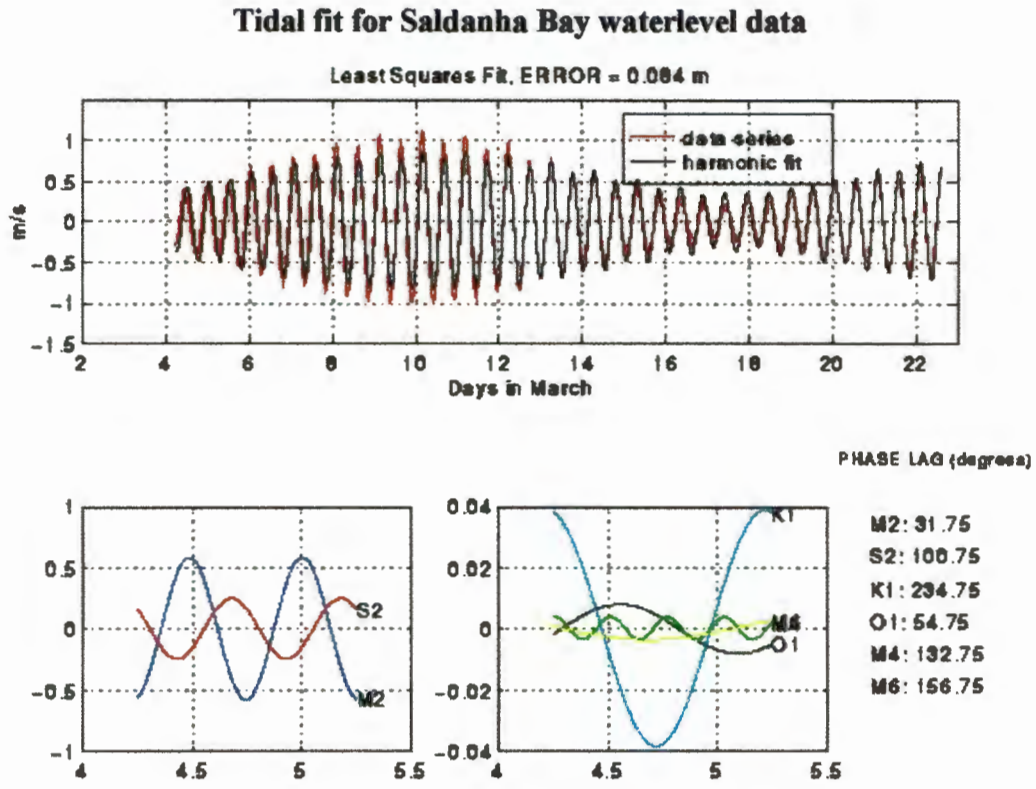

(a)

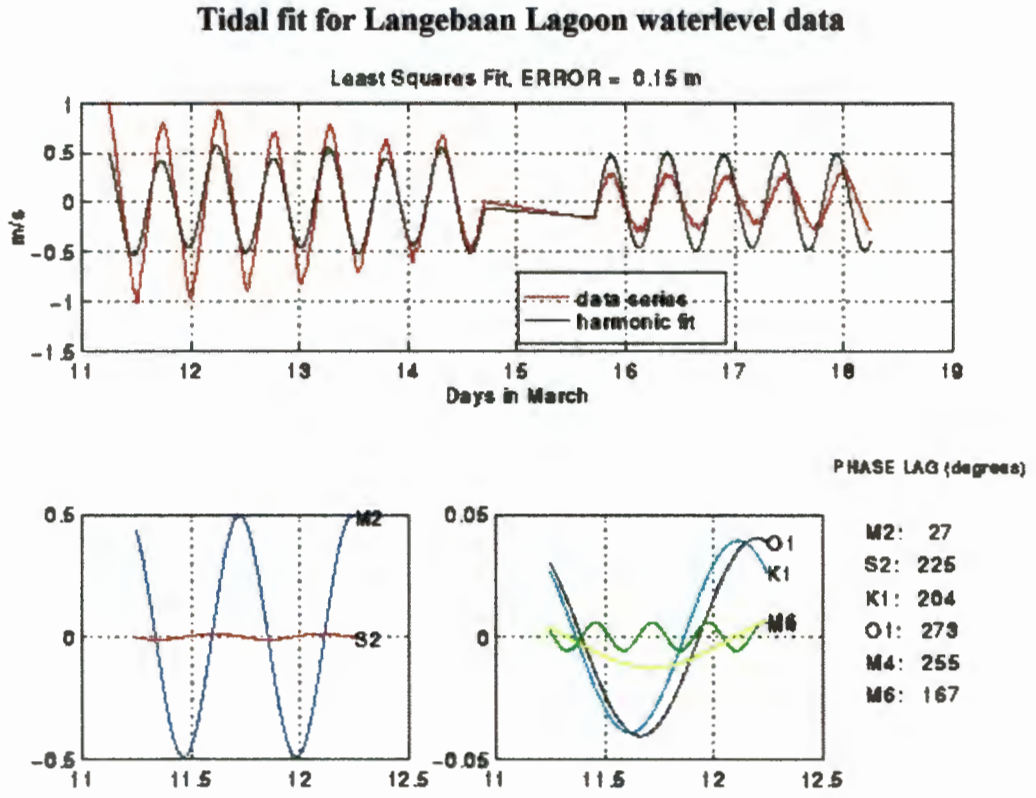

(b)

Figure 5-28: Tidal fit for the waterlevel data.

Tidal fit for the eastern inlet: along channel current, bin depth of 5.18 meters

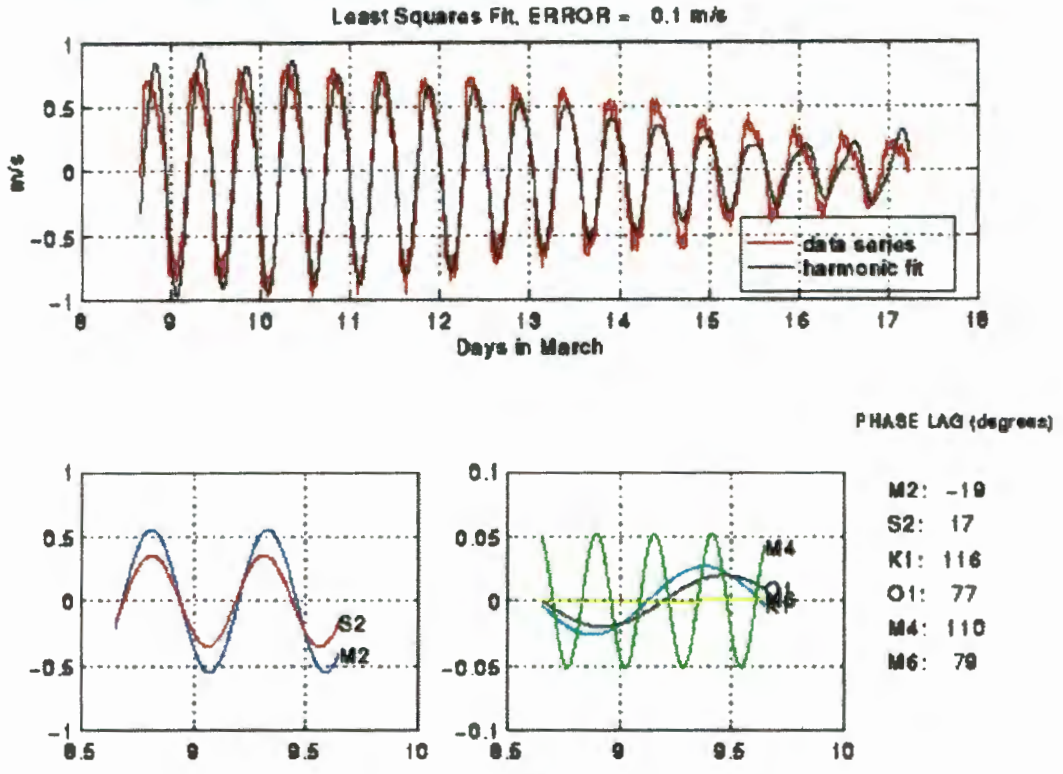

(a)

Tidal fit for the western inlet: along channel current, bin depth of 5.18 meters

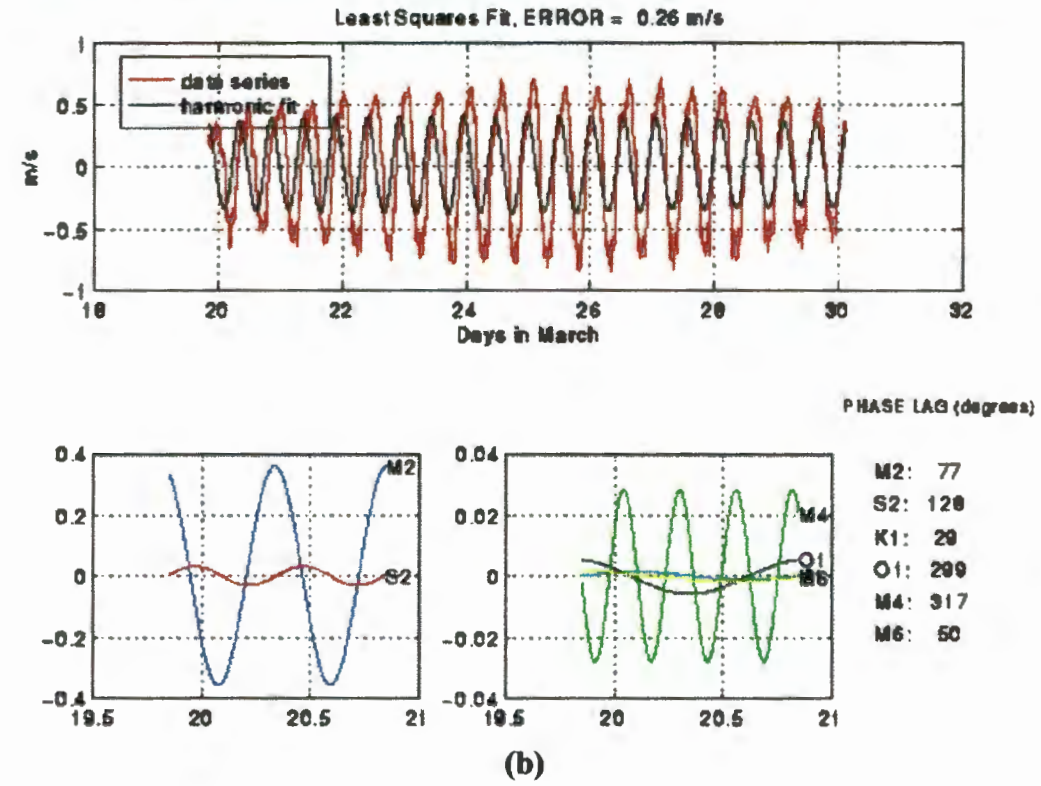

(b)

Figure 5-29: Tidal fit for the ADCP current data.

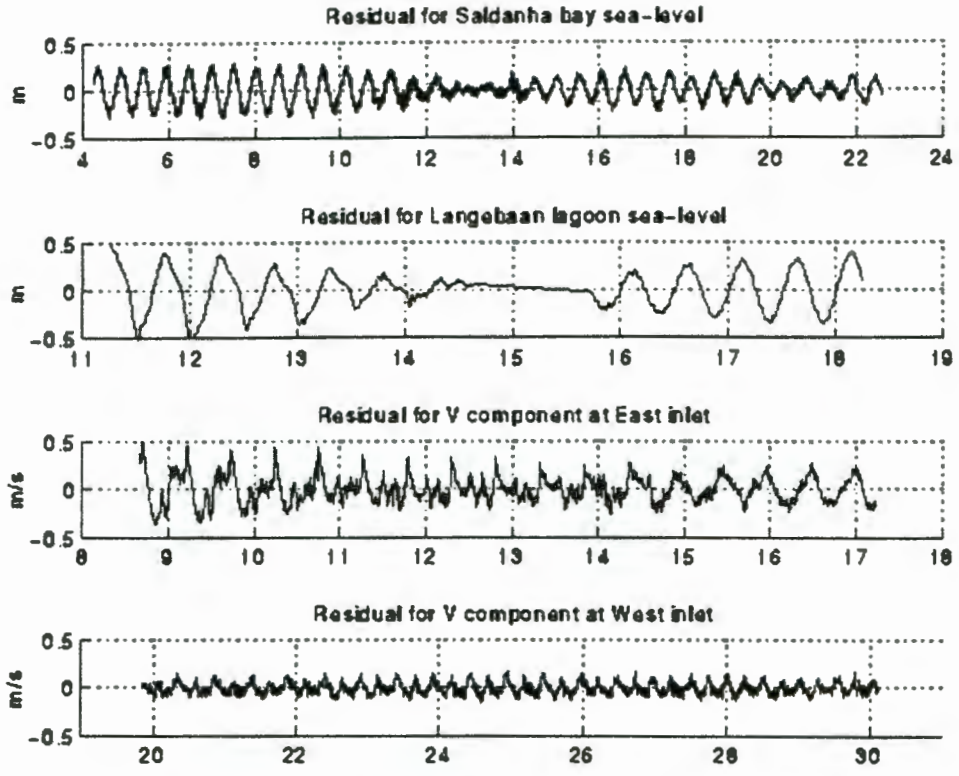

Figure 5-30: Residuals obtained after subtraction of the harmonic fit to the data records.

6. Water-level fluctuations in Langebaan Lagoon

Mixing and exchange between Langebaan Lagoon and Saldanha Bay strongly depend on the hydrodynamics at the lagoon entrance. It was noted in Chapter 3 however, that the waterlevels or density differences at the lagoon-bay interface are influenced by the circulation and the density properties of the lagoon basin. In Chapter 5, a strong relationship between waterlevel, current and temperature was observed at all sampling locations. The properties of the water-column at the lagoon entrance and within the lagoon basin, depend critically on waterlevel fluctuations experienced in the lagoon. A better understanding of the circulation in the Langebaan-Saldanha system can be achieved by addressing the problem of waterlevel changes in Langebaan Lagoon. In this section, we will consider waterlevel fluctuations arising in the lagoon as a result of tidal or low frequency forcing, before assessing how changes in the lagoon basin elevation affect the hydrodynamics at the lagoon entrance.

6-1 Tidal variations of water-levels in Langebaan Lagoon basin:

Several studies have been conducted in order to determine how waterlevel in a coastal lagoon responds to tidal forcing at the mouth. Some of this work is reviewed in Chapter 3. Often, waterlevel in coastal lagoons varies uniformly in a pumping or Helmholtz mode response and tidal inlets act as hydraulic low-pass filters, reducing the tidal amplitude and inducing a phase-lag between the ocean (or neighbouring bay) and the lagoon (Pugh, 1979; Mehta and Ozsoy, 1978).

Measurements provide us with some information on the set-up of the waterlevels near the lagoon mouth and within the interior basin. The results from the harmonic analysis conducted on the waterlevel data gathered in Saldanha Bay and in the southern part of the lagoon, showed a 9cm reduction in the M_2 amplitude between Saldanha Bay and the lagoon. However, the slight attenuation in the amplitude of the major tidal constituents at tidal and sub-tidal frequency is not directly visible on the time-series plots (figure 5-13). This shows that the amplitude attenuation experienced by the tidal wave as it propagates

from Saldanha Bay to the lagoon is, if existent, very small. Since the phase lags predicted through the harmonic analysis were not accurate, the lag between the tide in Saldanha Bay and Langebaan Lagoon was calculated directly from the data records. It was found that the lag between the tide in Langebaan Lagoon and Saldanha Bay depended upon the tidal range. During neap tides, the lagoon tide lagged that in the bay by about 16min, while during the spring cycle, the phase lag between the tide in the lagoon and in the bay increased to 49min on average, reaching a maximum of 1hr15 at spring low tide. From the time-series plots we can conclude that the tidal wave propagates into the lagoon with no significant attenuation in amplitude and that the lags between Langebaan Lagoon and Saldanha Bay tide are a function of the tidal range.

To gather information on the lateral variation of the waterlevel within the lagoon basin comparisons between the onset of the inflow and of the outflow at each of the lagoon inlets with the high and low tide in Saldanha Bay were made. Calculations made from the time-series showed that there was no evidence that the tidal wave reached one side of the lagoon's entrance before the other (figure 6-1 (a)) - it appears that the tidal wave reaches both inlets approximately at the same time. During the ebb, the timelag between the onset of the outflow at the inlets and the high tide in Saldanha Bay seems to show that Langebaan Lagoon water was expelled through the western inlet first (figure 6-1 (b)). Such a feature suggests that during the ebb, the lagoon surface does not drop uniformly over the basin and an West-East pressure gradient exists in the lagoon.

Due to the short length of the water-level record obtained for the lagoon, it is difficult to assess how Langebaan Lagoon responds to waterlevel fluctuations occurring within Saldanha Bay. In Langebaan Lagoon, we might wonder if the magnitude attenuation and the tidal phase lags are induced by the presence of two narrow inlets at the entrance of the lagoon, or if they result from the interaction of the tidal wave with the bathymetry in the lagoon basin. To better understand how the water level fluctuates in the lagoon and what controls these fluctuations, previous analytical theories are combined to observations.

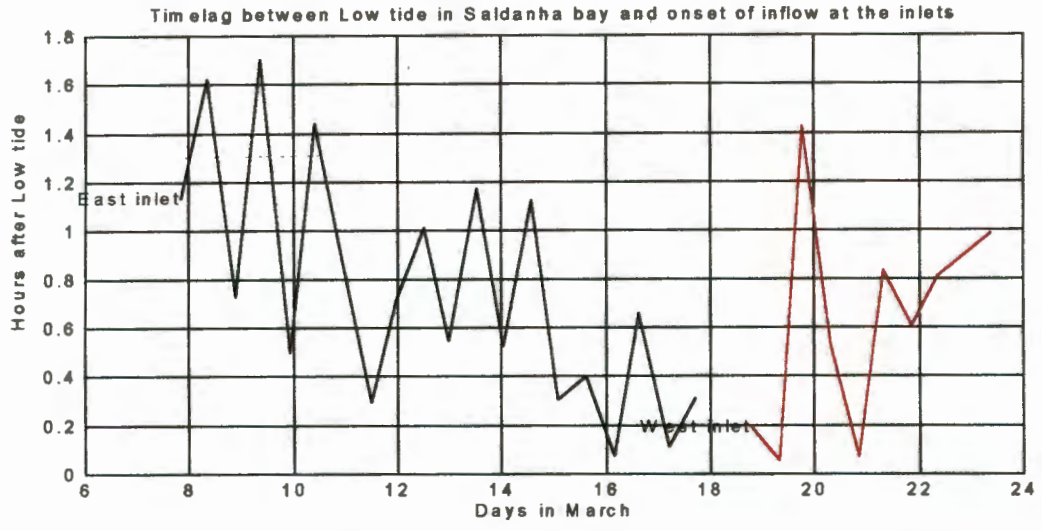

(a)

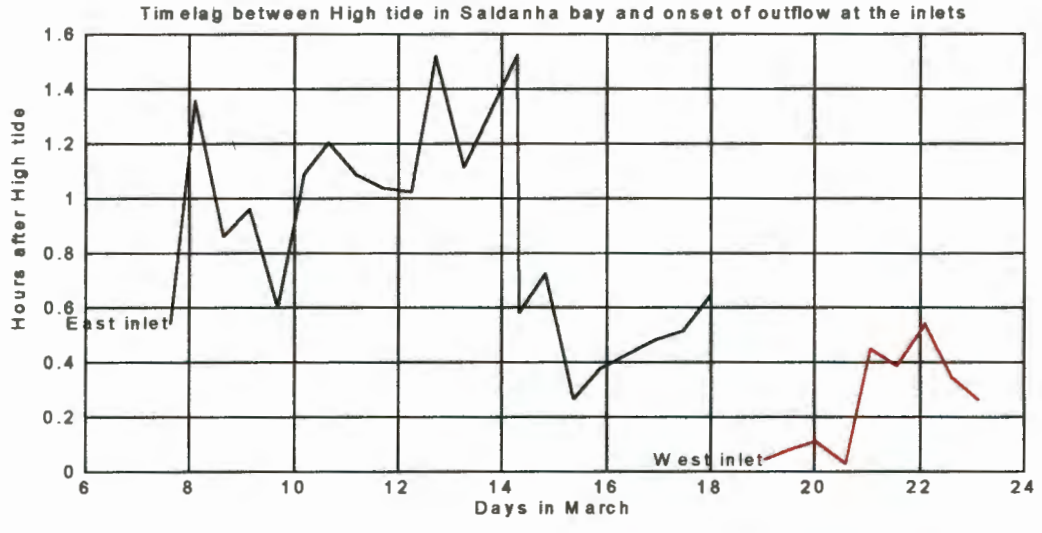

(b)

Figure 6-1: (a) Timelag between low tide in Saldanha Bay and the onset of the inflow at the Lagoon's inlets. (b) Timelag between high tide in Saldanha Bay and the onset of the outflow at the Lagoon's inlets.

According to previous findings, the amplitude and the phase-lag between Langebaan Lagoon and Saldanha Bay tidal constituents should depend essentially on three parameters: the Helmholtz frequency F_h (defined in equation 3-1), the frequency of the forcing tide $\omega = {}^{2\pi}/_{T}$ (where T is the period of the forcing tide) and the maximum dimension of the lagoon basin compared to the wavelength of the forcing frequency. The dimensionless forcing frequency as defined by Ozsoy (1977) is

$$\alpha = \frac{\omega}{F_h} \qquad \text{eq. 6-1}$$

For purpose of analysis, we assume that Langebaan Lagoon can be considered as a one-inlet system, with a cross-sectional area equal to the sum of the two inlets cross-sectional areas, and a length equal to the average length of the two inlets. Previous study (DiLorenzo, 1988) showed that for $\alpha < 0.1$, the rise and fall of the lagoon surface closely approximate that of the adjacent bay independently of damping. As α becomes greater than 0.1, the inlet serves as an increasingly effective filter. It is also seen from equation 6-1, that high frequency tides will experience larger amplitude attenuation and phase-lags as they propagate into the lagoon. In the Langebaan-Saldanha system where semi-diurnal tides dominate, the maximum dimension of the basin is small (<10% of the forcing wavelength) and the value of α associated with the M_2 tide is $\alpha = 0.11$. Water-levels are therefore expected to rise nearly simultaneously in Saldanha Bay and Langebaan Lagoon and tides should suffer no significant amplitude attenuation as they propagate into the lagoon. To confirm these assumptions, further analysis was conducted on the filtering capacity of the lagoon inlets using the findings of Spaulding (1994). Spaulding derived an empirical solution for surface elevation within a coastal lagoon. His method is based upon the assumption that the filtering capacity of the inlet depends primarily on one single parameter, the frictional dissipation term, which can be correlated to the elevation response of the lagoon basin. The non-dimensional frictional dissipation term is expressed as:

$$G_3 = \frac{L}{h}\left(\frac{A_l}{A_c}\right)^2 \frac{\eta_0}{gT^2} \qquad \text{eq. 6-2}$$

where A_l is the surface area of the lagoon, A_c is the inlet cross-sectional area, L is the inlet length, h is the depth average at the inlet, T is the period of the forcing tide and η_0 is the amplitude of the tide in the ocean (or adjacent bay). The amplitude response of the lagoon and the high and low water phase lags can be obtained by fitting a polynomial power series to G where

$$\log G = \frac{1}{\sqrt{G_3}} \qquad \text{eq. 6-3}$$

For small values of G, the inlet acts as a filter, decreasing the amplitude of the tidal wave and inducing phase lags between the lagoon and the neighbouring bay or ocean. As G increases, the filtering efficiency of the lagoon inlet decreases, until at a value of G = 1 or larger, sea-surface perturbations travel unimpeded through the inlet. A value of G = 4.21 was found for Langebaan Lagoon. Results obtained with the method of Spaulding show that water-level fluctuations travel through the Langebaan Lagoon inlets, with no attenuation in magnitude or induced phase-lags.

According our simplified model, the geomorphology of the lagoon mouth does not induce the phase-lags and the magnitude attenuation observed in the lagoon water-level record. The alteration of the tidal wave as it propagates from Saldanha Bay to Langebaan Lagoon must therefore result from the interaction of the tidal wave with the bathymetry of the lagoon basin. We may also note that the presence of two, rather than one inlet at the mouth of Langebaan Lagoon might explain some of the changes imposed on the tidal wave as it propagates from the bay to the lagoon. When the tidal range is high, the surface area of Langebaan Lagoon changes significantly over one tidal cycle due to the presence of numerous sand-banks and saltmarshes. Previous studies (Speer et al., 1991) revealed that when the surface area of a coastal lagoon changes substantially over a tidal cycle, longer lags can occur at high or low water. When the tide rises into Langebaan Lagoon, water first has to fill up intertidal areas and as a result, high waters occur later in the lagoon than in the bay. During the ebb, the frictional interaction of the tidal currents with the lagoon bed induces significant lags between the times of low waters in Langebaan Lagoon and in Saldanha Bay. The slightly longer duration of the ebb during periods of high tidal range indicates that the lagoon tide suffers greater distortion from bottom friction effects than from the presence of intertidal storage areas

Observations suggested that during the ebb, a West-East pressure gradient might exist in the lagoon basin. It is believed that the variable topography of the lagoon and the different properties of the tidal inlets contribute to the fact that waterlevels do not rise or drop uniformly over the whole lagoon. Tides propagate faster in deep waters, hence during the flood, the lagoon surface rises faster over the deep channels than over the shallow regions. Similarly during the ebb, waterlevels drop faster over deeper sections of

the lagoon. The effect of variable depth contours on the set-up of the pressure gradient is illustrated in figure 6-2.

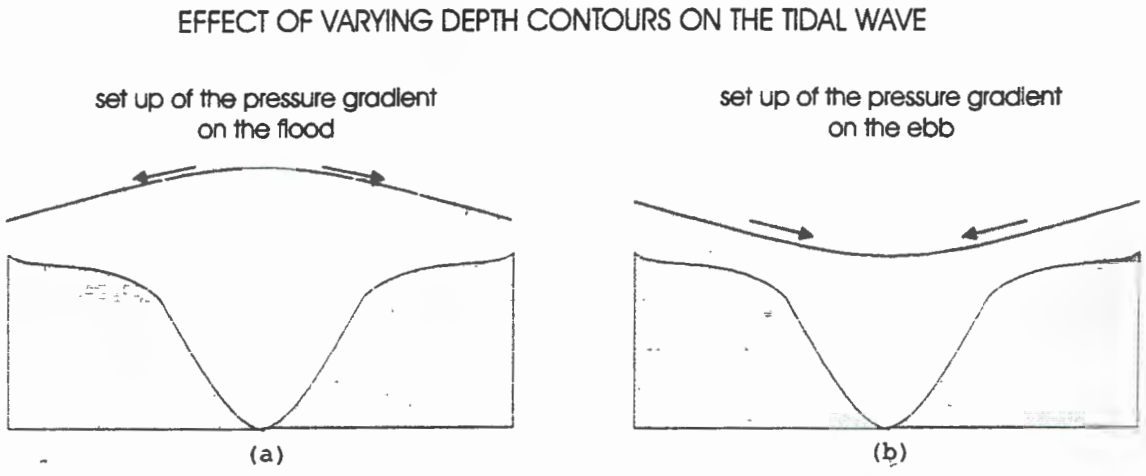

Figure 6-2: Pressure gradient resulting from the propagation of the tidal wave over variable depth contours from Chadwick and Morfett (1993).

When the tide interacts strongly with the lagoon bed, the retarding effect of bottom friction on the tidal currents exceeds the circulation driven by the pressure gradient and stronger currents are found in the channel. Drifter data collected in Langebaan Lagoon showed that during the flood, tidal currents experienced strong velocity loss as soon as they were advected away from the main channel. Such results underlie the predominant effect of bottom friction on the tidal currents. It is thus expected that in Langebaan Lagoon, the tide rises or drops more quickly over the deeper sections of the lagoon. The propagation of the tide should therefore be significantly retarded over the southern section of the lagoon, where extensive inter-tidal areas surround the main channel. The presence of two tidal inlets at the Langebaan Lagoon mouth could also influence the set-up of the water slope within the lagoon basin. The east inlet which is longer and narrower than the west inlet acts as a more efficient hydraulic filter. Tidal propagation might hence be retarded over the eastern section of the lagoon due to the constricting influence of the east inlet.

6.2 Subtidal and supertidal water-level fluctuations in the lagoon :

The waterlevel records showed that tides in the lagoon and in the bay are subject to high frequency forcing. The variations induced by high frequencies on the waterlevels was particularly noticeable during periods of small tidal range, when the strength of semi-diurnal forcing decreased. The shape of the tidal curve in Saldanha Bay was more 'bumpy' than in the lagoon, indicating that high-frequency events have a higher amplitude in the bay (figure 5-13). The subtidal fluctuations observed on the Saldanha Bay waterlevel record had periods of approximately 3 to 4min. These waterlevel fluctuations could result from edge waves which are fed by the swell. Langebaan Lagoon is sheltered and is therefore less subject to the influence of the swell. The waterlevel record obtained in the lagoon did not exhibit such rapid fluctuations. In the lagoon, high frequency fluctuations occurred over the neap tide. These high frequency fluctuations of the lagoon water-level probably reflect on the growth of compound tides due to the non-linear interaction of the tidal wave with the lagoon bed. The waterlevel records showed no evidence of a seiche.

Both the model and the observations showed that low-frequency waterlevel fluctuations propagated into the lagoon unimpeded. According to Garvine (1985), the wind's influence on the sea-level variations inside a bay or lagoon, results mainly from remote atmospheric fluctuations acting over the adjacent shelf. The local wind thus has minimal consequences on waterlevel fluctuations within the lagoon and can either contribute or act against the remote wind effect. Over the South-African west coast, the waterlevel fluctuates in the presence of upwelling and downwelling winds, or with the passage of coastal trapped waves (Shannon, 1985). In the presence of southerly winds, which dominate over the austral summer and drive the upwelling of the Benguela system, the coastal sea-level will slope downward toward the coast and the lagoon surface will drop. On the contrary, downwelling favourable winds will produce a rise of the waterlevel within the lagoon. The passage of coastal trapped waves along the South-African west coast will also generate a synoptic rise and drop of the waterlevels within the Saldanha Bay-Langebaan Lagoon system. Low-frequency variations of the waterlevel could not be related to the winds obtained at the Geelbek weather station. However, it appears that

synoptic variations of the waterlevels in the lagoon and in the bay resulted from atmospheric forcing occurring at Cape Colombine. Southerly winds (such as those occurring from the 10th to the 12th of March) induced a drop of the waterlevel in the lagoon and in the bay. Conversely, northerly winds were associated with a rise of the waterlevel (figures 5-12 and 5-14 (b)). Hence it seems that waterlevel variations in the bay and in the lagoon result mainly from remote atmospheric forcing occurring over the adjacent ocean. Atmospheric measurements at the Geelbek weather station indicated the predominance of south-easterly winds. Although those local winds did not seem related to variations in the Saldanha Bay waterlevel data, it is very likely that the waterlevel in Langebaan Lagoon would be affected by strong local winds. Previous study (Smith, 1990) suggested that even relatively light winds of 5-10m.s^{-1} could generate slopes in the free surface of the lagoon on the order of 0.5cm.km^{-1}. In Langebaan lagoon, where south-easterly winds are parallel to the longitudinal axis of the basin, the rise and fall of the waterlevel will be especially pronounced. The primary effect of the wind will be to set an upwind directed slope in the free surface of the lagoon. The resulting transport will be directed downwind in the surface layer of the water column, and upwind in the bottom layer or in the deeper waters along the middle of the lagoon. With longer records a more precise spectral analysis of the lagoon waterlevel could be conducted. This would allow one to estimate with more accuracy the effect that diurnal forcing by the wind has on the lagoon. Seasonal variations of the waterlevel can also occur. In winter, significant amounts of freshwater might be input into the Langebaan lagoon as a result of groundwater seepage or precipitation. It is believed that waterlevel in the lagoon will not be significantly raised by precipitation, as the water input into the system would quickly get flushed away by strong tidal currents. However, it is possible that a slightly greater waterlevel would be observed in the lagoon than in the bay, as a result of the lower density encountered over the lagoon basin.

6.3 Implications of variations in waterlevel in the lagoon on the hydrodynamics at the mouth:

Significant insight has been gained on the response of Langebaan Lagoon to barotropic or atmospheric forcing. Let us now consider how conditions at the lagoon entrance are affected by the waterlevel response of the lagoon basin.

During periods of weak tidal range, the free surface of the lagoon rises and drops with a slight lag with the Saldanha Bay tide and no apparent reduction in the tidal range. The distortion induced by the lagoon topography on the tide is weak and waterlevels fluctuate uniformly over the entire lagoon (figure 5-13). According to our theoretical analysis, the magnitude and the phase of the currents at the lagoon mouth should be approximately the same for both inlets. Observations show that during periods of high tidal range, there exists a significant phase lag between the tide in Saldanha Bay and in Langebaan Lagoon, with the tidal range suffering no significant attenuation. Data also show that in the lagoon, the duration of the ebb was slightly greater than that of the flood. It is thought that as the tidal range increases, the lagoon experiences longer ebbs than floods because the distortion imposed by bottom friction on the tidal wave exceeds that resulting from the presence of intertidal areas. The delay in the elevation response of the lagoon to tidal forcing in Saldanha Bay might cause significant phase lags between currents in the bay and in the lagoon. Lagoon water might be flowing with the ebb currents as the tide is rising in Saldanha Bay. Similarly, flood currents might be observed in parts of the lagoon when water in Saldanha bay is already being advected by ebb currents. During spring tides, the variability of the depth contours within the lagoon basin and the different filtering capacity of the two tidal inlets are expected to affect the propagation of the tidal wave. The larger intertidal areas in the south-eastern part of the lagoon and the more effective hydraulic filter imposed by the east inlet on the tides, should contribute to delays in the propagation of tidal fluctuations over the eastern section of the lagoon. A west-east energy gradient would result in the interior of the lagoon and the outflow of water would not occur simultaneously at both inlets. During periods of high tidal range, the ebb currents are therefore expected to be stronger and start sooner at the western inlet. Although insufficient data was collected to underlie the

presence of a west-east energy gradient within the lagoon basin, according to Flemming (1977) the disposition of the bedforms in the lagoon basin, with most intertidal flats and almost all salt marshes along the southeastern margin of the lagoon, supports the hypothesis that such energy gradient exists.

Low frequency events induced similar waterlevel fluctuations in both the bay and the lagoon (figure 5-14 (b)). However, it was noted that in the event of strong local winds, the waterlevel would fluctuate to a greater extent in the lagoon than that of the bay. Southerly winds should induce a residual circulation directed toward Saldanha Bay in the upper part of the water column with a return residual current in the deep sections of the channel. As a result, cold bay water would be advected toward the lagoon below a layer of warmer lagoon water and stratification would increase at the lagoon mouth. Northerly winds would have the opposite effect, generating a surface flow toward the lagoon and increasing the water-level over the salt-mash areas. Due to the shallow nature of Langebaan Lagoon it is very unlikely that in the presence of northerly winds, a return flow directed toward Saldanha Bay occurs in the lagoon basin. During the winter months, heavy rains would affect the density structure of Langebaan Lagoon. Significant input of freshwater (from rain or freshwater seepage) into the system would induce a higher waterlevel in the lagoon than in the bay. At the tidal inlets, the density of the water column would be reduced and the pressure gradient within the lagoon would favour the surface transport of lagoon water toward Saldanha Bay.

7. Tidal currents at the lagoon-bay interface

This section aims to build upon our observations and theoretical work undertaken on tidal inlets to define how water is advected in and out of the Langebaan Lagoon system. The transport of pollutants, nutrients and sediments in and out of the lagoon, or the impact of the Langebaan Lagoon effluent on Saldanha Bay result from the properties of the inflow and outflow at the lagoon-bay interface.

The properties of the tidal currents at Langebaan Lagoon inlets strongly depend upon the magnitude of the discharge, which reaches a maximum at spring tides and a minimum at neap tides. Based upon our measurements, we will first estimate the maximum and minimum water fluxes occurring through the lagoon mouth, before assessing the nature of the tidal inflow and outflow through each of the inlets. The effect of winds, baroclinic forcing or topographic boundaries on the tidal circulation will also be examined.

7.1 Water fluxes through the lagoon inlets:

To estimate the water fluxes through the inlets, it is assumed that the channel can be separated into a region with current velocity that was measured at the ADCP and a bottom boundary region, within which the velocity decreases logarithmically towards zero at the bottom. The flux of water Q through the inlets is then computed from equation

$$Q = \int A_c U dt \qquad \text{eq. 7-1}$$

where A_c is mean cross-sectional area at the inlet and U is the depth averaged velocity. The cross-sectional areas of the lagoon channel are obtained by integrating 10m depth contours cells with the ARCVIEW software program. Regions of the channel with a mean depth from 0m to 1m are not included in the calculations. Those regions correspond to the spring intertidal areas which are either dry or characterised by very weak currents and do not contribute significantly to the total flux of water through the inlets. The use of a mean cross-sectional area will result in an over-estimation of the fluxes during the later stages of the ebb and an under-estimation of the fluxes during the first stages of the ebb. It is thought that the error in the flux estimates at the beginning the ebb, will balance that occurring at the

end of the ebb, since the starting and ending current velocity within the inlet are comparable. The use of a mean cross-sectional area should thus not lead to significant errors. Currents were measured by the ADCP throughout most of the water-column but no measurements could be obtained in the immediate vicinity of the sea-bed (within the first 2.32m from the bottom) due to blanking by the ADCP. A logarithmic profile is therefore fitted to region of data blanking (near the sea bed) in order to obtain the depth-averaged velocity. The depth averaged velocity U is calculated by applying a modified universal velocity defect law equation proposed by Black and Healy (1986).

$$U = 5.75u_* \log\left(0.87\frac{d}{z_0}\right) \qquad \text{eq. 7-2}$$

where u_* is the shear velocity, d is the water depth and z_0 is the roughness length. The bed geometry must be known in order to estimate the roughness length. With no particular knowledge on the sea-bed characteristics, z_0 becomes an empirical factor in optimisation of experimental or field data and can be used as a means of tuning a particular predictive model. The shear velocity is assessed by applying the Karman-Prandt equation for rough turbulent flow (Dyer, 1986).

$$\frac{u}{u_*} = 2.5\log\left(\frac{z}{D}\right) + 8.5 \qquad \text{eq. 7-3}$$

where u is the current speed at height z (given by the ADCP measurements) and D is the mean sediment diameter.

Previous study on the sedimentation processes of Langebaan Lagoon (Flemming, 1977) showed that at a height z = 1m above the sea-bed, currents were 25% weaker than at the surface. The type of sediments on the lagoon channel bed was also determined. The western channel floor was constituted by very coarse sand, while the eastern inlet seabed consisted of coarse sand at the ADCP location and medium coarse sand at the inlet entrance. According to table 3, an average diameter for the sediment would then be 1.5mm at the west inlet, 0.5mm around the east inlet ADCP location and 0.35mm at the east inlet entrance. The roughness length is estimated empirically with the aim to provide realistic values of the depth-averaged velocity. In the west channel, we expect z_0 to be very small due to the coarse nature of the sediment. In the east channel, small sand dunes can develop

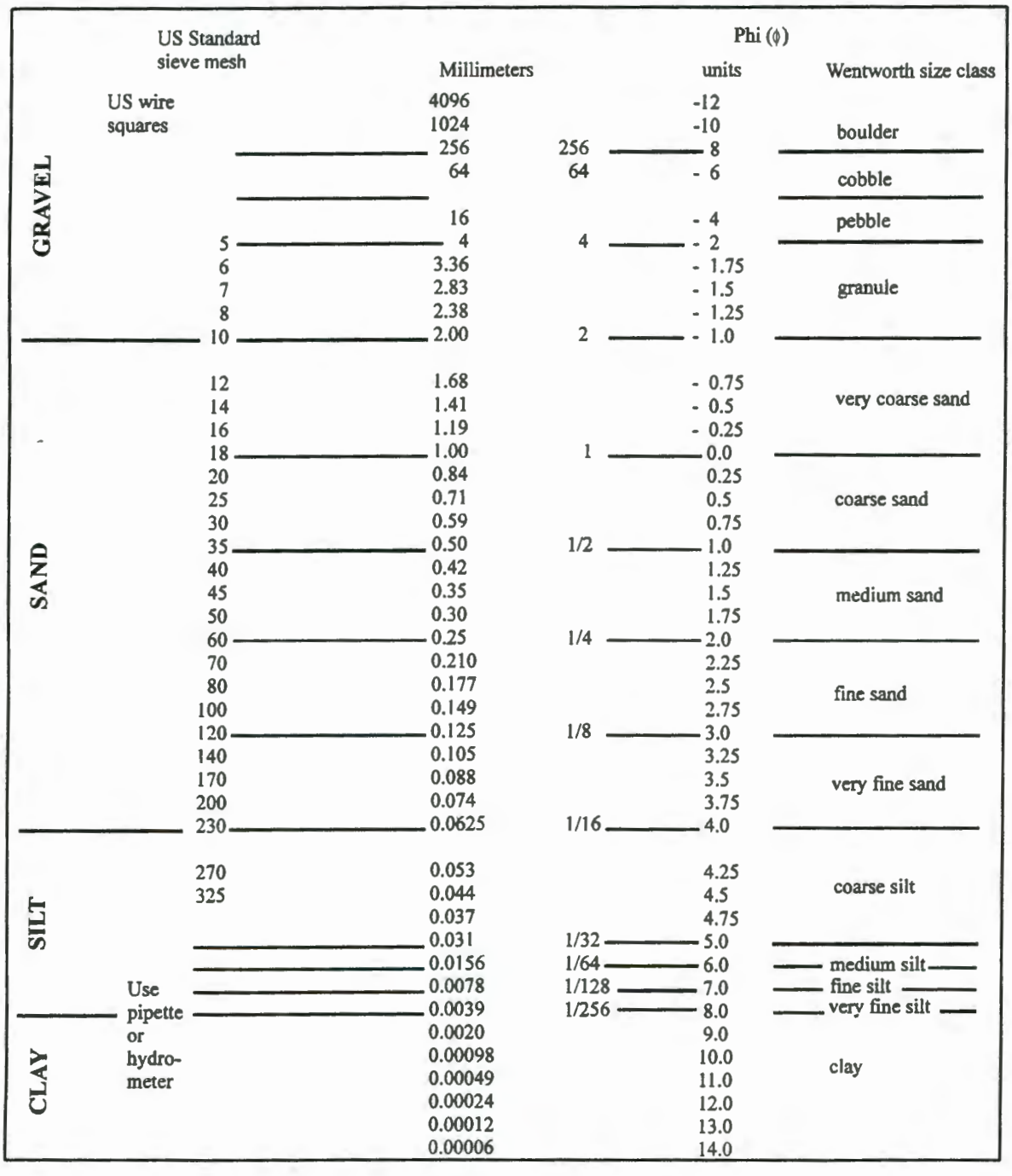

Table 3: Summary of the Udden-Wentworth size classification for sediment grains.

(Flemming, 1977) which implies that the roughness length should be greater. At the entrance of the east inlet, the sand is finer but due to the strength of the currents there, the formation of bedforms will be inhibited and the resulting roughness length should be small (Flemming, 1977). We find that reasonable values of U are obtained by setting $z_0 = 1.2D$ in the west inlet and $z_0 = 6D$ in the east channel. At the east inlet entrance, no current measurements were available. Assuming that fluxes at the ADCP and at the east channel entrance are equal, then the surface current at the east inlet entrance becomes

$$u_{inlet} = \frac{A_{inlet}}{A_{adcp}} \times u_{adcp} \qquad \text{eq. 7-4}$$

where u_{adcp} and A_{adcp} are the respective current velocity and cross-sectional area at the ADCP location and A_{inlet} is the cross-sectional area at the inlet entrance. We find that $u_{inlet} = 1 \cdot 46 \times u_{adcp}$. The depth averaged velocity at the east inlet entrance is then calculated from equation 7-2.

Once the depth averaged velocity has been obtained, it is possible to calculate the approximate flux of water through each inlet during the ebb or the flood using equation 7-1. Fluxes were calculated for the spring and the neap cycles in order to obtain maximal and minimal fluxes estimates (table 4). Discrepancies between the total inflow and outflow volumes result from the fact that current measurements in the east and the west channel were not simultaneous.

East channel	Total flux (m^3)	Maximum flux (m^3/s)	**West channel**	Total flux (m^3)	Maximum flux (m^3/s)	Sum of fluxes in east and west inlets (m^3)
Spring tide						
inflow	3.0952×10^7	2116		1.7348×10^7	1502	4.83×10^7
outflow	2.2342×10^7	1512		3.7996×10^7	2603	6.0338×10^7
Neap tide						
inflow	1.0899×10^7	818		1.015×10^7	887	2.6283×10^7
outflow	6.3084×10^6	573		1.9975×10^7	1636	2.1049×10^7

Table 4: Volumes of water advected through Langebaan Lagoon inlets during the spring and neap tides.

Note that the values obtained for the tidal prism compare favourably with that derived by Weeks (1990), who found values of 5.84 $\times 10^7 m^3$ and 1.94 $\times 10^7 m^3$ for the spring and the neap tidal cycles, respectively.

7.2 Inflow:

Following previous studies (Wolanski and Imberger, 1987; Chadwick et al., 1997) described in detail in Chapter 3, the inflow into the lagoon should resemble that of an irrotational sink providing the bottom slope in the withdrawal region is gentle. In such case, water is drawn uniformly from the offshore region and the potential lines are semi-circular arcs with velocity decreasing away from the mouth, in proportion to x^{-1} (Ozsoy, 1977). The shape of the withdrawal region thus corresponds to a portion of a circle. Using the inflow volumes calculated in section 7-1 of this chapter, the extent of the sink region L_{sink} is

$$L_{sink} = \sqrt{\frac{V_{inflow}}{w\pi h}} \qquad \text{eq. 7-5}$$

where V_{inflow} is the volume of bay water entering the lagoon during the flood, h is the mean depth over the withdrawal region and w is the portion of a circle of the withdrawal area. The mean depth of the withdrawal regions, calculated with ARCVIEW, are 4.7m and 4.3m for the east and west inlet respectively. During the spring tide, there was significant overlap between the two inlets withdrawal regions. The extent of the withdrawal zone at the lagoon mouth was hence calculated as if only one inlet connected the lagoon to the bay. A value of 0.333 was used for w. On the neap tide, there were hardly any interactions between the two inlets withdrawal zones. It was assumed that the inlets withdrew water from two separate regions. The values used for w on the neap tide were 0.5 and 0.333 for the east and the west inlet respectively. Using table 4 we obtain:

East channel	spring tide	neap tide	**West channel**	spring tide	neap tide
L_{sink} (meters)	2628	1215	L_{sink} (meters)	2628	1500

Table 5: Extent of the withdrawal area from the lagoon inlets when 'Big Bay' water is drawn into the lagoon during the flood.

In an environment with a quickly varying bathymetry, the shape of the flood withdrawal zone and the associated velocity distribution might become affected by local gradients in waterlevels or bottom friction. The extent to which the flood withdrawal region becomes affected by a rapidly varying bathymetry, depends upon the influence of bottom friction on the pressure-gradient induced circulation. When the effect of bottom friction dominates, the deeper sections of the withdrawal region are associated with stronger currents and as a consequence, water is drawn from farther offshore. In Chapter 6, it was seen that tidal currents in Langebaan Lagoon were strongly influenced by bottom friction and as a consequence, the channel regions were characterised by stronger flows throughout the tidal cycle. It is therefore likely that during the flood, the west inlet withdrawal zone extends slightly further offshore than predicted, with most of the water originating from the channel region. Ambient currents will also alter the properties of the inflow. Wolanski (1987) showed that the combined effect of a deepening shelf and an ambient longshore flow, results in the selective withdrawal of water from the region offshore and up current of the entrance.

The ADCP transect undertaken by the CSIR across Langebaan Lagoon mouth provides us with some insights on the current distribution on the flood (figure 7-1). One kilometre from the lagoon entrance, the west inlet draws water uniformly over the channel width. Flood currents have a southerly direction and a velocity approximately equal to $0.3m.s^{-1}$. As water is advected through the west inlet, the flow narrows and accelerate due to the reduction of the channel width and current velocities of approximately $0.8m.s^{-1}$ are reached. Flood currents in the vicinity of the west inlet are strongly affected by the channel topography. The geometry of the west inlet withdrawal zone should reflect the strong horizontal variations observed in the velocity field and we therefore expect that most of the water withdrawn by the west inlet will originate from the channel. The withdrawal of water by the east inlet seems to approximate more closely that of a potential sink. Currents are directed toward the centre of the inlet in a south-easterly direction and have a greater magnitude in the centre than in the periphery of the withdrawal zone. Similarly to the west inlet, the flood currents in the east inlet are affected by changes in the channel geometry. The advection of water through the east inlet is associated with a widening and a slackening of the flow with current velocities dropping from $0.8m.s^{-1}$ to $0.5\text{-}0.6m.s^{-1}$ (figure 7-1).

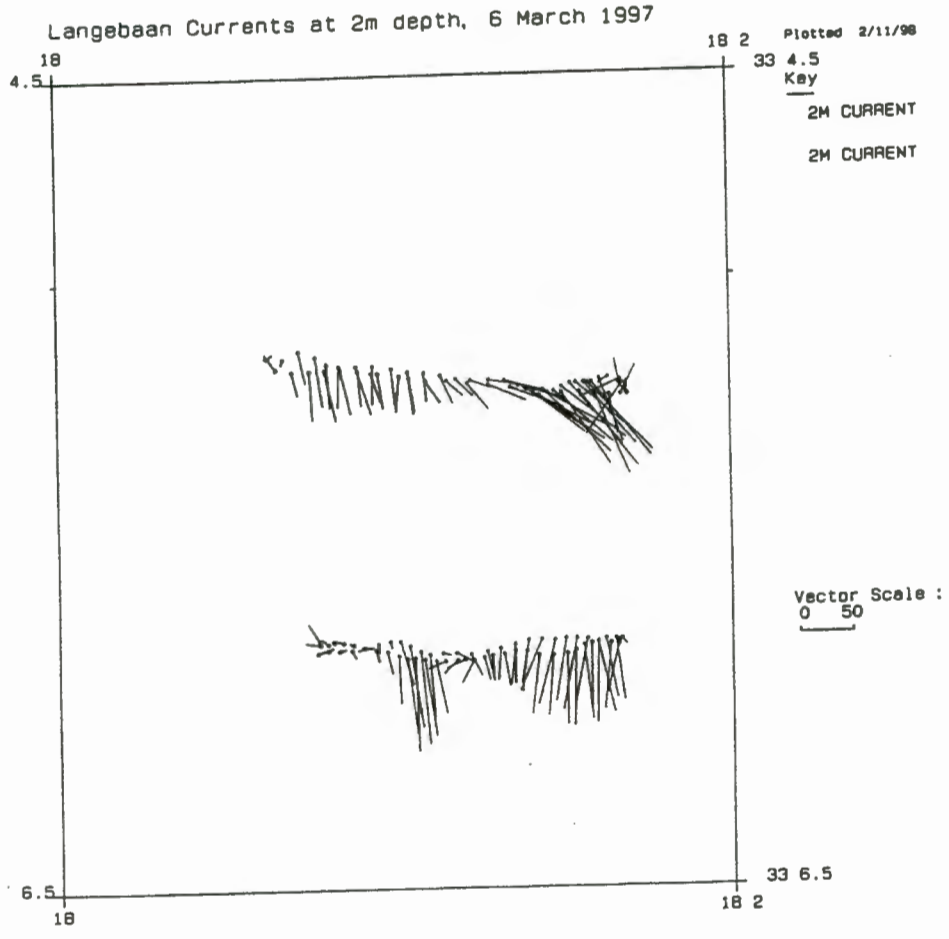

Figure 7-1: Current transects undertaken by the CSIR, on the inflow of the 6.03.97 across the mouth of Langebaan Lagoon (refer to Figure 4-3 for position). The vector scale indicates the current velocity in $cm.s^{-1}$.

To summarise, water entering the east inlet originates from the shallows surrounding the inlet and is drawn from a region which closely corresponds to that of a potential sink. During the flood, water enters the west inlet mainly from the deep channel. The west inlet is thus subjected to the influence of colder and denser water originating from the deeper sections of Big Bay.

7.3 Outflow:

During the neap cycle, the depth averaged velocity at the lagoon inlets is weak. It is thus expected that during periods of small tidal range, the ebb currents are driven by the tide induced pressure gradient and should have properties similar to that of an inverse sink flow.

Figure 7-2: Aerial photograph taken over the mouth of Langebaan Lagoon on the 26.01.89.

the discharge and the receiving fluids have different densities, the jet will sometimes lift off the bottom due to buoyancy forcing. The properties of buoyant jets and bottom attached jets differ significantly and it is therefore necessary to determine if the jets issuing from Langebaan Lagoon will detach from the sea-bed. The criteria of Safaie (1979) and Hauenstein (1983) for bottom attachment of the jets are used to determine the lift off depth for the east and the west inlets ebb flows. Safaie (1979) deduced from a series of experiments that a tidal jet is attached to the bottom if the water depth h satisfies:

$$h < 0.914 \frac{u_0^{1/2} h_0^{3/4}}{(g')^{1/4}} \qquad \text{eq. 7-6}$$

where u_0 is the depth-averaged velocity at the inlet, h_0 is the average depth of the inlet, $g' = g\frac{\Delta\rho}{\rho}$ is the discharge reduced gravity, $\Delta\rho$ is the density anomaly (the difference in density between water in the jet and in the receiving water-body), and ρ is the reference

density (the density of the receiving fluid). Hauenstein (1983) analysed empirical data, including that of Safaie to obtain the following criterion for bottom attachment:

$$h < 0.71 \frac{u_0}{(g')^{1/2}} (b_0 h_0 S)^{1/4} \qquad \text{eq. 7-7}$$

where S is the downward slope of the seabed in the jet direction and b_0 is the inlet half-width. Equations 7-6 and 7-7 were applied to the east and west inlet outflows during the spring tides. For the east and the west outflows, the lift off depth is plotted against the density anomaly $\Delta\rho$ in figures 7-3 and 7-4, respectively.

According to the criteria of Hauenstein (1983), lagoon water that is advected through the inlets during the ebb will never lift off the bottom even when the density anomaly becomes equal to 0.18 (which represents the maximum density anomaly measured during the field survey). The criteria developed by Safaie shows that the lagoon effluent might detach from the sea-bed beyond the 8m depth contour if a significant density anomaly exists between the lagoon effluent and Big Bay waters. Observations showed that the water-column at the lagoon inlets has temperature and salinity properties similar to that encountered in Saldanha Bay throughout most of the ebb (figures 5-1, 5-5 and 5-6). Temperature at the lagoon inlets only increased briefly at the end of the ebb, when warmer water from the middle region of the lagoon reached the mouth. Throughout most of the outflow, the difference in density between the lagoon effluent and the Big Bay waters is small and it is expected that the ebb jets issuing from the lagoon inlets will remain bottom attached during periods of high tidal range.

The strong homogeneity of the water-column at the lagoon inlets and the generally weak buoyancy forcing, enable us to define the hydrodynamics at the Langebaan Lagoon inlets based upon the solutions derived by Ozsoy (1977) for the depth-averaged equations of motions at tidal inlets.

The properties of a self similar plane jet are expressed in terms of normalised co-ordinates (Ozsoy and Unluata, 1982):

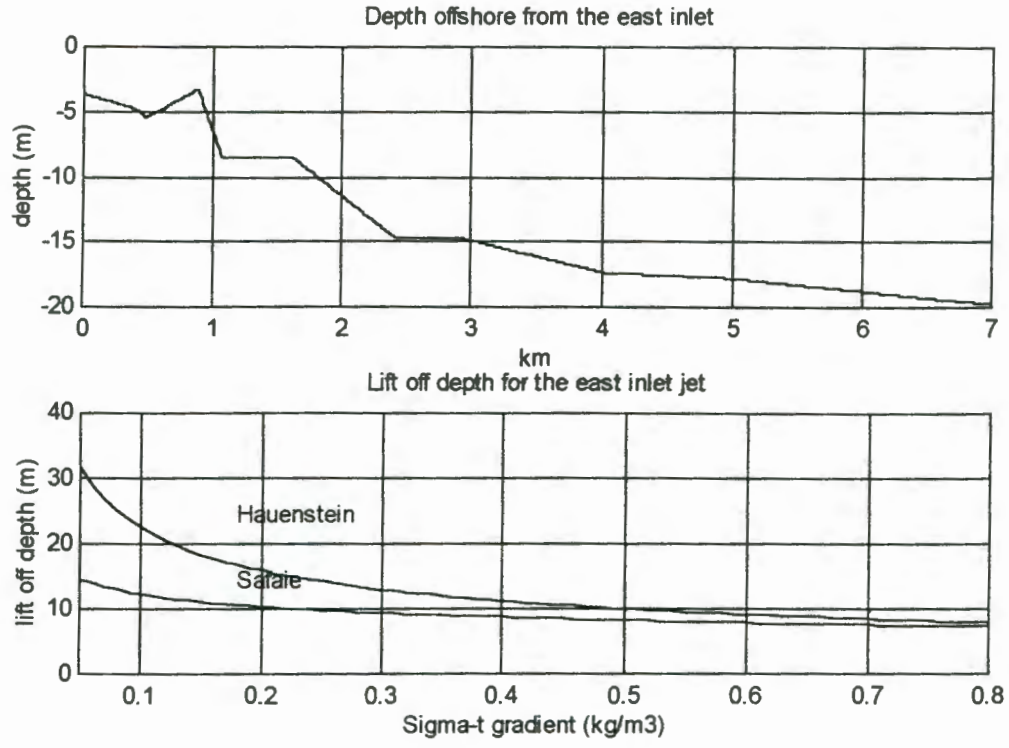

Figure 7-3: In the upper panel are the variations of the depth contours from the east inlet. Below, lift off depth for the east inlet outflow for different values of the density anomaly according to the criteria of Hauenstein (1983) and Safaie (1979). $S = 0.0023$, $u_0 = 0.80 m.s^{-1}$, $b_0 = 264m$, $h_0 = 3.67m$.

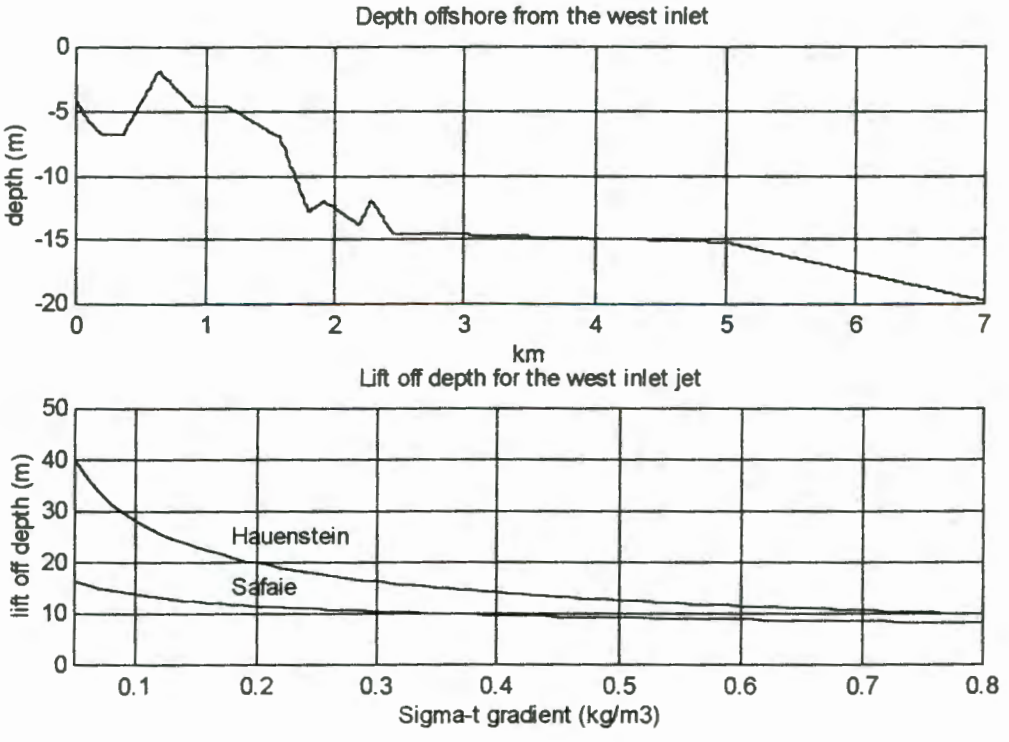

Figure 7-4: In the upper panel are the variations of the depth contours from the west inlet. Below, lift off depth for the west inlet outflow for different values of the density anomaly according to the criteria of Hauenstein (1983) and Safaie (1979). $S = 0.0022$, $u_0 = 0.83 m.s^{-1}$, $b_0 = 523m$, $h_0 = 4.15m$.

$$\xi = \frac{x}{b_0}\ ,\ \mu = \frac{fb_0}{8h_0}\ ,\ H(\xi) = \frac{h}{h_0}\ ,\ R(\xi) = \frac{r}{b_0}\ ,\ B(\xi) = \frac{b}{b_0}\ ,\ U(\xi) = \frac{u_c}{u_0}$$

x is the distance from the inlet, h is the depth, b is the jet half-width. b_0 , h_0 , and u_0 are respectively the half width, depth and depth-averaged velocity at the inlet. u_c is the centreline velocity of the jet, r is the length of the core region, f is the friction factor and μ is a non dimensional number accounting for the effect of friction. The friction factor f , can be expressed in terms of the Manning coefficient n (Mehta and Joshi, 1988). The Manning coefficient was determined from the Chezy coefficient C , which is, according to Bruun and Gerritsed (1960) obtained from the empirical relationship

$$C = \alpha_2 + \alpha_3 \log(A_c) \qquad \text{eq. 7-8}$$

where A_c is the cross sectional area of the inlet, $\alpha_2 = 30$ and $\alpha_3 = 5$. The suggested value for the constants α_2 and α_3, based on measurements of many sandy inlets with a maximum velocity on the order of $1 m.s^{-1}$, should be appropriate for our study. The relationship between C and A_c can be stated in terms of the Manning equation:

$$n = \frac{h_0^{1/6}}{C} \qquad \text{eq. 7-9}$$

where h_0 is the mean depth of the inlet channel. Following the method of Metha and Joshi (1988), the friction factor f is

$$f = 8g \times \frac{n^2}{h^{1/3}} \qquad \text{eq. 7-10}$$

In the ZOFE, $U(\xi) = 1$. The half-width of the jet $B(\xi)$ can subsequently be obtained from equations 3-5 and 3-6. In the ZOEF, the bottom frictional jet is subject to linear depth variations $H(\xi) = 1 + \nu\xi$ where $\nu = m\frac{b_0}{h_0}$ and m is the bottom slope.

The centerline velocity U and the half-width B can then be expressed as (Ozsoy, 1977):

$$B(\xi) = \frac{H^{\mu/\nu - 1}}{I_2}\left[H_s^{-2\mu/\nu} + \frac{2\alpha I_2}{I_1(2\mu - \nu)}\left(H^{2-\mu/\nu} - H_s^{2-\mu/\nu}\right)\right] \qquad \text{eq. 7-11}$$

$$U(\xi) = H^{-\mu/\nu}\left[H_s^{-2\mu/\nu} + \frac{2\alpha I_2}{I_1(2\mu - \nu)}\left(H^{2-\mu/\nu} - H_s^{2-\mu/\nu}\right)\right]^{-1/2} \qquad \text{eq. 7-12}$$

$I_1 = 0.45$ and $I_2 = 0.316$ are both constants of integration. $H_s = H(\xi_s)$ where ξ_s represents the extent of the core region and is given by the solution of the transcendental equation:

$$I_1 e^{-\mu\xi_s} - I_2(1 + \alpha\xi_s) = 0 \qquad \text{eq. 7-13}$$

α is the entrainment coefficient at the jet boundary. The values of α are those determined experimentally by Morton et al. (1956). $\alpha = 0.036$ in the ZOFE and $\alpha = 0.050$ in the ZOEF. To determine the extent of the core region (r), or ZOFE, the transcendental equation (eq. 7-13) is solved graphically for both values of α.

The model output for the east and the west inlets appears in Figure 7-5 and 7-6 respectively.

Large values of μ were found for both of the inlets outflows, implying that the Langebaan Lagoon effluent is strongly influenced by bottom friction as it propagates into Saldanha Bay. As a result, the jets issuing from the lagoon inlets lose energy rapidly and are characterised by a strong decay of the centerline velocity. At a distance of 1km from the lagoon mouth, the centerline velocity of the tidal jets has dropped by nearly 50% (figures 7-5 and 7-6). Farther away from the lagoon mouth, at a distance of approximately 1.5km from the inlets, bottom friction is lessened and the centerline velocities of the jets decrease gradually. The offshore extent of the jets, L_{jet}, was derived by assuming that the total flux through the inlets during the ebb equals the volume of water within the jet. During the spring cycle, the length scales for the east and the west inlet jets were respectively equal to 6.4km and 7.2km.

The effect of bottom friction on the west inlet outflow is especially pronounced. At a distance of 1km from the inlet, the half width for the west inlet jet already exceeds 1km. The rapid expansion of the west inlet jet will result in strong interactions between the west inlet ebb flow and Donkergat and Meeu Islands. The process of entrainment in the vicinity of the inlet might also contribute to initially attach the west inlet outflow to the Donkergat island coastline. The paths followed by drifters on the 13th and the 14th of March (figure 5-15) revealed that the west inlet outflow bends in a north-westerly direction, following the

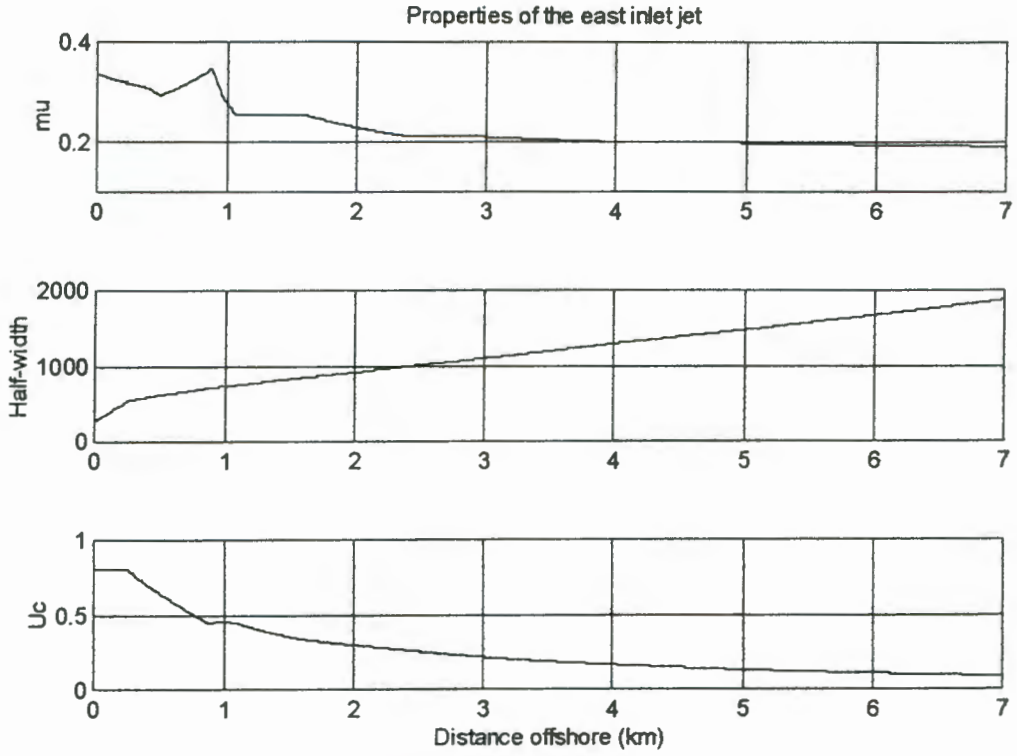

Figure 7-5: Properties of the jet issuing from the east inlet during the spring tide. The jet half-width is expressed in meters and Uc is the centerline velocity of the jet in $m.s^{-1}$. mu = μ is a non-dimensional parameter accounting for bottom friction. Linear variations in depth were assumed and the bottom slope was calculated to be m = 0.0023. U_0 = 0.80, v = 0.1701, Bo = 267m.

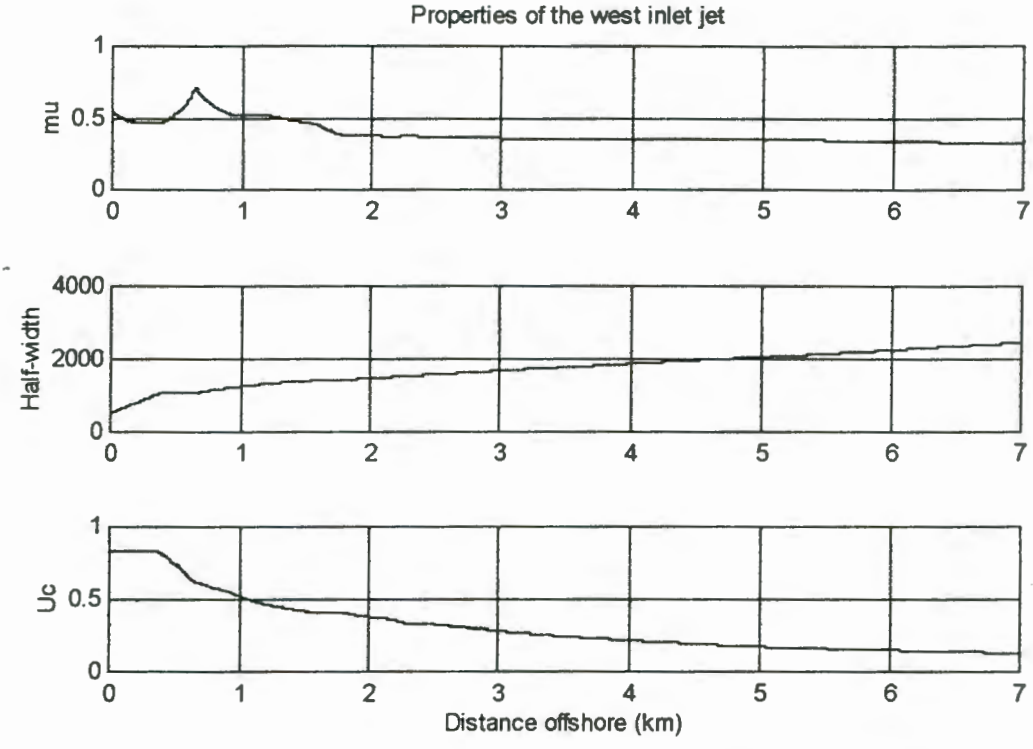

Figure 7-6: Properties of the jet issuing from the west inlet during the spring tide. mu = μ is a non-dimensional parameter accounting for bottom friction. The jet half-width is expressed in meters and Uc is the centerline velocity of the jet in $m.s^{-1}$. Linear variations in depth were assumed and the bottom slope was calculated to be m = 0.0022. U_0=0.83, v = 0.2888, Bo = 529m.

coastline of Donkergat island. This feature tends to confirm the hypothesis that flow issuing from the west inlet attaches to Donkergat island due to the entrainment process. The strong interactions of the west inlet outflow with natural boundaries limit the applicability of Ozsoy's theory. With strong shear occurring between the land and the flow, the west inlet ebb flow loses its 'jet' nature and the flow properties become dependent upon the strength of the pressure gradient between Saldanha Bay and the inlet, relative to the kinetic energy losses experienced by the flow through frictional interactions with land boundaries. As a result, the velocity structure, the flow width and the offshore extent of the west inlet ebb flow will differ from that predicted. On the 13th of March, the drifter released at the west inlet at the beginning of the ebb travelled 4.3km into Saldanha Bay, a distance significantly less than the jet length-scale estimated on the spring tide (7.2km). The value of L_{jet} derived for the west inlet jet is thought to greatly overcome the length of the west inlet ebb flow. It is presumed that the ebb flow from the west inlet might initially take the form of a turbulent jet, to then become a pressure gradient driven flow. Strong shear between the west inlet ebb flow the sea-bed and land boundaries would act to reduce the momentum and the offshore extent of the flow. Entrainment on one side of the west inlet outflow is impeded by the presence of solid land boundaries and as result, the flow expansion should be less than that predicted with the model. It is expected that the interaction between the west inlet effluent and Donkergat island will lead to the formation of eddies, which might subsequently be carried with the mean flow further into Big Bay. Such eddies will contribute toward the formation of residuals and strong mixing is likely to occur within Rietbaai and along the Donkergat island coastline.

The east inlet outflow propagates into Saldanha Bay without interference with land boundaries and less interactions with the sea-bed (μ, plotted in Figure 7-5, is significantly less). It is therefore able to develop into a bottom frictional jet. It is thus hoped that the model provides us with a fairly realistic characterisation of the east inlet outflow properties. The flow issuing from the east inlet is also strongly affected by bottom friction, although to a less extent that the west inlet outflow. The jet half width increases linearly and reaches a value of 1km at a distance located 2.5km from the lagoon mouth (figure 7-4). Comparisons between ADCP and drifters current data showed that water issuing from the east inlet during the ebb, loses a lot of momentum within the first 1.5km. A similar decrease of the

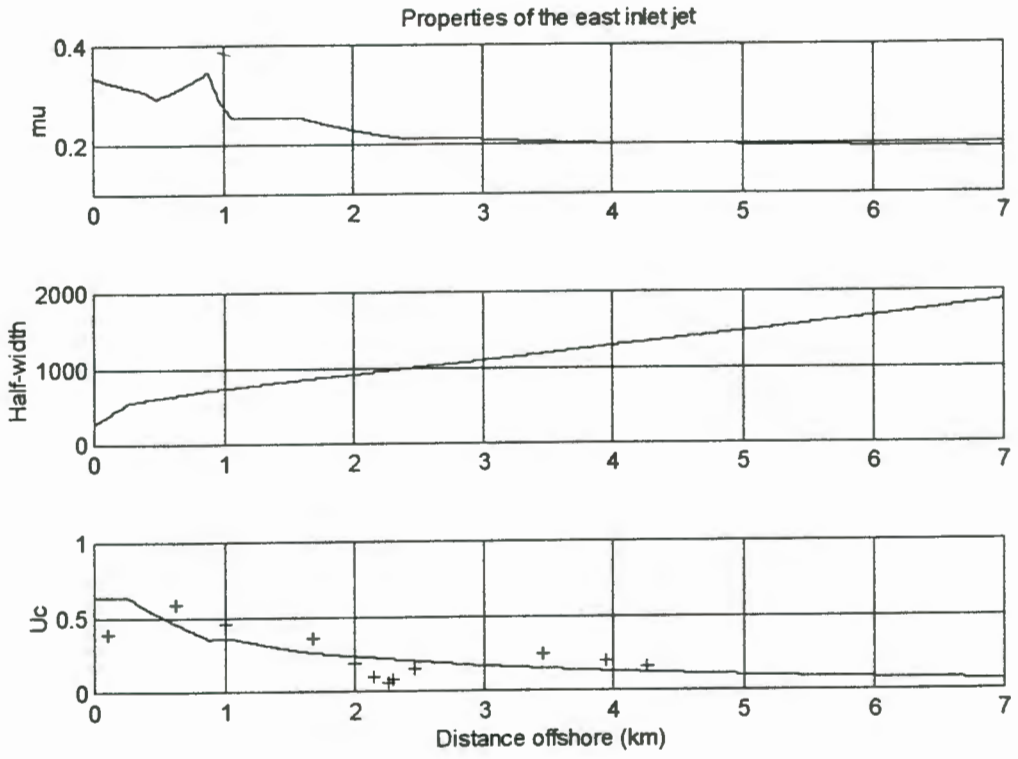

Figure 7-7: Properties of the jet issuing from the east inlet during on the 13.03.97. The jet half-width is expressed in meters and Uc is the centerline velocity of the jet in $m.s^{-1}$. The black crosses represent the surface current velocity obtained with the drifters. mu = μ is a non-dimensional parameter accounting for bottom friction. Linear variations in depth were assumed and the bottom slope was calculated to be $m = 0.0023$. $U_0 = 0.63$, $\nu = 0.1701$, $Bo = 267m$.

centerline velocity was predicted by the model, building our confidence that the model outlines the main features of the east inlet ebb flow (figure 7-7). The lengthscale derived for the east inlet jet on the 13th of March is equal to 5.4km and exceeds by 12.5% the distance travelled by the drifter (released at the beginning of the ebb) on that same day. It is therefore likely that the value of L_{jet} obtained on the spring tide (6.4km) constitutes a higher bound for the offshore extent of the east inlet ebb jet.

Although some of the features outlined by the model agree with observations, discrepancies are bound to occur between the theoretical and the real flow due to the assumptions made in derivation of the model. For example, the model assumes a constant velocity at the inlet, while in reality, the velocity is only constant over a limited time period, which might be less than the time needed by the jet to become fully developed and quasi steady. In the case of Langebaan Lagoon however, the currents at the inlets quickly reach their maximum velocity and display a fairly constant velocity throughout the ebb. The assumption that the velocity is constant at the inlets is therefore reasonable and should not lead to major discrepancies between the modelled and the real flow. The theory of Ozsoy also assumes a linear variation of the depths contours. In real flows however, water carried with the jet is advected over a complex and quickly varying topography. As a consequence, sudden contractions of the jet which would occur if the flow propagated over a steep slope (such as that occurring 1.6km away from the east inlet) are not represented in the model output. Comparisons between the drifter velocity and the centerline velocity of the east inlet jet (figure 7-7) build our confidence in the capacity of the model to reproduce the principal features of the east inlet ebb flow. However, the values for L_{jet} proved too large when compared to the drifter data. There exist many factors which would lead to an over-estimation of the jet centerline velocity. For example, the depth-averaged velocity at the inlet, or the total flux of water going through the inlets, might have been over-estimated. Discrepancies between real and modelled flow can be attributed to assumptions made in the derivation of the model's equations or non-linearity resulting from the interaction of the flow with solid boundaries. Eventually, at some distance from the inlet orifice, the jet behaviour becomes influenced by environmental parameters, such as ambient currents, stratification, or winds, which have not been accounted for in the model. The effect of environmental parameters on the tidal ebb jets will be considered in section 7-4. Still, the model provided us with useful information on

the nature of the ebb flow issuing from Langebaan Lagoon. The model served to outline the predominant effect of bottom friction on the ebb tidal currents, the rapid flow expansion and the significant momentum loss experienced by the currents within the first kilometre of propagation into Big Bay. Also, it should be remembered that the goal behind the use of this mathematical model is to provide us with an understanding of the system's hydrodynamic, not to give an exact representation of the flow. A numerical model would provide a better more realistic simulation of the flow fields.

7.4 Impact of environmental features on the ebb jets:

At some distance from Langebaan Lagoon inlets, the strength of the tidal currents has significantly decreased and other forcing mechanisms are likely to affect the nature of the tidal jets. In this section we will consider how winds, ambient currents in Saldanha Bay, or baroclinic forcing in the bay and in the lagoon, might alter the nature of the Langebaan Lagoon outflow. The changes experienced by tidal jets due to their mutual proximity will also be considered.

Local and remote wind events will alter the propagation of the Langebaan Lagoon effluent into Saldanha Bay by generating baroclinic forcing, ambient currents or, as outlined in Chapter 6, by modifying the hydrodynamic conditions at the lagoon inlets. In summer, upwelling favourable winds sometimes provide suitable conditions for the development of stratification in Saldanha Bay. Previous studies (Monteiro and Brundrit, 1995) have shown that during the summer, temperature gradients of up to 10°C can occur between the surface and the bottom layers of Saldanha Bay. Since the east inlet withdraws water from the shallow regions of Big Bay, temperature gradients between the east inlet tidal jet and the deep sections of Big Bay should be similar to those existing between the mixed and the bottom layers of Saldanha Bay. Hence, density anomalies of 0.8 to 1kg.m^{-3} might occur between the east inlet ebb jet and the deep sections of Big Bay during the summer months. The significant vertical mixing resulting from the interaction of the west inlet outflow with land boundaries should impede any buoyancy forcing and we expect the ebb flow to mix throughout the water-column. According to figure 7-4, with density anomalies of approximately 0.8kg.m^{-3} the east inlet ebb jet will lift off the seabed as it reaches the 8m

depth contour, at a distance approximately equal to 1.5km from the inlet. If the east inlet ebb jet becomes buoyant, vertical entrainment will be generated at the bottom boundary of the jet. The jet half-width will increase due to the shallower depth of the lifted interface but for the same reason, the offshore extent of the jet will be greater. Eventually, if the density anomaly between the jet and the surrounding waters is high, the two large scale vortices formed just after the start of the discharge will increase in size with distance offshore and constitute a region of strong mixing at the front end of the jet. During the winter months, northerly winds predominate over the Benguela system. The water-column in Saldanha Bay is largely isothermal and the temperature in the lagoon is similar to that encountered in the bay (Shannon and Stander, 1977). Therefore, the ebb jet issuing from the east inlet should not lift off the bottom unless a significant volume of freshwater has been input into the lagoon basin, through precipitation or groundwater seepage.

Winds can also alter the property of the Langebaan Lagoon outflow by raising (depressing) the water level, thus increasing (decreasing) the discharge at the lagoon inlets, or by intensifying (acting against) the tidal currents at the lagoon mouth. Local southerly winds (measured in Geelbek) have a strong diurnal signal (figure 5-11) and should influence the circulation at the inlets daily by enhancing the seaward propagation of the lagoon effluent. Wind measurements at Cape Colombine showed that waterlevels in the bay and in the lagoon responded quickly to remote atmospheric forcing (figures 5-12 and 5-14). It is expected that when drops in the waterlevel are combined with strong southerly winds over the lagoon and the bay, the lagoon discharge will be more affected by winds rather than by variations in the waterlevel, and the offshore extent of the lagoon effluent will increase. From the 10^{th} to the 12^{th} of March, strong southerly winds blowing at Cape Colombine (reaching maximum velocities of $15 m.s^{-1}$) induced a 0.2m decrease of the waterlevel over the lagoon and the bay. Such a drop in the waterlevel at the lagoon inlets would only reduce the ebb and flood discharge by approximately 5%.

Ambient currents in Big Bay will also affect the behaviour of the outflow from both inlets. In the presence of ambient flow, the jet will bend according to the strength of the surrounding current and the jet equations have to be expressed in terms of a curvilinear co-ordinate that follows the bending of the jet.

Eventually, the Langebaan Lagoon effluent enters Saldanha Bay in the form of two strong flows, very close to one another and with different properties. The proximity of the two inlets means that both outflows will become attracted and eventually attached to each other due to mutual entrainment. In the immediate vicinity of the lagoon mouth, the east and the west inlet outflows tend to merge together due to the entrainment process (figure 5-23). At both tidal inlets, the ebb tidal currents have a similar velocity. Very quickly though, it is thought that the west inlet ebb flow loses momentum due to frictional interactions with solid boundaries. Joshi (1982) showed that as bottom friction, or alternatively μ increased, the surrounding fluid entered the jet almost radially and the influence of the jet was confined to a small distance offshore. Therefore, past the lagoon's mouth region, entrainment will only be significant at the boundaries of the east inlet ebb jet. As the distance from the lagoon inlets increases, the influence of the east inlet jet on the surrounding waters should grow and some of the water issuing from the west inlet might be entrained into the east inlet jet.

In this section, significant insight has been gained upon the nature of the flood and ebb flows at the Langebaan Lagoon inlets. It is hoped that based upon these findings, it will become possible to characterise, and to a certain extent quantify, the mixing and the exchange of water between Langebaan Lagoon and Saldanha Bay.

8. Exchange and mixing across the Langebaan Lagoon-Saldanha Bay interface

Exchange and mixing between coastal lagoons and the adjacent ocean or bay are important processes which provide for the distribution and fate of nutrients, pollutants, sediments or other water-borne materials. Langebaan Lagoon is a natural protected environment (Robinson, 1989) which is subject to environmental stress due to its vicinity with Saldanha Bay, a region of industrial growth. Understanding the processes controlling the exchange and mixing across the Langebaan Lagoon-Saldanha Bay interface is vital for the preservation of the lagoon system. Also, Langebaan Lagoon is a shallow and evaporative environment which constitutes a source of heat for Saldanha Bay. Depending on the mixing and on the magnitude of the exchange between Langebaan Lagoon and Saldanha Bay, the lagoon outflow might significantly affect the density field, and hence the water-quality, within Saldanha Bay. This section seeks to determine how water is exchanged and mixed across the Langebaan Lagoon-Saldanha Bay interface. Measurements showed that the circulation at the Langebaan Lagoon inlets is predominantly driven by the tide. Based on observations and a theoretical understanding of tidal inlet hydrodynamics, it was suggested that at the lagoon mouth, a strong asymmetry would be encountered between the ebb and the flood flows. Previous studies have revealed that when there exists an asymmetry between ebb and the flood, tidal currents rapidly exchange and mix material near tidal inlets (Signell and Butman, 1992; Chadwick et al., 1997; Awaji et al., 1980). In the first section of this chapter, we will address the rapid mixing and exchange induced by tidal currents through the Langebaan Lagoon mouth and consider the implications on the flushing of Langebaan Lagoon. The second section of this chapter will focus on the slower flushing induced by residual currents.

8.1 Mixing and exchange induced by tidal currents through the Langebaan Lagoon mouth:

When the tidal range is significant, particles released in the vicinity of the lagoon inlets during the ebb have large drifts (figure 5-15). At the east inlet, the ebb flow would take the

form of a turbulent jet while at the west inlet, the jet development would be impeded by the presence of land boundaries. The offshore extent of the west inlet flow could not be determined using the theory derived by Ozsoy on tidal inlets. It appeared that the east and the west inlet outflows mutually attracted each other north of the inlets (figure 5-23) and that the ebb tidal excursion was slightly less at the west inlet than at the east inlet (figure 5-15). During periods of weak tidal range, the ebb and the flood took the form of potential flows at both inlets and the overlap between the ebb and the flood region increased. Zimmerman (1986) has shown that tidal dispersion is typically due to horizontal current variations on the scale of the tidal excursion. The theoretical analysis on the tidal currents at the lagoon mouth and the drifter data obtained on the 13th and 14th of March showed that the offshore extent of the Langebaan Lagoon effluent decreased with the tidal range. It is therefore expected that the mixing induced by tidal currents near the lagoon mouth will decrease with the tidal range.

8.1.1 Tidal mixing near the lagoon mouth:

When the tidal range is large, the eastern jet contributes toward the mixing and flushing in Saldanha Bay through lateral entrainment at its boundaries, while on the western side of Big Bay, lateral entrainment by the west inlet outflow is inhibited by the presence of coastal features. Analysis conducted in chapter 7 showed that north of the west inlet, the greater frictional interactions between the ebb flow and solid boundaries might add vorticity to the flow and enhance vertical mixing. The aerial photograph taken over the mouth of Langebaan Lagoon (figure 7-2) seems to support the hypothesis that eddies are generated at the western boundary of the Langebaan Lagoon effluent.

In the absence of a well defined stratification in Saldanha Bay, the outflow from both inlets appears to remain attached to the bottom (figures 7-3 and 7-4). In such case, water advected from the lagoon into the bay during the ebb would act to keep the water-column mixed over significant regions of Big Bay. The impact of the Langebaan Lagoon outflow on the temperature profile in Big Bay is illustrated by figure 8-1. In the region of influence of the Langebaan Lagoon ebb flow, the temperature gradient between the surface and the bottom layers weakens considerably as a result of the strong vertical mixing associated with the propagation of Langebaan Lagoon effluent.

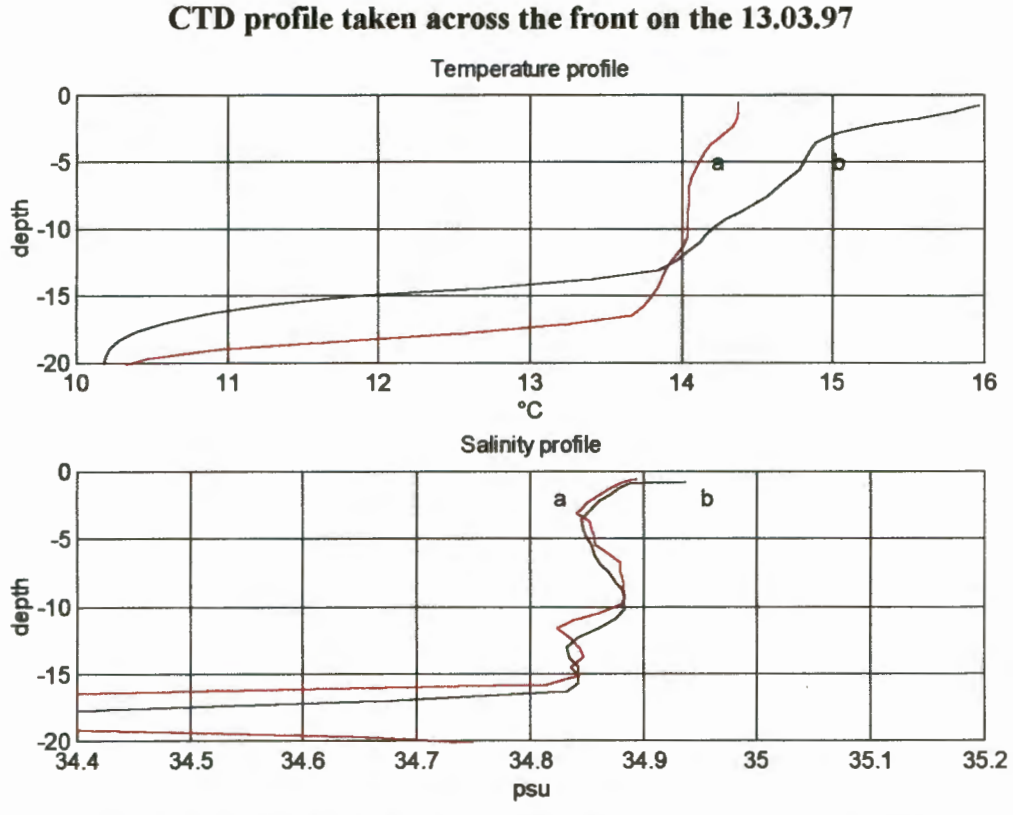

Figure 8-1: Profile (a) was taken within the outflow, near the front and between the Langebaan Lagoon effluent and the Saldanha Bay water. Profile (b) is characteristic of Saldanha Bay water at this time. The CTD profile at station (a) shows colder surface temperature resulting from the mixing between the bottom layer and the surface layer of Saldanha Bay water.

When strong stratification occurs in the bay, the lagoon effluent is considerably lighter than the bottom layer in Saldanha Bay and buoyancy forcing on the lagoon effluent is significant. The west inlet outflow is thought to remain bottom attached as it is subject to stronger vertical mixing and hence, less buoyancy forcing. We hence realise that although the cold and dense bottom water might intrude as far as the west inlet during the flood, stratification north from the west inlet is broken down during the following ebb. While Saldanha Bay water might be stratified in nature and might be advected through the west inlet during the flood, the water that exits the west inlet during the subsequent ebb will generally be well mixed due to the shallow nature of the lagoon basin. During the first stages of the ebb, well mixed lagoon water is advected through the west inlet and as the ebb progresses, barotropic forcing through the west inlet increases. Stratification which might have been present at the west inlet during the flood is broken down. Figure 8-2 shows that stratification between the

surface (2m) and the bottom (5m) layers reached a maximum during the neap tide inflow, but was soon broken down as the ebb started.

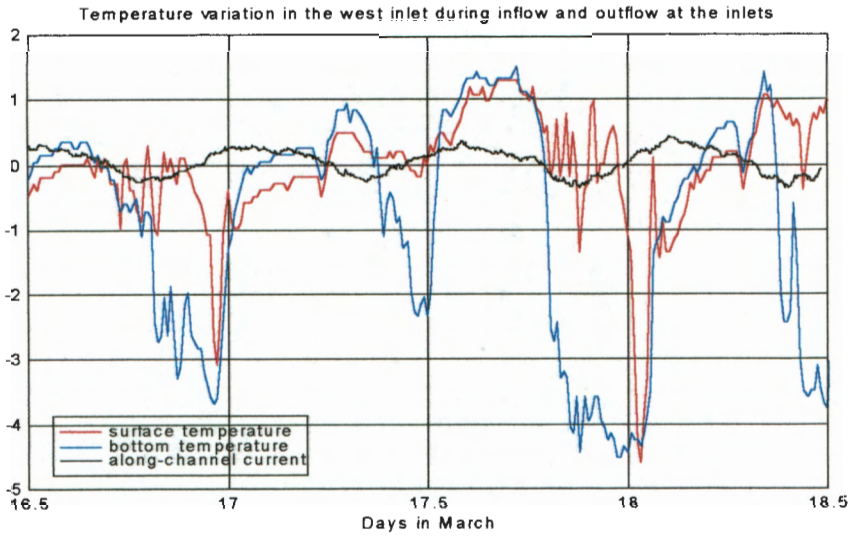

Figure 8-2: Tidal fluctuations from the mean for the west inlet temperature plotted alongside the along-channel current in the east inlet (at a bin depth of 5-18m). Positive values of the along-channel current indicate that Langebaan Lagoon water is flowing into Saldanha Bay with the ebb currents. Stratification between the surface (2m) and the bottom (5m) layers of the west inlet channel during the inflow, is broken down at the start of the ebb.

During the spring tide the east inlet ebb flow might lift off from the seabed as it reaches the 8m depth contour, at a distance of approximately 2km from the mouth of Langebaan Lagoon (figure 7-3). If the east inlet jet lifted off, vertical entrainment would be generated at the bottom boundary of the jet, rich nutrient waters would be brought into the surface layer of the water column and a bottom return current would be generated.

8.1.2 Tidal exchange near the lagoon mouth:

Rapid tidal exchange near tidal inlets often results from a process termed "tidal pumping" (Fisher et al., 1979). Tidal pumping results from an asymmetry between the ebb and the flood. On the ebb, particles released at the lagoon inlets during the ebb have large drifts, while on the flood, the sink nature of the inflow implies that particles are withdrawn from a region closer to the inlet (figure 3-1). Depending on the strength of the ebb-flood asymmetry, we hence see that significant volumes of water issuing from the lagoon during the ebb might not return into the lagoon during the subsequent flood. The material

exchanged between the lagoon and the bay is thus limited to the region where the sink overlaps the jet.

In Chapter 7, it was seen that the ebb tidal excursion for the east inlet would decrease with the tidal range. On the spring tide, the length-scale of the east inlet jet was estimated to be approximately 6.2km, while on the 13th of March, the tidal range was smaller and the east inlet ebb jet was predicted to extend 5.4km offshore from the lagoon mouth. Drifter data also underlined the dependency of the ebb tidal excursion on the tidal range. From the 13th of March to the 14th of March, the ebb tidal excursion for the east inlet was reduced from 4.8km to 4.3km. The offshore extent of the west inlet outflow could not be estimated using the analysis conducted in Chapter 7. However, the deployments of drifters on the 13th and 14th of March showed that the length of ebb tidal excursion was similar, or slightly less, at the west inlet than at the east inlet. On the 13th and the 14th of March, drifter released at the beginning off the ebb at the west inlet drifted into Saldanha Bay for 4.3km and 3.5km, respectively. In Chapter 7, it was seen that on the neap tide, the offshore extent of the ebb and the flood flows would be reduced and the induced exchange should therefore be much less. Based on the knowledge that the length scale of the ebb jet increases more rapidly than the length scale of the flood withdrawal zone (figure 8-3), we expect that the exchange will vary primarily as a function of the tidal range. Since large tidal excursions were experienced by particles released near the lagoon mouth during the ebb, significant exchange should occur across the interface between the lagoon and the bay. It is also expected that during periods of high tidal range, direct exchange between the lagoon and the outer ocean occurs. In Chapter 6, it was seen that when the tidal range was large, the water-level in the lagoon significantly lagged that of the bay. Lags between the lagoon and the bay water-levels might enhance the tidal exchange as the inertia of the lagoon outflow might continue to carry water offshore after transition to the flood flow.

It is thought that the exchange between Langebaan Lagoon and Saldanha Bay strongly depends upon the tidal range and that tidal pumping is the dominant mode of exchange across the Langebaan Lagoon-Saldanha Bay interface. Previous studies have underlined the dependency of tidal exchange on tidal range (figure 8-4) and have suggested that in coastal embayments with narrow entrances and large tides, such as Langebaan Lagoon, tidal

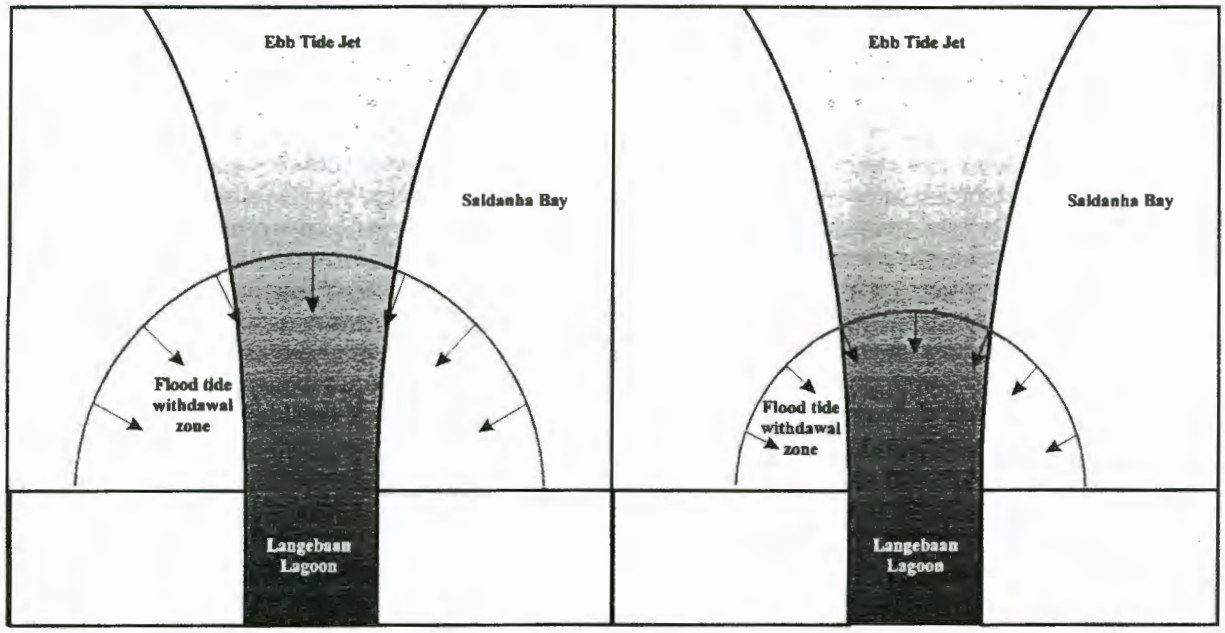

(a) Strong tide **(b) Weak tide**

Figure 8-3: Schematic of Langebaan Lagoon-Saldanha Bay exchange during (a) a strong tide event, and (b) a weak tide event. Note how the ratio of lagoon-water to bay-water within the withdrawal zone increases with decreasing tidal range.

pumping is the dominant mode of exchange (Chadwick et al., 1997). The tidal exchange of water between a basin and the neighbouring ocean or bay is often expressed in terms of the tidal exchange ratio (TER), as defined in equation 3-10. Based upon the hypothesis that tidal pumping dominates the tidal exchange across the interface between Langebaan Lagoon and Saldanha Bay, the tidal exchange ratio should be controlled by the overlap between the ebb and the flood. Following Chadwick (1997), TER can be estimated as

$$TER = 1 - \sqrt{\frac{1}{w\pi}\left(\frac{b_0}{l_x}\right)} \qquad \text{eq. 8-1}$$

where w is a fraction of a complete circle occupied by the withdrawal zone, b_0 is the width of the lagoon mouth and l_x is the ebb tidal excursion. This expression of the TER was derived based upon the assumption that the inflow and the outflow of water through the mouth of the lagoon are equal and can be estimated by assuming a standing wave tide within the lagoon. This expression of the tidal exchange ratio also assumes complete mixing in the lagoon. Equation 8-1 is equivalent to equation 3-14 and has the advantage of allowing us to estimate TER on the 13th and the 14th of March, days when the length of the

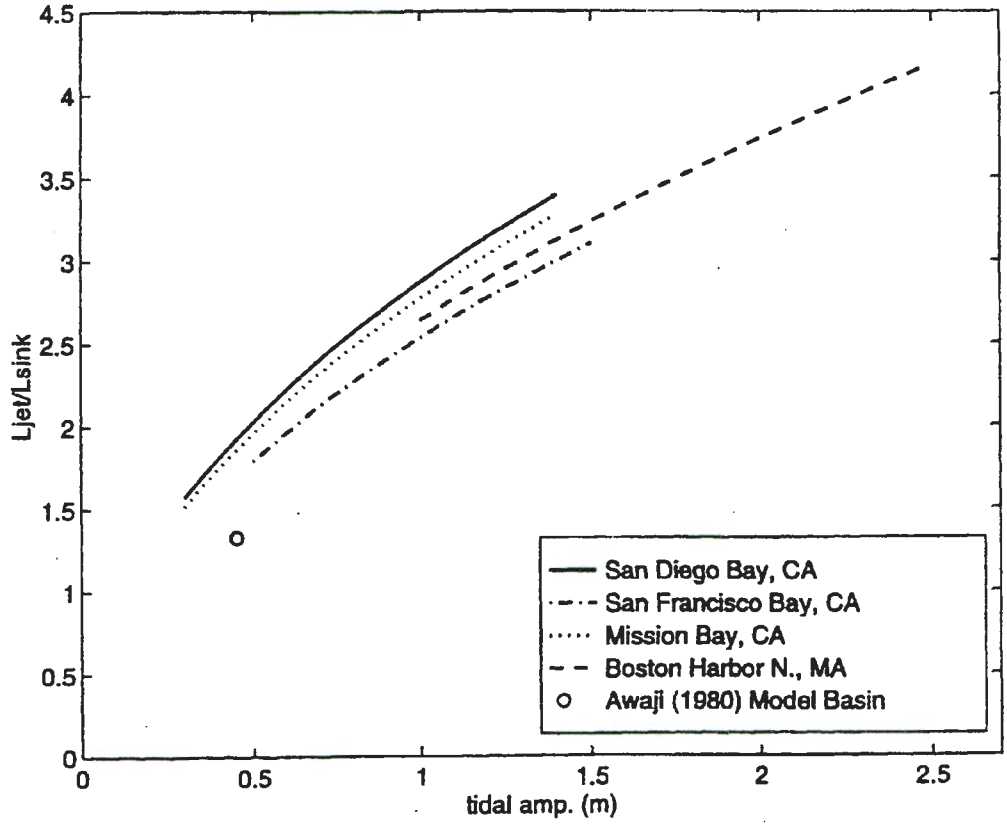

Figure 8-4: Tidal range variations in the ratio of length scales for the ebb and flood sink in San Diego Bay, San Francisco Bay, Mission Bay, Boston Harbour, and for the numerical model basin of Awaji et al.(1980). This plot was taken from Chadwick (1997).

sink inflow could not be estimated due to a lack of data. In the estimation of TER, we assume that during periods of large tidal range, the tidal excursion for the lagoon outflow can be approximated by the tidal excursion at the east inlet. The width of the lagoon mouth, b_o, is taken as the sum of the two inlets width. On the spring tide, on the 13th and on the 14th of March, w is set to a value of 0.333. On the neap tide w is set to 0.5.

The values derived for the tidal exchange ratio can be used to determine the flushing capacity of the lagoon. According to Chadwick (1997) the residence time assuming complete mixing in Langebaan Lagoon can be expressed as

$$T_{res} = \frac{V_l}{P} \times \frac{T}{TER} \qquad \text{eq. 8-2}$$

where V_l is the volume of the lagoon, T is the tidal period and P is the tidal prism. The tidal prism (expressed in equation 3-11) is obtained by assuming a standing wave tide in the

lagoon. The calculated values of tidal exchange ratio and the residence time appear in table 7.

Day	Tidal range (m)	TER	Residence time (days)
Spring tide	2	0.5124	1.16
13.03.97	1.4	0.4370	1.36
14.03.97	1.2	0.4051	1.47
Neap tide	0.5	0.1244	19.13

Table 7: Tidal exchange ratio and residence time for different values of the tidal range in Langebaan Lagoon.

Depending on the tidal range, the residence time for Langebaan Lagoon varies from about 1-20 days. Those results are based upon the assumption that complete mixing occurs within Langebaan Lagoon basin. In reality, the efficiency of mixing will vary at locations in the lagoon basin. Previous study have revealed that in a long and narrow basin, such as Langebaan Lagoon, dispersion and residence time vary as a function of distance from the lagoon mouth (Largier et al., 1997). Regions located near the mouth of the lagoon are subject to strong tidal exchange and are characterised by large tidal diffusivity. As one progresses towards the lagoon heads, the tidal exchange and the diffusivity decrease. CTD profiles taken in the lagoon showed that salinity increased with distance from the lagoon mouth. Near the lagoon inlets, the water-column had a salinity similar to that of the neighbouring bay, while far into the lagoon, hypersalinity occurred (figures 5-5 and 5-6). The observed salinity distributions indicate decreasing exchange towards the head of the lagoon. It is therefore expected that in the southern regions of the lagoon where tidal dispersion is weak, the residence time for water particles will significantly exceed that derived in this chapter. However, for regions where tidal dispersion is significant, the values derived for the tidal exchange ratio and for the residence time should be realistic. According to Zimmerman (1986), tidal dispersion is typically due to horizontal current variations on the scale of the tidal excursion. The movement of the isotherms and isohalines obtained from the CTD data (figures 5-5 and 5-6) provided an estimate of the tidal excursion on the flood. The flood tidal excursion was seen to approximately equal 8km and 4km on the spring tide and on the neap tide, respectively. It is therefore expected that on the spring tide,

tidal dispersion will be significant for regions located up to 8km from the lagoon mouth, while on the neap tide, tidal dispersion will be significant for regions located up to 4km from the lagoon mouth. For particles located within those regions, the tidal exchange ratio and the residence times estimated previously should be realistic. In regions located farther into the lagoon, the tidal exchange will be reduced and the residence time for water particles will be greater. Arabonis (1995) estimated the residence time at different locations in Langebaan Lagoon from the salinity distribution. His estimates might represent with more accuracy the flushing capacity for regions of Langebaan Lagoon which are not in the vicinity of the lagoon mouth. The residence times calculated by Arabonis were equal to zero day at the lagoon mouth, 10 days in the mid-sections of the lagoon and approximately one month at the lagoon's heads.

Superimposed on the back and forth motion of the tide through the inlets, there exists a steady circulation, often called the "residual circulation". The residual circulation, generally defined as the velocity field obtained by averaging the velocity at each point over the tidal cycle, might contribute toward the exchange. Residual currents can result from atmospheric forcing, baroclinic forcing or from the non-linear interaction of the tide with the lagoon geometry. When non-tidal currents contribute extensively to the residual circulation, estimates of embayment flushing based on tidal calculation alone can significantly overestimate the flushing time that would be expected under typical environmental conditions. In the next section of this chapter we will attempt to determine the extent to which tidal currents contribute toward the residual circulation and then consider how residual currents affect the mixing and exchange between Langebaan Lagoon and Saldanha Bay.

8.2 Influence of residual currents on the mixing and exchange through the lagoon mouth

Current measurements at the mouth of the Langebaan Lagoon showed evidence of a residual circulation, with a net inflow into the east inlet and a net outflow out of the west inlet (figures 5-25 and 5-26). At both inlets, Eulerian residual currents had typical magnitudes of 0.1-0.2m.s^{-1}.

Before considering how these residual currents might affect the exchange or the mixing of material near the Langebaan Lagoon mouth, it is first necessary to determine whether the 'measured' Eulerian residual currents are indicative of a Lagrangian residual circulation, or if they just represent some local and isolated asymmetry between the ebb and the flood. It is difficult to say whether the net outflow of water from the west inlet is representative of what happens over the inlet width. The complex morphology of the west inlet and the presence of features such as Meeu Island, Rieetbaai and Donkergaat island are likely to produce strong non-linearity within the inlet flow. Also, the direction of the channel at the west inlet is variable (figure 5-20) and this is represented on the direction taken by the flow during the flood and the ebb (figure 5-19). Hence, the velocity field at the west inlet might exhibit strong horizontal variations. At locations in the west inlet, the Eulerian residual flow might be very different to that measured at the ADCP and might indicate for example, that there exists a net flux of water directed from the bay to the lagoon. Making conclusions on the mean flux of water through the west inlet based on the residual circulation measured at one point is thus hazardous. The east inlet has a very different morphology. The presence of a narrow channel inhibits spatial variation in the location of the maximum current throughout the tidal cycle. We expect the migration of the maximum current during the tide to be associated with a slight change in direction of the principal axis component. Still, the ADCP data showed that inflow and outflow occurred along the same axis. This strong polarisation of the flow suggests that the ADCP was located at the point of maximum current during the ebb and the flood. The strong topographic gradients encountered along the east channel, also make reasonable the assumption that the currents throughout the channel width are approximately equal to those measured at the ADCP. If the mean flux through the east inlet and into the lagoon is positive then for mass conservation purposes, there must be a net loss of water from the west inlet and the residual circulation revealed by the ADCP data is real. Depending on the strength and on the periodic, or episodic nature of the residual currents, the residual circulation might have a significant impact on the transport and mixing of particles between Langebaan Lagoon and Saldanha Bay. To understand how the residual circulation at the lagoon inlets affect the exchange of particles between Langebaan Lagoon and Saldanha Bay it is therefore necessary to determine the different sources of residual velocity.

In coastal lagoons, the non-linear interaction of the tide with the lagoon irregular bathymetry and coastline often constitutes a considerable source of residual circulation. However, wind or density-driven flows will also contribute to the overall residual velocity field. Langebaan Lagoon is a well mixed body of water and is not subject to significant fresh water input by rivers or groundwater seepage. Observations (figures 5-5 and 5-6) and previous studies on the Langebaan Lagoon system (Christie, 1981; Arabonis, 1995) have shown that in the southern sections of the lagoon, hypersalinity occurs as a result of strong evaporation over the shallow sections of the lagoon. During the summer months, when strong evaporation occurs, an inverse density gradient is encountered in the lagoon basin, with salinity in the southern part of the lagoon exceeding that at the lagoon mouth. If the lagoon basin is sufficiently hypersaline, it will be denser than Saldanha Bay water and lagoon water will tend to drain out of the basin, being replaced by less dense bay water. A residual circulation directed from Langebaan lagoon toward Saldanha Bay should hence result. According to the study of Largier et al. (1997) on several hypersaline systems, including Langebaan Lagoon, the longitudinal density gradient in hypersaline estuaries is generally insufficient to generate a strong inverse circulation. It is therefore expected that in Langebaan Lagoon, the residual circulation results mainly from the wind and the tide.

Theoretical analysis (chapter 7) and observations (figures 5-15) showed that there existed a strong asymmetry between the ebb and the flood flows at the east inlet. During the ebb, the east inlet outflow takes the form of a turbulent jet and Saldanha Bay water is advected toward the inlet as a result of lateral entrainment at the jet boundaries. On the flood, the flow takes the form of a potential sink. This ebb/flood asymmetry hence contributes to the formation of a residual circulation with Saldanha Bay water being 'pumped' into the east inlet of the lagoon. In Chapter 6, it was also found that during periods of high tidal range the tidal wave experienced significant distortion as it propagated into the lagoon basin. The distortion imposed by the lagoon geometry on tides would result in the tidal wave having a smaller amplitude and a greater lag at the east inlet. In a two inlets situation, residual flow arises as a result of differences in the mean water level, tidal amplitudes and phases at the inlets, and differences in the inlet themselves. Van de Kreeke and Dean (1975) have shown that in a two-inlet situation, the residual flow will be toward the inlet at which the tidal amplitude is smaller, or at which the tidal phase is lagged, all other factors being equal.

Alternatively, a residual transport will be directed toward the inlet of greater length, narrower width or greater depth, again all other factors being equal. Hence, the tidal pump generated by ebb/flood asymmetry and the distortion imposed by the lagoon bathymetry on the tidal wave would both contribute toward the generation of a residual circulation directed from Big Bay toward and into the east inlet. During periods of high tidal range, 'tidal pumping' and tidal wave distortion increase and as a result, we expect the residual current at the east inlet to have a greater magnitude. Measurements undertaken at the east inlet (figure 5-24) show that the residual current velocity was maximum during periods of high tidal range and minimal at neap tides. Both theory and measurements support the idea that the residual current at the east inlet is induced mainly by tidal currents and is representative of a Lagrangian residual transport.

If the lagoon were connected to Saldanha Bay by the east inlet only, the Lagrangian residual flow into the lagoon would be compensated by an opposing Eulerian flow in order to maintain a steady state condition. At the east inlet however, both the Eulerian and the Lagrangian residual transport are directed toward the interior of the lagoon. It is believed that the positive flux of water into the east inlet is compensated by a net loss through the west inlet. The low passed component of the along-channel current in both the east and the west channel had similar magnitude, comforting us in the idea that the residual circulation measured at the west inlet balances the residual transport of water into the east inlet. At the west inlet, the strength of the Eulerian residual current did not seem to be correlated to the tidal range and it only fluctuated slightly around a mean value of $0.16 m.s^{-1}$ (figure 5-26). It is possible that the residual flow at the west inlet has a different behaviour than that encountered at the east inlet, because the flow out of the west inlet is a secondary response to the tidal pumping mechanism and is thus more remotely related to tidal range variations.

In Chapter 5 and 6, some relation was observed between the winds at Cape Colombine, the waterlevel in Saldanha Bay and the residual current at the east inlet. Strong southerly winds at Cape Colombine induced a drop of the waterlevel in Saldanha Bay and a weaker residual flow from Big Bay into the east inlet. As explained in Chapter 6, southerly winds will induce a residual circulation directed toward Saldanha Bay in the upper part of the water column with a return residual current in the deep sections of the channel. The water-column at the

east inlet was never strongly stratified probably because the shallow regions located north of the inlet inhibit the intrusion of deep, cold water from Saldanha Bay. It is therefore expected that over the whole water-column of the east inlet southerly winds will induce a residual circulation directed from the lagoon to the bay. Time series of the temperature showed that cold water from the bottom layer of Saldanha Bay sometimes intruded at the west inlet during the flood. During the flood, southerly winds could hence strengthen the flood currents in the deep sections of the west inlet channel, thus favouring the intrusion of deep and cold water from Saldanha Bay into the west inlet. It is therefore possible that in the deep section of the west inlet channel, southerly winds induce a residual circulation which opposes the residual flow observed in the surface layer. From the 10^{th} to the 12^{th} of March, strong southerly winds (exceeding $10m.s^{-1}$) blew at Cape Colombine and within that same period of time, the magnitude of the residual current at the east inlet decreased by approximately $0.04m.s^{-1}$ (figures 5-12 and 5-25). From the 10^{th} to the 12^{th} of March however, the residual current at the east inlet was still directed from Big Bay into the lagoon, that is, in a direction which opposed the wind driven circulation. Also, the magnitude variation induced by the wind on the residual circulation at the east inlet was small. These observations suggest that although strong wind events will markedly affect the residual circulation at the lagoon inlets, the residual velocity field near the east inlet of the lagoon is dominated by tidal residual currents.

It is thought that the 'measured' Eulerian residual currents at the lagoon inlets result primarily from the asymmetry and the phase lags of tidal currents near the lagoon mouth and reflect on the Lagrangian transport occurring at the lagoon mouth. We hence suspect that the ebb/flood asymmetry encountered at the mouth of the Langebaan Lagoon dominates the exchange between the lagoon effluent and Big Bay waters. Values of the TER and the residence times obtained previously should hence provide reasonable estimates of the total exchange across the interface between Langebaan Lagoon and Saldanha Bay. The tidal residual circulation observed at the mouth of Langebaan Lagoon will continuously act to transport water-borne particles or sediments from the bay to the east inlet and from the west inlet to the bay. Previous study (Sharon, 1997) have underlined the unsteady behaviour of the east inlet. In the past years, sediments have been accumulating north of the east inlet. The unbalanced sediment flux at the east inlet, probably results from the fact that

tidal pumping is compensated by a stronger outflow at the west inlet rather than at the east inlet. It is very difficult to predict the evolution of bedload transport in a two-inlet situation. It is possible that at Langebaan Lagoon entrance, we witness a situation similar to that of Big Hickory Pass and New Pass in Florida, where the smaller inlet has a history of closing and reopening (Joshi, 1982). In the vicinity of the western inlet, the strong ebb flow will probably prohibit the accumulation of sediment around the mouth area.

It was seen that strong exchange arises across the Langebaan Lagoon-Saldanha Bay interface. The exchange of water between the lagoon and the bay varies with the tidal range and is predominantly driven by the ebb-flood asymmetry at the lagoon mouth. The lagoon effluent contributes effectively to the stirring and flushing of the water-column in Big Bay. It appeared that the residual circulation observed at the lagoon inlets is mainly tidal and that wind events have a sporadic and smaller influence on the overall residual velocity field. Residual currents affect the transport of material near the lagoon mouth, by creating a residual circulation directed from the bay toward the east inlet and from the west inlet to the bay.

the ebb and the flood was maximum and the exchange of water between the lagoon and the bay was minimal. As the tidal range increased, the geometry of the tidal inlets and the tidal distortion imposed by the lagoon basin on the tidal wave both contributed to generate an asymmetry between the ebb and the flood flows. On the flood, the flow took the form of a potential sink while on the ebb, water propagated into Saldanha Bay with high momentum and particles released at the lagoon inlets on the ebb experienced large drifts. It was suggested that when the tidal range was large, the east inlet outflow took the form of a turbulent jet while at the west inlet, the ebb flow would strongly interact with the seabed and coastal features and would not develop into a jet. The proximity of the lagoon inlets implied that the east and the west inlet flows merged together during the ebb. On its eastern boundary, the lagoon outflow participated toward the mixing and flushing of Big Bay water through lateral entrainment. On its western boundary, it was thought that the strong shear between the lagoon outflow and solid boundaries would contribute toward the generation of eddies. The large drifts resulting from the sink-like nature of the inflow and the jet-like nature of the outflow induced a very rapid and strong exchange between the lagoon, Saldanha Bay and possibly the outer ocean waters. Throughout the ebb, temperature at the lagoon inlets increased as a result of warmer water from the southern sections of the lagoon being advected through the mouth. Despite buoyancy forcing being present most of the time, the lagoon effluent generally remained attached to the bottom, keeping the water-column mixed over significant regions of Big Bay. However, when strong stratification occurred in Saldanha Bay, the east inlet ebb jet would lift off from the bottom as it reached the 8m depth contour in Big Bay. The detachment of the east inlet ebb jet could hence be responsible for local increases in stratification within Big Bay, but even in such case, the jet would enhance vertical mixing in the bay and favour the uptake of nutrient from the bottom layer of the bay to the surface mixed layer. The tidal exchange across the lagoon-bay interface was controlled by the asymmetry between the ebb and the flood flows at the tidal inlets. The strength of the asymmetry increased with tidal forcing and as a result, tidal exchange varied strongly with the tidal range.

One important feature revealed by this study was the existence of a residual circulation, with the east inlet constituting the entrance route for Saldanha Bay water and the west inlet being the exit route for the lagoon water. The Eulerian residual currents measured at the lagoon

inlets were thought to be related to the Lagrangian transport of material near the lagoon mouth. The residual circulation measured at the east inlet increased during periods of high tidal range and it was suggested that the tidal pump induced by the ebb/flood asymmetry was the predominant mechanism for the generation of residual velocity at the east inlet. The Langebaan lagoon hydrodynamic was singular in that tidal pumping at the east inlet was compensated by a stronger Eulerian flow at the west inlet. Although tidal residual current dominated the overall residual velocity field, the residual circulation at the lagoon mouth was markedly affected by wind events.

This study combined measurements and a theoretical understanding of coastal lagoons hydrodynamics to provide a new description of the Eulerian and Lagrangian flow fields at the interface between Langebaan Lagoon and Saldanha Bay. Significant insight was gained on the spatial and temporal variations of the currents near the mouth of Langebaan Lagoon. It is hoped that this work will provide a framework for investigating a wide range of transport and mixing problems, may they be related to protecting the ecology of Langebaan Lagoon or to monitoring the water quality in Saldanha Bay.

The region located near the lagoon mouth is characterised by strong horizontal gradients in the velocity field. Therefore, additional field data should be obtained to test some of the hypothesis made in this study and to enable a more quantitative description of the flow at the interface between the lagoon and the bay. For example, current measurements across the mouth and into Saldanha Bay would help picture the horizontal gradients encountered in the flow field as the lagoon effluent propagates into the bay. More drifter experiments could also be undertaken in order to gain farther information on the dispersion induced by tidal currents. Eventually, longer data records should be obtained to conduct a more meaningful statistical analysis and also, for the purpose of better understanding how extreme events affect the system.

References

AMBRAMOVICH, G. N., 1963. The theory of turbulent jets, *Massachusetts Institute of Technology Press*, Cambridge, Massachusetts.

ARABONIS, J. P., 1995. Analysis of water exchange in Langebaan Lagoon. *BSc of Honours*, University of Cape Town.

AWAJI, T., IMASATO N., KUNISHI, H. , 1980. Tidal exchange through a strait: a numerical experiment using a simple model basin. *Journal of Physical Oceanography*, Vol. 10, 1499-1508.

AWAJI, T., 1982. Water mixing in a tidal current and the effect of turbulence on tidal exchange through a strait. *Journal of Physical Oceanography*, Vol. 12, 501-514.

BARNES, R. S. K., 1980. *Coastal lagoons*. Cambridge UK: Cambridge University Press.

BENDAT, J. S., PIERSOL, A., 1971. *Random data: analysis and measurement procedures*. 2nd ed., New-York: John Wiley & Sons.

BILSKI, S., 1995. A report on the results of drogue studies in Saldanha bay and the use of a differential global positioning system in achieving these results. *Data Report*, University of Cape Town.

BILSKI, S., 1996. The characteristics of synoptic circulation patterns in Saldanha Bay. *MSc Thesis*, University of Cape Town.

BLACK, R. E., LUKATELICH, R. J., MCCOMB, A. J., ROSHER, J. E., 1981. Exchange of water, salt, nutrients and phytoplankton between Peel Inlet, Western Australia and the Indian ocean. *Australian Journal of Marine and Freshwater Research*, Vol. 32.,709-720.

BORICHANSKY, L. S., MIKHAILOV, V. N., 1966. Introduction of river and sea-water in the absence of tides. *Proceedings of the Symposium on Scientific Problems of the Humid Tropical Zone Deltas and Their Implications, Pakistan, Dacca*, Paris:UNESCO, 175-180.

CHADWICK, A., MORFETT, J., 1993. *Hydraulics in civil and environmental engineering*. London: E & F. N. SPON.

CHADWICK, D. B., 1997. Tidal exchange at the bay-ocean boundary: the breath of the bay. *PhD Thesis*, University of San Diego.

CHADWICK, D. B., LARGIER, J. L., CHENG, R. T., 1997. The role of thermal stratification in tidal exchange at the mouth of San Diego Bay. In *Buoyancy Effects on Coastal and Estuarine Dynamics*, Aubrey, D. G., Friedrichs, C. T., ed., (Coastal and Estuarine Studies; 53), Washington: American Geophysical Union, 139-154.

CHAO, S. Y., 1988. Wind driven motion of estuarine plumes. *Journal of Physical Oceanography*, Vol. 18, 1144 -1166.

CHRISTIE, N. D., 1981. Primary production in Langebaan lagoon. In *Estuarine Ecology*, Day, J. H., ed., Cape Town: Balkema, 101-106.

CODE, 1985. CODE-2: Moored array and large-scale data report. *Technical Report WHOI*, Woods Hole Oceanographic Institute.

COOPER, J., 1981. *Saldanha Bay-Langebaan: a unique heritage full of history and full of promise for the future*. Cape Town: CALTEX, 20-21.

CSIR, 1995. *Draft Summary Report Environmental Impact Assessment. Proposed Extension of the General Cargo Quay*. Port of Saldanha.

CSIR, 1997. Draft Main Report. Strategic Integrated Port Planning, Port of Saldanha. *Report No ENV/S-C97152A*.

DILORENZO, J. L., 1988. The overtide and filtering response of small inlet/bay systems. In *Hydrodynamics and Sediment Dynamics of Tidal Inlets*, Aubrey, D. G., Weishar, L., ed., (Lecture Notes on Coastal and Estuarine Studies; 29), New-York: Springer-Verlag, 24-53.

DRONKERS, J. J., 1964. Tidal computations in rivers and coastal waters. North Holland. Amsterdam.

DYER, K. R., 1973. *Estuaries: a physical introduction*. London: John Wiley & Sons.

DYER, K. R., 1986. *Coastal and Estuarine Sediment Dynamics*. London: John Wiley & Sons.

FISHER, H. B., LIST, E. J., KOH, R. C. Y., IMBERGER, J., BROOKS, N. H., 1979. *Mixing in Inland and Coastal Waters*. Boston: Academic Press.

FLEMMING, B. W., 1977. Depositional processes in Saldanha Bay and Langebaan lagoon. *PhD Thesis*. University of Cape Town.

FRENCH, J. L., 1960. Tidal flow in entrances. *Technical bulletin No. 3, U. S. Army Corps of Engineers, Waterway experiment Station, Committee on Tidal Hydraulics*, Vicksburg, Miss.

GADGIL, S., 1971. Structure of jets in rotating systems. *Journal of Fluid Mechanics*, Vol. 47, 417-436.

GARVINE, R. W., 1985. A Simple Model of Estuarine Subtidal Fluctuations Forced by Local and Remote Wind Stress. *Journal of Geophysical Research*, Vol. 90, No. C6, 11945-11948.

GODIN, G., 1991. The analysis of tides and currents. In *Tidal Hydrodynamics*, Parker, B., ed., New York: John Wiley & Sons.

HANSEN, D. V., RATTRAY, M., 1966. New dimensions in estuary classification. *Limnology and Oceanography*, Vol. 11, 319-325.

HAUENSTEIN, W., 1983. "Zuflussbedingte Dichtestromungen in Seen.". Institute for Hydromechanics, *Technical Report No. R20-83*, ETH, Zurich.

HEARN, C. J., HUNTER, J. R., IMBERGER, J., VAN SENDEN, D., 1990. Tidally induced jet in Koombana Bay, Western Australia. *Australian Jouranl of Marine and Freshwater Research*, Vol. 95, 3189-3197.

HEARN, C. J., LUKATELICH, R. J., MCCOMB, A. J., 1991. Coastal lagoon ecosystem modelling. In *Tidal Hydrodynamics*, Parker, B., ed., New York: John Wiley & Sons, 471-502.

HOLLOWAY, P. E., 1996. A Field Investigation of Water Exchange Between a Small Coastal Embayment and an Adjacent Shelf. In *Mixing in Estuaries and Coastal Seas*, Pattiaratchi, C., ed., (Coastal and Estuarine Studies; 50), Washington: American Geophysical Union, 145-158.

IMASATO, N., 1983. What is tide-induced residual current?. *Journal of Physical Oceanography*, Vol. 13, 1307-1317.

JAY, D. A., MUSIAK, J. D., 1996. Internal tidal asymmetry in channel flows: origins and consequences. In *Mixing in Estuaries and Coastal Seas*, Pattiaratchi, C., ed., (Coastal and Estuarine studies; 50), Washington: American Geophysical Union, 211-249.

JOSHI, P. B. 1982. Hydromechanics of tidal jets. *ASCE, Journal of the Waterway, Port, Coastal and Ocean division*, Proceedings of the American society of Civil Engineers, Vol. 108, No. WW3, 239-253.

JURY, M. R., MACARTHUR, C. I., BRUNDRIT, G. B., 1990. Pulsing of the Benguela upwelling region: large scale atmospheric controls. *South African Journal of Marine Science*, Vol. 9, 27-41.

KAPOLNAI, A., WERNER, F., BLANTON, J., 1996. Circulation, mixing, and exchange processes in the vicinity of tidal inlets: a numerical study. *Journal of Geophysical Research*, Vol. 101, No. C6, 14253-14268.

KJERFVE, B., KNOPPERS, B. A., 1991. Tidal choking in a coastal lagoon. In *Tidal Hydrodynamics*, Parker, B., ed., New York: John Wiley & Sons, 169-181.

KJERFVE, B., 1994. *Coastal Lagoon Processes*, Amsterdam: Elsevier.

KRAUSS, T. P., LOREN, S., LITTLE, J. N., 1994. *Signal processing toolbox*. Natick, Mass: The Mathworks, Inc.

LARGIER, J. L., 1988. Internal shelf tides, wind-driven motion and their role in deepening the surface mixed layer. *PhD Thesis*, University of Cape Town.

LARGIER, J. L., 1992. Tidal Intrusion Fronts. *Estuaries*, Vol. 15, 26-39.

LARGIER, J. L., HOLLIBAUGH, J. T., SMITH, S. V., 1997. Seasonally hypersaline estuaries in mediterranean-climate regions. *Estuarine, Coastal and Shelf Science*, Vol. 45, 789-797.

LESSA, G., 1996. Tidal dynamics and sediment transport in a shallow macrotidal estuary. In *Mixing in Estuaries and Coastal Seas*, Pattiaratchi, C., ed., (Coastal and Estuarine Studies; 50), Washington: American Geophysical Union, 338-360.

LINDEN, P. F., SIMPSON, J. E., 1986, Gravity driven flows in a turbulent fluid. *Journal of fluid mechanics*, Vol. 172, 481-497.

LUKETINA, D. A., IMBERGER, J., 1987. Turbulence and entrainment in a buoyant surface plume. *Journal of Geophysical Research*, Vol. 94, 12619-12636.

MEHTA, A. J, JOSHI, P. B, 1988. Tidal inlet hydraulics, *Journal of Hydraulic Engineering*. Vol. 114, No 11, 1321-1337.

MEHTA, A. J, OZSOY, A. E., 1978. Inlet hydraulics. *Stability of Tidal Inlets-Theory and Engineering*, Bruun, P., ed., New-York: Elsevier.

MIDDLETON, J. G., 1975. The asymptotic behaviour of a starting plume. *Journal of Fluid Mechanics*, Vol. 72, 753-771.

MONTEIRO, P. M. S., BRUNDRIT, G. B., 1990. Interannual chlorophyll variability in South Africa's Saldanha Bay system. *South African Journal of Marine Science*, Vol. 9, 281-287.

MONTEIRO, P. M. S., BRUNDRIT, G. B., 1995. Shelf-Bay interactions in the southern Benguela upwelling system: implications for eutrophication. *Unpublished.*

MONTEIRO, P. M. S., LARGIER, J. L., 1999, Thermal stratification in Saldanha Bay, South Africa and subtidal, density driven exchange with the coastal waters of the Benguela upwelling system, *Estuarine, Coastal and Shelf Science*, submitted.

MORTON, B. R., TAYLOR, G. I., TURNER, J. S., 1956. Turbulent gravitational convection from maintained and instantaneous sources. *Proceedings*, Royal Society, Vol. A234, 1-23.

NUNES, R. A., SIMPSON, J. H., 1985. Axial convergence in a well-mixed estuary. *Estuarine, Coastal and Shelf Science*, Vol. 20, 637-649.

OTNES, R. K., 1978. Applied time series analysis. New-York: A Wiley-Interscience publication.

OZSOY, E., 1977. Flow and mass transport in the vicinity of tidal inlets. *Technical Report No. TR-0.36*, Coastal and oceanographic engineering laboratory, University of Florida, Gainsville, FL.

OZSOY, E., UNLUATA, U., 1982. Ebb-tidal flow characteristics near inlets. *Estuarine, Coastal and Shelf Science*, Vol. 14, 251-263.

PATTIARATCHI, C., 1996. *Mixing in Estuaries and Coastal Seas*. (Coastal and Estuarine Studies; 50), Washington: American Geophysical Union.

PRANDLE, D., 1985. On salinity regimes and the vertical structure of residual flows in narrow tidal estuaries. *Estuarine, Coastal and Shelf Science*, Vol. 20, 615-635.

PRANDLE, D., 1991. Tides in estuaries and embayments (review). In *Tidal Hydrodynamics*, Parker, B., ed., New York: John Wiley & Sons.

PRESTON-WHYTE, R. A., TYSON, P. D., 1988. *The atmosphere and weather of Southern Africa.* Cape Town: Oxford University Press.

PUGH, D. T., 1979. Sea levels at Aldabra atoll, Mombasa and Mahé, western equatorial Indian Ocean, related to tides, meteorology and ocean circulation. *Deep Sea Research*, Vol. 26A, 237-258.

PUGH, D. T., 1987. *Tides, surges and mean sea-level.* Chichester: John Wiley & Sons.

RIDDERINKHOF, H., ZIMMERMAN, J. T. F., 1990. Mixing processes in a numerical model of the Dutch Wadden Sea. In *Residual Currents and Longterm Transport*, Cheng, R. T., ed., (Coastal and Estuarine Studies; 38), Wahsington: American Geophysical Union, 194-209.

ROBINSON, G. A., 1989. *West coast National Park: a master plan for Langebaan nature area.*

ROZENTHAL, G., GRANT. S., 1989. Simplified tidal prediction for the South African coastline. *South African Journal of Marine Science*, Vol. 85, 104-107.

SAFAIE, B., 1979. Mixing of buoyant surface jet over slopping bottom. *ASCE, Journal of the Waterway, Port, Coastal and Ocean division*, Proceedings of the American society of Civil Engineers, Vol. 105, No WW4.

SAVAGE, S. B., SOBEY, R. J., 1975. Horizontal momentum jets in rotating basins. *Journal of Fluid Mechanics*, 71(4), 755-768.

SCHULZE, B. R., 1965. Climate of South Africa. General survey, South African Weather Bureau, part 8.

SHANNON, L. V., 1985. The Benguela ecosystem part 1: Evolution of the Benguela, physical features and processes. *Oceanography and Marine Biology Annual Review*, Vol. 23, 105-182.

SHANNON, L. V., NELSON, G., 1996. The Benguela: large scale features and processes and system variability. In *The South-Atlantic: present and past circulations*, Wefer, G., Berger, W. H., Siedler, G., Webb, D. J., ed., Berlin: Springler-Verlag, 163-210.

SHANNON, L. V., STANDER, G. H., 1977. Physical and chemical characteristics of water in Saldanha Bay and Langebaan Lagoon. *Transaction of the Royal Society of South Africa*, Vol. 42, 441-459.

SHARON, J., 1997, The morphological changes of the Langebaan sand spit, *BSc of Honours*, University of Cape Town.

SHENG, Y. P., PEENE, S., YASSUDA, E., 1996. Circulation and transport in Sarasota Bay, Florida: the effect of tidal inlets on estuarine circulation and flushing quality. In *Mixing in Estuaries and Coastal Seas*, Pattiaratchi, C. ed., (Coastal and Estuarine Studies; 50), Washington: American Geophysical Union, 184-210.

SIGNELL, R. P, BUTMAN, B., 1992. Modelling tidal exchange and dispersion in Boston harbour. *Journal of Geophysical Research*, Vol. 97, No. C10, 15591-15606.

SMITH, N. P., 1985. The decomposition and simulation of the longitudinal circulation in a coastal lagoon. *Estuarine, Coastal and Shelf Science*, Vol. 21, 623-632.

SMITH, N. P., 1994. Water, salt and heat balance of coastal lagoons. In *Coastal Lagoon Processes*, B. Kjerfve ed., New-York: Elsevier, 69-101.

SPAULDING, M. L., 1994. Modelling of circulation and dispersion in coastal lagoons. In *Coastal Lagoon Processes*, Kjerfve, B., ed., New-York: Elsevier, 103-131.

SPEER, P. E, AUBREY, D. G., FRIEDRICHS, C. T., 1991. Nonlinear hydrodynamics of shallow tidal inlet/bay systems. In *Tidal Hydrodynamics.*, Parker, B., ed., New York: John Wiley & Sons, 321-339.

SPOLANDER, B., 1995. Entrainment in Saldanha Bay. *MSc Thesis*, University of Cape Town.

STOMMEL, H., FARMER, H. G., 1952. On the nature of estuarine circulation. *Woods Hole Oceanographic Institute References Nos. 52-51, 52-63, 52-88 (3 vols. Containing chapter 1-4 and 7).*

SWAN, A. R. H., SANDILANDS, M., 1995. *Introduction to geological data analysis.* Oxford: Blackwell Science Ltd.

TAYLOR, R. B., DEAN, R. G., 1974. Exchange characteristics of tidal inlets. *ASCE, Journal of the Waterway, Port, Coastal and Ocean division*, Proceedings of the 14th coastal engineering conference, Copenhagen, Denmark, Vol. 3, 2268-2289.

TOLLMIEN, W., 1945. "Berechung Turbulenter Ausbreitungsvorgänge". *U. S. Government Publication TM 1085*, National Advisory Committee on Aeronautics, Washington.

TRITTON, D. J, 1988. *Physical fluid dynamics.* 2nd ed., New-York: Oxford University Press.

VAN BALLEGOOYEN, R. C., 1995. Forced synoptic coastal-trapped waves along the southern African coastline. *MSc Thesis*, University of Cape Town.

VAN DE KREEKE, J., DEAN, R. G., 1975, Tide induced mass transport in lagoons. *ASCE, Journal of Water resources, Harbors and Coastal Engineering division*, Vol. 101, 393-402.

VAN DER MERWE, E., 1990. Water structure and circulation in Saldanha Bay. *BSc of Honours*, University of Port Elisabeth.

WEEKS, S. J., 1990. The current and circulation in Saldanha Bay: post 1975, Water budgets in the Saldanha Bay and Langebaan Lagoon systems under differing hydrological conditions, implications for the residence times of pollutants, Marine eutrophication project: report 1. *BSc of Honours*, University of Cape Town.

WEEKS, S. J., BOYD, A. J., MONTEIRO, P. M. S., BRUNDRIT, G. B., 1991(a). The currents and circulation in Saldanha Bay after 1975 deduced from historical measurements of drogues. *South African Journal of Marine Science*, Vol. 11, 525-535.

WEEKS, S. J., MONTEIRO, P. M. S., NELSON, G., COOPER, R. M., 1991(b). A note on wind-driven replacement flow of the bottom layer in Saldanha Bay, South Africa: implications for pollution. *South African Journal of Marine Science*, Vol. 11, 579-583.

WILKINSON, D. L., 1978. Periodic flows from tidal inlets. *Proceedings of the 16th ASCE coastal engineering conference*, Vol. 2, 1336-1346.

WOLANSKI, E., IMBERGER, J., 1987. Friction-controlled selective withdrawal near inlets. *Estuarine, Coastal and Shelf Science*, Vol. 24, 327-333.

WOLANSKI, E., 1986. Water circulation in a topographically complex environment. In *Lecture Notes on Coastal and Estuarine Studies*, Van de Kreeke ed., Berlin: Springler-Verlag, Vol. 16, 154-167.

WONG, K. C., 1987. Tidal and subtidal variability in Deleware's inland bays. *Journal of Physical Oceanography*, Vol. 17, 413-422.

ZIMMERMAN, J. T. F, 1976. Mixing and flushing of tidal embayments in the western Dutch Wadden sea, II: analysis of mixing processes. *Netherland Journal of Sea Research*, Vol. 10, 397-439.

ZIMMERMAN, J. T. F, 1981. Dynamics, diffusion and geomorphological significance of tidal residual eddies. *Nature*, Vol. 290, 549-555.

ZIMMERMAN, J. T. F, 1986. The tidal whirlpool: A review of horizontal dispersion by tidal and residual currents. *Netherland Journal of Sea Research*, Vol. 20, 133-154.